Universität für Bodenkultur Wien
University of Natural Resources
and Applied Life Sciences, Vienna

Decellularized vascular structures and substances from human placental tissue

A source for small-diameter vascular grafts and human collagen

Dissertation
zur Erlangung des Doktorgrades
an der Universität für Bodenkultur Wien

Eingereicht von

Dipl.-Ing. Karl Heinrich Schneider

Wien, Februar 2016

Institut für Biotechnologie
Vorstand: Ao.Univ.Prof. Dr. Florian Rücker
Betreuer: Ao.Univ.Prof. Dr. Johannes Grillari

Durchgeführt am Ludwig Boltzmann Institut für Experimentelle und Klinische Traumatologie / AUVA Forschungsinstitut
Vorstand/Betreuer: Ao.Univ.Prof. Dr. Heinz Redl

Acknowledgement

There are numerous people I would like to thank who supported me during the course of my thesis. But in order to keep this acknowledgement short I will mention only a few ones here by name:

Successful supervision is not only based on providing factual knowledge but also by inspiring and guiding others to give their best. I am grateful and I appreciate that Prof. Dr. Heinz Redl was able to provide me both during the elaboration of my thesis. I also express my gratitude to my other supervisor Prof. Dr. Johannes Grillari, who encouraged me to do this thesis in the first place.

I am deeply grateful to Dr. Andreas Teuschl for his constant support in all aspects of my work and Dr. Wolfgang Holnthoner and his research group, for the inspiring working environment and their help whenever I needed it. Special thanks go to Jonathan Bernhard, M.Sc. for his revision of the manuscript.

Last but not least, I would not be where I am now without my family and close friends who where there for me at all times and in every circumstance of my life.

Zusammenfassung

Die menschliche Plazenta, meist nur als klinisches Abfallprodukt angesehen, stellt bei jährlich rund 5 Millionen Geburten in Europa eine vielversprechende Quelle für humanes Gewebe dar [1], welches ohne Schaden für die Spenderin in großen Mengen gewonnen werden kann. Die Plazenta setzt sich aus verschiedenen Gewebsschichten zusammen. Diese können im Bereich der Geweberegeneration unterschiedlich genutzt werden. Außerdem wird diesem Gewebe durch Ursprung und Beschaffenheit eine besonders hohe Qualität zugesagt. Im Rahmen dieser Studie wurde ein Verfahren zur Isolation und Dezellularisation von Blutgefäßen mit einem Innendurchmesser von weniger als 5 mm aus dem Plazenta Chorion etabliert. Eine besondere Herausforderung bei der Dezellularisation von biologischem Gewebe ist es, sämtliche Zellbestandteile aus der extrazellulären Matrix (ECM) zu lösen, ohne dabei großen Schaden an ihrer Grundstruktur zu verursachen. Hierbei wurden enzymatische, chemische, und mechanische Methoden kombiniert, um optimale Ergebnisse zu erzielen. Als Kontrolle wurden spezielle histologische und biochemische Analyseverfahren sowie mechanische Tests durchgeführt. In einem ersten Experiment wurden Stücke aus dezellularisierten Einzelgefäßen mit Endothelzellen reendothelialisiert und in eine Fibrinmatrix gemeinsam mit Fettstammzellen (ASC) eingebettet. Durch das verwendete Co-Kultursystem wird das Wachstum neuer Kapillargefäße induziert, welche in die Fibrinmatrix einwachsen. Dieser sogenannte „dual-level approach“ repräsentiert eine neue Strategie zur Neovaskularisation im Bereich des Tissue Engineering. Für eine mögliche Entwicklung eines Gefäßtransplantats wurden Oberflächenmodifikationen mit Heparin an dezellularisierten Blutgefäßen durchgeführt und erste Tests für eine zukünftige klinische Anwendung gemacht. Im Zuge dieser Arbeit wurden zusätzlich Kollagenproben, isoliert aus dem Basalgewebe der Plazenta, charakterisiert. Ihre Sekundärstruktur und Reinheit wurde mittels Zirkulardichroismus Spektroskopie bestimmt und erste Tests in einem Zellkultursytem mit primären Hepatozyten durchgeführt. Diese Studie setzt weitere Schritte zur Nutzbarmachung von Plazentagewebe für klinische Anwendungen oder als Grundlage für Zellkultursysteme in der Forschung.

Abstract

The placenta is normally deemed as clinical waste. Due to the amount of over 5 million births per year in the European Union [1], the placenta is likely the most easily accessible human tissue of consistent quality that does not cause any additional harm to the donor. Furthermore, the placenta develops together, from the mother and with the baby, during pregnancy. This fetal or neonatal origin of the tissue could have a positive impact on the quality of graft material. In this work, we established a decellularization procedure for small-diameter human vascular scaffolds harvested from placenta chorion. The scaffolds were characterized biochemically, histologically and examined for their cytocompatibility with endothelial cells. The ability to decellularize the vascular tissue using this protocol, and the demonstrated ability to recellularize indicates the ability of the material to function as a versatile tool for novel tissue engineering approaches and regenerative medicine. With our experiments we demonstrate the biocompatibility of decellularized vascular tissue from the human placenta. The tissue was successfully recellularized with endothelial cells (ECs), which, in co-culture with ASCs, displayed vascular tube formation from the scaffold. A prospective target of this project will be to facilitate a complete re-endothelialization of human vascular grafts with endothelial cells for further applications in tissue engineering and regenerative medicine. Our dual-level approach should ensure oxygen and nutrient supply in varying tissue sizes and thus represent a novel vascularization strategy. Initial experiments were performed to evaluate the quality of decellularized vascular grafts to be used in clinical applications as small diameter vascular grafts. Therefore, the anticoagulant heparin was covalently linked to the collagen matrix of the decellularized vessel graft. Furthermore, to determine the potential of placental substances, pure collagen isolated from human placenta tissue was characterized. Circular Dichroism (CD) Spectroscopy analysis of collagen isolated from the human placenta confirmed a natural secondary structure of the purified molecules. Moreover, using this collagen for cell cultivation showed no cytotoxicity and a supporting effect on cell adhesion and proliferation of primary hepatocytes in vitro.

Table of Contents

1 Aim of the study

In this thesis we wanted to examine the potential of human placenta tissue as a source for decellularized small diameter vascular grafts vascular scaffolds for prevascularization purposes. We tried to provide an understanding of the qualities of raw human placenta material, and to demonstrate the importance of an appropriate placenta decellularization protocol, as this process affects cell-tissue compatibility, mechanical properties and biocompatibility of the resulting acellular tissue. Moreover, this study uses in vitro assays to characterize the effect of decellularization, and surface modification techniques on the tissue matrix to modulate the performance of the grafts in an in vivo application.

Besides vascular structures, molecular substances can be extracted from the placental tissue. A satellite project determined the secondary structure of collagen isolated from the placenta using circular dichroism (CD) spectroscopy and to determine the cell compatibility of the material using primary anchorage dependent cells.

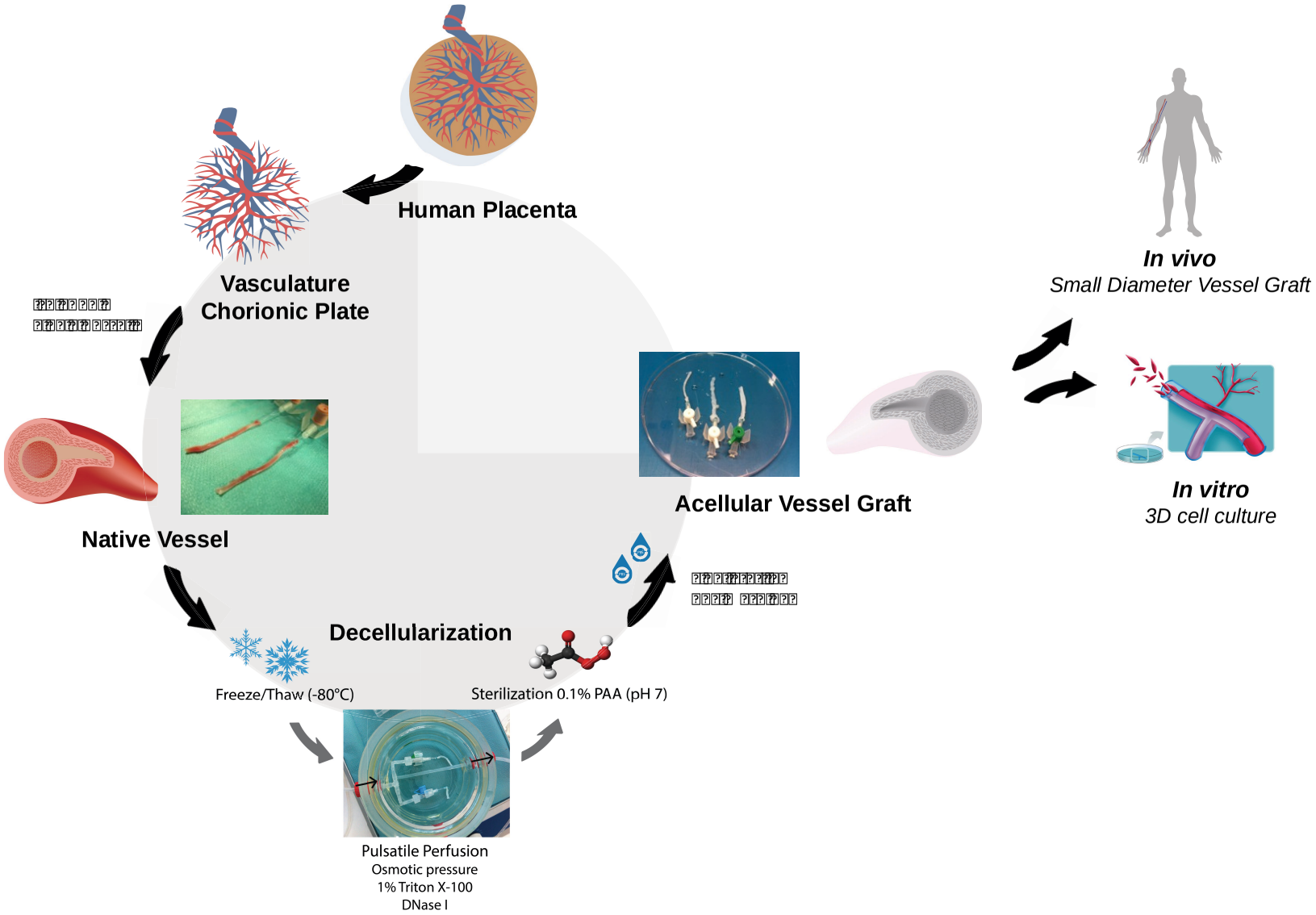

Figure 1: Graphical abstract. Flow scheme of the preparation, decellularization, and application of human placenta vascular tissue structures [121].

2 Introduction

2.1 Tissue engineering and regenerative medicine

For more than three decades, the terms tissue engineering and regenerative medicine have been used to describe the field of regeneration and rehabilitation of inherent or acquired defects in tissues and organs. In fact, tissue engineering and regenerative medicine have grown to resemble a singular research entity [2]. A persistent theme in the field is the challenge of imitating nature and translating new materials into clinical treatments and therapies. Therefore, a combinations of cells, cell culture techniques, biomaterials, bioreactor systems, and suitable biochemical and physicochemical factors are being utilized [3]. By simulating a native environment through the use of all or some of these components, cells can act naturally when reseeded on scaffolds *in vitro* or migrate into a scaffold after implantation [4]. Biodegradable scaffolds play an important role as templates for 3D tissue growth or as artificial implants to guide and stimulate in situ regeneration [5]. Many different biomaterials and a variety of ways to isolate, generate or process them are known and are already being investigated.

2.1.1 Vascular tissue engineering

Rates of death attributed to cardiovascular diseases (CVD) have declined in the United States, but CVD is still the leading cause of mortality and accounted for over 30% deaths in 2011 [6]. Despite an increasing number of therapies for vascular dysfunctions, including approaches in tissue engineering [7], the demand for vascular transplants far exceeds the number of available donor tissues or organs. Currently, the standard grafts used to treat CVD are autologous grafts from the patient, using saphenous vein or mammary artery. Autologous grafts have the best outcome and are considered the gold standard in this field. However, there are big disadvantages due to the fact that this method requires multiple surgical procedures and there is a limited amount of adequate vessels available.

A common alternative, synthetic grafts have shown positive outcomes only when used in large diameter (>6 mm) vessel substitution. In small diameter vascular grafts the use of synthetic materials often leads to thrombosis or hyperplasia [8]. Noting these limitations, the use of decellularized allogenic blood vessels could be an effective alternative to established methods. Elsewhere, new sources of grafts for small-caliber replacements (<6 mm) have become a major focus in CVD research [9,10]. Indeed, these vascular grafts require certain attributes for clinical use.

Ideal vascular grafts should show sufficient mechanical strength to withstand long-term hemodynamic stresses. They should be non-toxic, non-immunogenic and show biocompatibility with the host tissue. In addition, for suitability in clinical applications, availability of various sizes is needed. So-called “off-the-shelf” availability and a definite simplicity in surgical handling are important for the use in situations of emergency care [11]. A vascular graft should not promote thrombosis and completely incorporate into the host tissue with adequate ability to grow for use in children [12]. In short, there are many requirements, but still no ideal vascular graft that fulfills all requirements at once.

2.1.2 Biomaterials

By definition, biomaterials are structures or substances used to create scaffolds as a replacement or support of injured tissue [13]. They can be of natural or synthetic origin, alive or lifeless, and interact with biological systems. Biomaterials are often used in medical applications to augment or replace a natural function. Key features of biomaterials are biocompatibility, bioactivity, and mechanical strength. Bioactive biomaterials elicit biological activity. For example, in the case of vascular grafts, bioactivity can prevent blood coagulation, encourage endothelial cell attachment, promote capillary infiltration, and prevent excessive collagen expression of smooth muscle cells migrated to the tissue [14]. Bioresorbable materials undergo degradation in the body with non-toxic dissolution products and are slowly replaced by newly formed tissue [15]. Ideally, biomaterials should have mechanical and physical properties consistent with the anatomical site into which it is implanted.

Furthermore, they should be readily available and manufactured at reasonable costs [16].

In tissue engineering, biomaterials play an important role as the scaffold for cultured cells, and require additional properties such as an interconnected porosity to ensure efficient cell migration, nutrient supply, metabolic waste elimination and oxygen transport [17]. Biomaterials can be derived from nature (e.g. ECM, collagen, fibrin, silk) or synthesized in the laboratory using metallic components, polymers, ceramics, or composite materials. Synthetic biomaterials have the advantage that they can be formed and processed to fulfill necessary functions. A combination of synthetic biomaterials and biological ligands reactive for cell receptors and signaling molecules has been investigated to create a new type of cell scaffold [18]. In contrast, naturally derived biomaterials can be chosen by their qualities and isolated while still conserving their original properties. For example, the extracellular matrix from decellularized tissues has been shown to affect cell proliferation [19], direct cell differentiation [20,21], and induce constructive host tissue remodeling responses [22,23]. However, processing of the tissue, including decellularization, has to ensure preservation of native surface topology, 3D ultrastructure and composition of the ECM to allow clinical success [24,25].

2.1.3 Fibrin

Fibrin is the activated “glue” of plasmatic blood clotting. During blood coagulation, fibrinogen, a circulating inactive precursor, is cleaved by thrombin to release two sets of fibrinopeptides (A and B). Quickly after cleavage, a formation of non-covalent monomer assembly forms a weak clot. The formation of covalent crosslinks, which are stabilized by a transglutaminase Factor XIIIa, adds additional crosslinks into the fibrin mesh and enhances the stability of the fibrin clot [26]. The activity of the transglutaminase factor requires the presence of Ca^{2+} ions as a cofactor. Fibrin is clinically used as a tissue adhesive or as a sealant for wound treatment. In tissue engineering, 3D fibrin gel matrices are used for applications including engineering of adipose, cardiovascular, liver, skin and

cartilage tissue [27,28]. Furthermore, fibrin hydrogels are used for cell cultivation and promotion of vascularization [29].

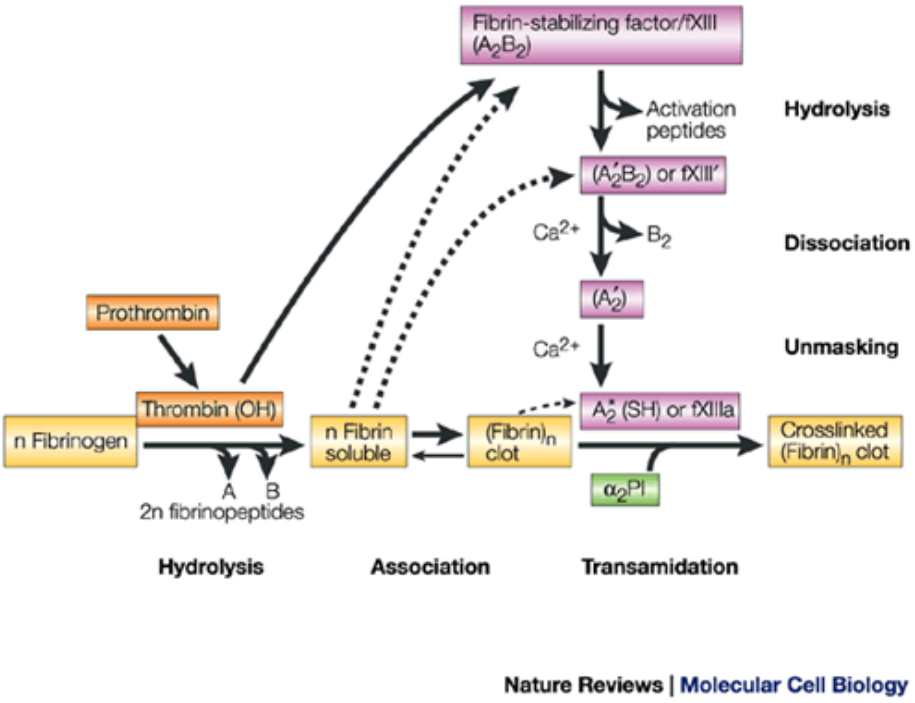

Figure 2: Cleavage of fibrinogen molecules to fibrin and the interaction with the stabilization factor XIIIa for enhanced stability of the fibrin clot. Nature Reviews [152].

2.1.4 Extracellular matrix

The extracellular matrix (ECM) is a structure consisting of proteins, glycoproteins and polysaccharides secreted by the resident cells of each tissue. It fills the space between the cells, provides physical support and plays an important role in cell regulation and development [30]. The ECM and its molecules are known to affect migration, function and homeostasis of the cells. More precisely, certain domains of collagen, the main protein of the ECM, have the potential to bind to cell surface receptors, other proteins like fibronectin or laminin, glycosaminoglycans (GAGs), nucleic acids, and growth factors [31].

Previous studies have proposed that growth factors and structural proteins of the ECM can be preserved in decellularized tissues. Biological activity was

retained in decellularized porcine mesothelium and stimulated fibroblast cell growth and expression of growth factors *in vitro* [32,33]. Indeed, physical and biochemical properties are strongly interconnected and one can influence the other [34]. It is therefore not surprising that each tissue type has a unique and specialized ECM organization and composition depending on its function. However, there are controversies regarding the mechanisms that best promote cell migration and tissue reconstruction and there is a discrepancy about the relevance of the specific 3D ultrastructure and the molecular composition of a tissue [35].

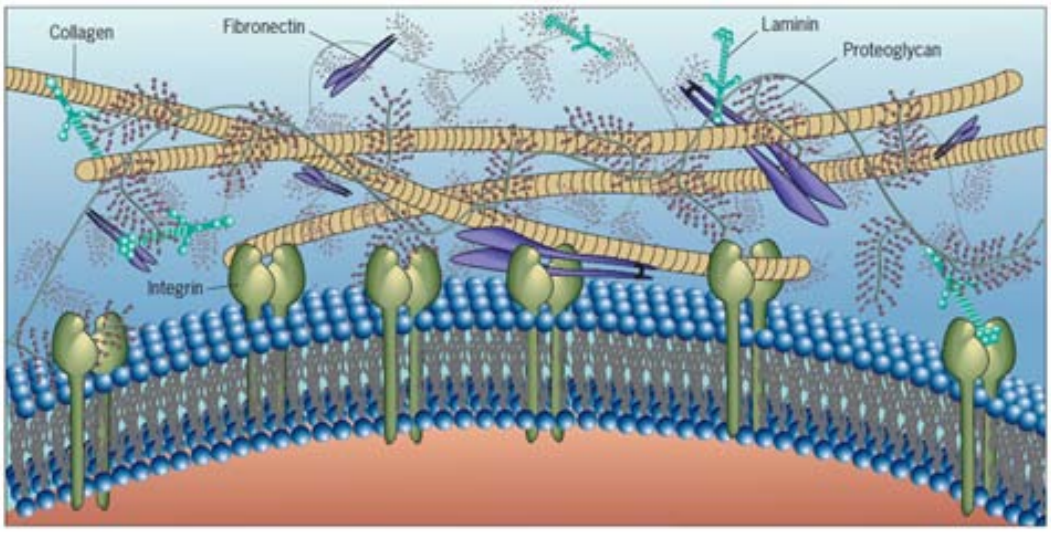

Figure 3: Schematic of ECM main proteins connected to cell membrane integrins. Collagen, fibronectin, laminin and proteoglycans are the main groups of molecules composing the ECM. Picture from NPTEL (E-learning platform) [153]

2.1.5 Collagen

Collagen is an abundant structural protein in the human body and is a main component of the extracellular matrix (ECM). Approximately one-quarter of the protein in the body is collagen and they are mainly produced by fibroblasts performing a Vitamin C dependent collagen synthesis [36]. There are several types of collagens, each with a unique shape, but all collagen types are built around a core structure of three strands of proteins, $(ProHypGly)_4$–

(ProHypAla)–(ProHypGly)$_5$, forming a triple helical structure [37]. This triple helical conformation is responsible for the structure and stability of tissues. Furthermore, the different collagen types show divergent characteristics. Some specific properties are mechanical strength, thermal stability or specific interactions with other biomolecules to support cell-cell interactions. Consequently, the use of collagen or a collagen consisting ECM can give strength and biocompatibility to a biological scaffold. Furthermore, it is known that collagen can play a role in adhesion, migration and differentiation of cells and may be an attractant for fibroblasts in vivo during wound repair, fracture healing and embryogenesis [38]. Many cell surface proteins can interact with the collagen fibrils. Furthermore, collagen based biomaterials can be combined with other biomolecules like glycosaminoglycans (GAG), elastin, or chitosan [36,39] for advanced cell-scaffold interactions, producing biomaterials with a large potential in tissue engineering applications.

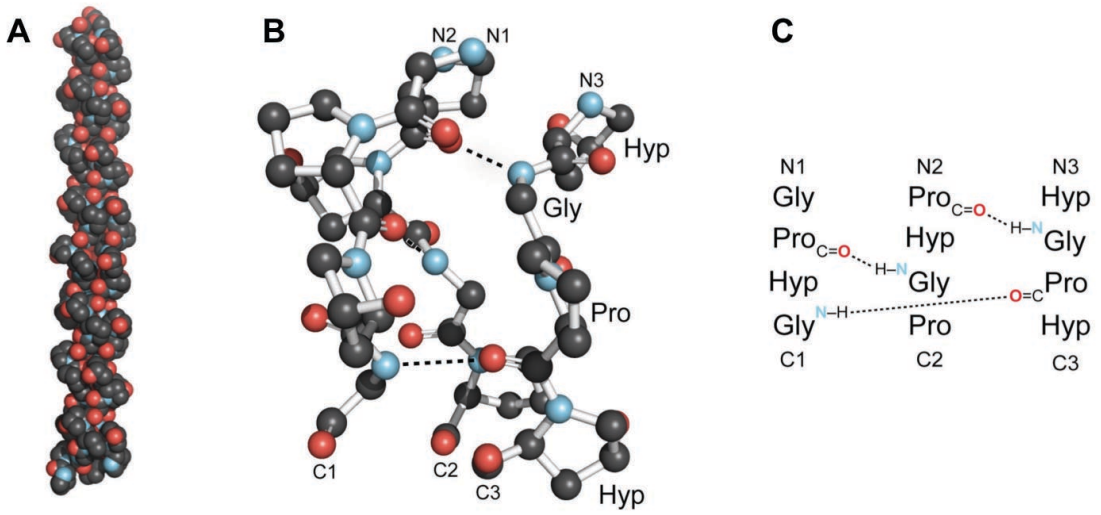

Figure 4: The three strands of collagen are wound around each other in a tight left-handed triple helix. (A) Crystal structure of collagen triple-helix with three repeating amino acids per turn and with glycine as every third amino acid in red [Protein Data Bank (PDB) entry 1cag]. (B) Ball-and-stick image of a short segment. (C) Stagger of the 3 strands in the segment in panel B [37].

2.1.6 Decellularized tissues

Biomaterials based on decellularized tissues are increasingly attractive as a functional alternative to other natural or synthetic materials [40]. In fact, decellularized tissue have been produced from a variety of animal sources and tissues, including aorta, skin, urinary bladder, liver, and placenta [41]. One major advantage of decellularized tissues is that the removal of cells and cell fragments eliminates the immune rejection responses of the host after transplantation. Indeed, factors that affect host response include decellularization efficacy, the use of chemical crosslinking agents, and the age of the tissue which is harvested [42].

Decellularized materials are naturally derived and inherently support various cell functions. The structure and composition of the ECM helps maintain tissue structure and cell-matrix interactions. For instance, the arrangement of tissue fibers has been proven to support cell migration and proliferation, including gene expression and cell-cell interactions [43–45]. As described before (2.1.3), the choice of a specific tissue source, similar in characteristics to the needs of the resulting application, can lead to a successful treatment. The main goal will always be to completely decellularize the tissue while causing the least alteration in structure and composition in order to preserve major properties of the native tissue.

Table 1: Schematic overview of the most commonly used decellularization and recellularization techniques for vascular tissue

Tissue	Decell. Method	Recell. Method	Ref
Human umbilical cord	Comparison of detergents	In vitro seeding of EC	[46]
Human umbilical artery	CHAPS and SDS	In vitro seeding of EC and In vivo implant in nude rats	[47]
Human common femoral arteries	Freeze-thaw, hypotonic buffer, SDS	In vitro seeding of mouse 3T3 cells	[48]
Human umbilical arteries	Trypsin -EDTA, SDS	In vitro seeding of MSC	[49]
Swine arteries	SDS	None	[50]
Porcine carotid arteries	Comparison of non ionic treatment, osmotic pressure, ionic detergent	In vitro seeding of porcine carotid artery SMC	[51]
Calf tibial arteries and veins	SDS, Trypsin, PDGE, drying	In vitro seeding of EC	[52]
Porcine carotid arteries	Triton X-100, ammonium hydroxide,	In vitro seeding of EC	[53]
Porcine abdominal aorta	Mechanical shaking device	None	[54]
Porcine tissue-engineered vessels	CHAPS and SDS	In vivo after homologous cell seeding	[55]
Porcine descending aorta	Sonication	None	[56]
Rat iliac arteries	SDS, DNase-I,	In vivo after homologous cell seeding	[57]
Rat aortic conduit graft	SDS	In vivo heterotopic implantation	[58]

2.1.7 Applications of decellularized tissues and organs

During the past 10 years, different studies of decellularized donor organs such as heart [59], trachea [60], or liver [61], showed that they can provide an acellular scaffold matrix that can be seeded with appropriate cell types and support their respective characteristic/specific cell functions. Each tissue has a specific chemical and structural composition that can be selected to support certain tissue engineering approaches [62]. Nevertheless, finding a sufficient tissue source with the necessary properties for the desired application can be

difficult. Presently, clinical products like bioprosthetic heart valves, skin grafts, demineralized bone grafts, and acellular biological meshes, have been successfully used in millions of patients [63–65].

Commercially available products are allogenic or xenogenic in origin. Nevertheless, xenografts may elicit significant immune response in the recipient due to differences in the primary structure of the residual proteins in the ECM [66,67]. Therefore, an appropriate source of human material without limitation in access would be beneficial. The human placenta, a clinical waste product, could solve this need for a certain range of applications.

To overcome a shortage of donor organs, the whole organ of interest should be decellularized to obtain an acellular, but complex, tissue geometry in addition to the natural vascular network, which can be connected to the host circulation at the time of implantation [41]. However, numerous challenges in the field of whole organ engineering remain, including the decision of the organ donor source, the ideal decellularization and recellularization procedures, and the establishment of an appropriate ex-vivo bioreactor system, among others [62].

In this work, we propose that blood vessels isolated from the placenta chorion can be used as small diameter vascular grafts. Compared with other research groups that use various origins for vascular tissues and processed them with different decellularization and recellularization techniques (Table 1), we are the first group to describe the use of arteries isolated from the placenta chorion.

2.1.8 Re-endothelialization of vascular tissue

Various cell seeding techniques have been established over the past decades, but no efficient seeding technique with an adequate clinical applicability has been developed [68]. After characterization of the decellularized grafts, including biocompatibility studies, a re-endothelialization of the decellularized grafts prior to an *in vivo* application could make the tissue-engineered blood vessels more favorable for clinical applications [69]. However, correlations between the cell number of reseeded cells and results

in long-term graft function have not yet been demonstrated. Many important questions, such as cell seeding efficiencies of vascular grafts or translation to clinical applications, have to be addressed in the future. Also, the use of autologous cells for reseeding techniques can extend the preparation time of vascular grafts and can cause difficulties in terms of clinical applicability [70]. Nevertheless, further progress in the field of vascular tissue engineering and future investigations to optimize long-term vascular graft patency are needed.

2.1.9 Surface modification – heparin immobilization

Improvements in the field of biomaterials and tissue engineering have led to several surface modification techniques. Synthetic biomaterials often lack potent biological activity needed for initial cell adherence and cell-scaffold mediated functions [71]. As well, decellularized biomaterials contain their own shortcomings. Hence, extensive efforts have focused on the modification of acellular matrices to enhance scaffold characteristics. A chemical immobilization of bioactive molecules should help to guide cell adhesion and provide the necessary properties [72]. In the field of small diameter vascular grafts, thrombosis and neointimal hyperplasia are the main causes of graft failure [73]. A quick re-endothelialization is necessary to regain a normal and healthy function of the graft [74]. Therefore, a surface modification with heparin can improve the qualities of the graft and serve two purposes: a reduction of thrombogenicity and to provide a substrate for heparin-binding factors. Heparin is a well-known and highly prescribed anti-coagulation drug. It consists of highly sulfated linear polysaccharides. The mechanism that induces anti-coagulation is an interaction of heparin with two serine inhibitors, anti-thrombin III (AT III) and factor Xa. Due to a conformation change of AT III, additional bindings of serine proteases are accelerated, which prevents blood coagulation [75]. To create a nonthrombogenic luminal surface with positive healing characteristics, decellularized blood vessels can be chemically cross-linked with heparin molecules. The bound heparin should reduce thrombogenicity and promote cell infiltration and remodeling due to the heparin binding growth factors. These growth factors accumulate on the luminal surface after implantation [76]

2.1.10 Functional blood anticoagulation tests

Severe reactions like thrombosis or a rejection of the graft could lead to disease or even death of the recipient. Functional tests upfront to implantation can maximize the success rate of effective vessel grafts without objectionable secondary effects [76]. To prove the anticoagulant influence of heparin covalently bound to the surface of acellular vascular grafts two methods have been used in this study. Direct incubation of whole blood with heparinized vessel grafts showed a prevention of clot formation when compared to control samples that had been incubated with untreated acellular grafts. Simultaneously, a new assay has been established to evaluate the efficacy of heparinization on a rotation-thromboelastometer (ROTEM). The ROTEM instrument is a haemostasis analyzer that measures kinetic changes of the clot elasticity of whole blood samples [77]. With this instrument, normally used as monitoring tool in acute clinical situations, the thromboelastic and platelet response to biomaterials can be measured [78].

2.2 Human placenta

The mature placenta is a discoid organ with an approximate diameter of 20 cm, a thickness of 3-4 cm, and a weight of 500-600 g. On the fetal side, the approximately 50 cm long umbilical cord connects the placenta and the fetus. The main function of the placenta is to facilitate nutrient exchange between the fetus and the mother. Both mother and fetus give rise to the placenta. However, a majority of the placental tissue is composed of fetal elements [79]. More specifically, the maternal part of the placenta is bordered by connective tissue of the basal plate. From the basal plate, numerous Septa reach into the placental space and divide it into 10 to 15 lobules or cotyledons. The chorionic plate, a tissue covered with a distinctive vascular network, borders the fetal part, from where large amounts of small vascular trees, so called villi, reach into the space of the cotyledons. These dense vascular networks, including the villi, are composed of fetal origin [80].

2.2.1 Placental circulation

Placenta is a unique, highly vascularized organ that receives blood from both circulatory systems, the mother and the fetus [81]. Scores of villi are connected to the basal plate and the septa. This allows the delivery of nutrients between the mother and the baby during pregnancy. Maternal blood flows into the intervillous space, small gaps between the villi and the basal tissue. From there the blood is carried through the capillaries of the villi to the embryo by the small vessels of the chorionic plate and the umbilical vein [80]. Blood of low oxygen content flows back through two umbilical arteries into the placenta tissue to the villi and is loaded with nutrients and oxygen before it closes the circle and flows back to the fetus.

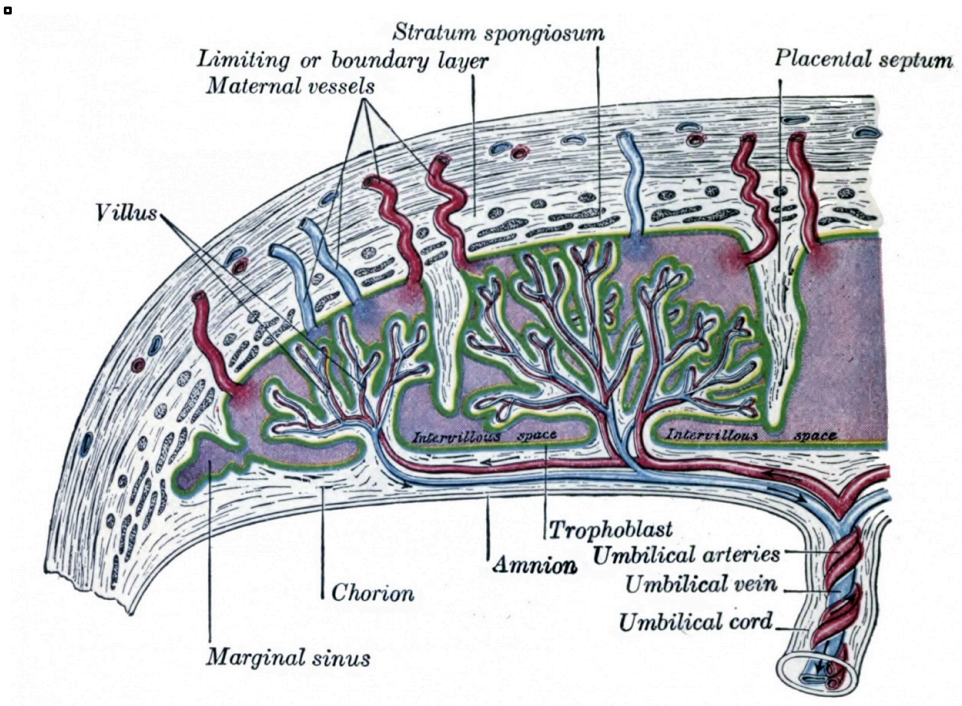

Figure 5: Schematic of placenta, longitudinal section [80]. Fundamental structures are visible: the umbilical cord with its vasculature, the amnion, the chorionic plate, the multi-branched villus reaching into the intervillous space, the placental septum, and the basal plate including the maternal vessels filling the intervillous space with the mother's blood.

2.2.2 Human placenta material as tissue source

There are approximately 5 million births in Europe every year (statista.com) and evidence has been accumulated over the last decades that suggests placenta tissues have clinical benefits in a wide range of wound repair and surgical applications [82]. In particular, the amniotic membrane showed superior therapeutic benefits and has been successfully used in numerous clinical applications. From the beginning of the 20th century there have been various reports of the use of amniotic tissue for treating skin lesions [83], surgical reconstruction of the vagina [84], burn wound dressings [85,86], abdominal wall defects [87] and for different applications in ophthalmology [88]. The amnion matrix was shown to reduce pain, decrease infection and increase the rate of re-epithelialization of the traumatized tissues. Hence, today many commercially available amniotic membrane products are on the market and there is increased interest in this material among clinicians. Nevertheless, the largest part of the material that could be utilized from the human placenta often stays unused and is deemed to be clinical waste. There is still great potential for new applications utilizing this material. Structures from the chorionic plate, isolated substances from the soft tissue of the basal plate protein isolation could all be utilized.

2.3 Placental structures

Its distinctive vasculature and the villous capillaries are the main structures of the placenta and can act as human tissue source for vascular grafts with high diversity. The umbilical cord extends from the fetal umbilicus to the chorionic plate. It consists of two arteries and one vein covered with Wharton´s jelly. At the intersection of the umbilical cord and the chorionic plate, the umbilical arteries branch to form eight or more chorionic arteries with an average of 1.5 mm in diameter that further branch to four to eight horizontal cotyledonary vessels of secondary order with an average diameter of 1 mm. For maternal-fetal exchange, as described above, the vessels divide into third-order villous branches toward the basal tissue and enter the cotyledons with about 30-60 branches in each cotyledon with capillaries of 0.1-0.6 mm diameter. The mature placenta consists of 15-28 cotyledons [81].

2.3.1 Vascular structures

Mainly one structure of the placenta tissue, the amnion, is used in diverse fields of research as well as in the clinic e.g. ophthalmology and wound treatment [89–91]. Only a few studies have taken advantage of the chorionic plate and its highly distinctive vascular structures. Former studies only described the decellularization of placental matrices as a potential scaffold for soft tissue augmentation, using the existing vasculature for delivering the decellularization agents into the tissue, but not to utilize the vasculature itself [92]. There are different approaches to developing a suitable process to facilitate decellularization of vascular structures from the placenta tissue. In the beginning of this study a few approaches were considered, decellularize the whole organ at once to utilize the microvasculature [93], to separate a segment of the chorionic plate before decellularization [92], or to isolate single blood vessels of the required shape and decellularize. After preliminary tests of all three approaches we have decided to isolate single vessels and directly decellularize them to give proof of concept in a small-scale approach. Due to a large number of branches, the average length of a single isolated vessel is about 3-4 cm without branches. However, the range of the inner diameter reaches from 4 mm down to less than 1 mm in diameter. These vascular structures are suitable to be isolated and processed for use as small diameter vascular grafts (SDVG).

2.3.2 In vivo study of small diameter vascular grafts

To confirm that the decellularized small diameter vessel grafts from the placenta chorion are suitable for further clinical applications a short implantation trial has been performed. This pre-study was carried out in cooperation with the biomedical research center of the Medical University of Vienna. The implantation of a decellularized small diameter vascular graft isolated from the placenta chorion should display the mechanical functionality and suggest the feasibility of a larger study.

2.4 Placental substances

In addition to the use of solid structures from the placenta tissue, molecular substances of the tissue can be isolated. Human placenta contains sufficient amount of collagen and other extractable proteins such as albumin [94] laminin [95], growth factors [96]. Single ECM components, like collagen or laminin can be extracted, purified, and used as biomaterials. As described above, collagen is a widely investigated and utilized ECM material with large potential in tissue engineering [36]. Therefore, an easily available source for human collagen can be beneficial. Collagen, the major protein of the ECM, was isolated using pepsin and salt fractionation [97].

2.4.1 Characterization of human collagen

In this present work human placenta collagen was characterized to confirm purity, structural conformation, and potential cytotoxicity. Circular dichroism (CD) spectra of pure collagen solution were studied to determine the secondary structure and folding properties of collagen isolated from human placenta tissue compared to commercially available collagen isolated from rat-tail and human tissue [98]. In CD-Spectroscopy the difference in absorption of left-handed circularly polarized light (L-CPL) and right-handed circularly polarized light (R-CPL) is detected while measuring solutions of proteins containing one or more light-absorbing groups (chiral chromophores). To generate specific absorption spectra for each protein composition and conformation, the CD of the molecule is measured over a range of wavelengths. A triple helical conformation of collagen molecules can be determined by specific CD spectra defined by an approximate maximum peak at 221 nm and a minimum peak at 197 nm. Characteristic CD curves display a high purity of the native conformation of the collagen [99]. Another objective of this study was to give evidence that human placental collagen supports primary cells in vitro. Collagen has been proven to support cell attachment and provides a natural environment for cells [38]. Natural morphology and proliferation can indicate that there is no cytotoxic effect caused by possible impurities or remnants of chemicals used during isolation. Therefore, primary

hepatocytes were cultivated in vitro on tissue culture plates coated with placental collagen.

2.5 Vascularization strategies

A sufficient vascularization of engineered tissues *in vitro* or *in vivo* represents a key challenge in tissue engineering and regenerative medicine. Functional scaffolds repopulated with cells are often limited in size due to insufficient nutrient supply and the elimination of toxic waste products [100]. In nature a distinctive vasculature meets these demands. Strategies to overcome these limitations are numerous. Hence, there are many different strategies to overcome limitations of an insufficient vasculature in engineered tissues. Host cells may achieve vascularization after implantation triggered by scaffold functionalization. Incorporation of angiogenic growth factors [101,102] or other stimuli mediate ingrowth of newly formed blood vessels into implanted tissue [103]. However, a more rapid nutrient supply of tissue constructs may be achieved by inosculation [104]. This means that a pre-formed vasculature in the scaffold has to accelerate functional anastomosis with the host vasculature instead of performing a time-consuming ingrowth of vasculature. There have been estimations that the physiological growth rate of microvessels is about 5 µm/h [105,106]. The strategy of inosculation has promoted the development of prevascularization approaches in the field of tissue engineering. An *in vivo* prevascularization approach is to implant the scaffold in a tissue other than the defect site, stimulating vascularization. After the scaffold has established a sufficient vascularization, it may be transferred into the final defect site [107]. Despite the advantage of a natural vascularization, this method requires multiple surgical interventions that may cause postoperative complications. For *in vitro* prevascularization, scaffolds are seeded with relevant cell types (i.e. endothelial cells, mural cells, progenitor cells and tissue-related cell types) and cultured *in vitro* with the purpose of building three-dimensional (3D) vascularized structures prior to implantation [108]. However, due to the lack of microsurgical connections to the host vasculature, perfusion is slower than in the in vivo prevascularization [109]. In this study, we followed a new dual-level strategy to create *in vitro*

prevascularized tissues using endothelial cells, combined with larger acellular blood vessels to provide a microsurgical connection site for the scaffold. Decellularized blood vessel matrix was used for EC integration, to support new micro vascular structure formation and provide connection sites for anastomosis. (Figure 6). Preliminary experiments of the dual level approach were performed in this study. After an initial recellularization of decellularized blood vessel pieces with endothelial cells, the tissue was embedded into a 3D fibrin matrix and mixed with ASCs to initiate a 3D co-culture system. The experiment demonstrated tube formation from endothelial cells reseeded to decellularized blood vessel scaffolds.

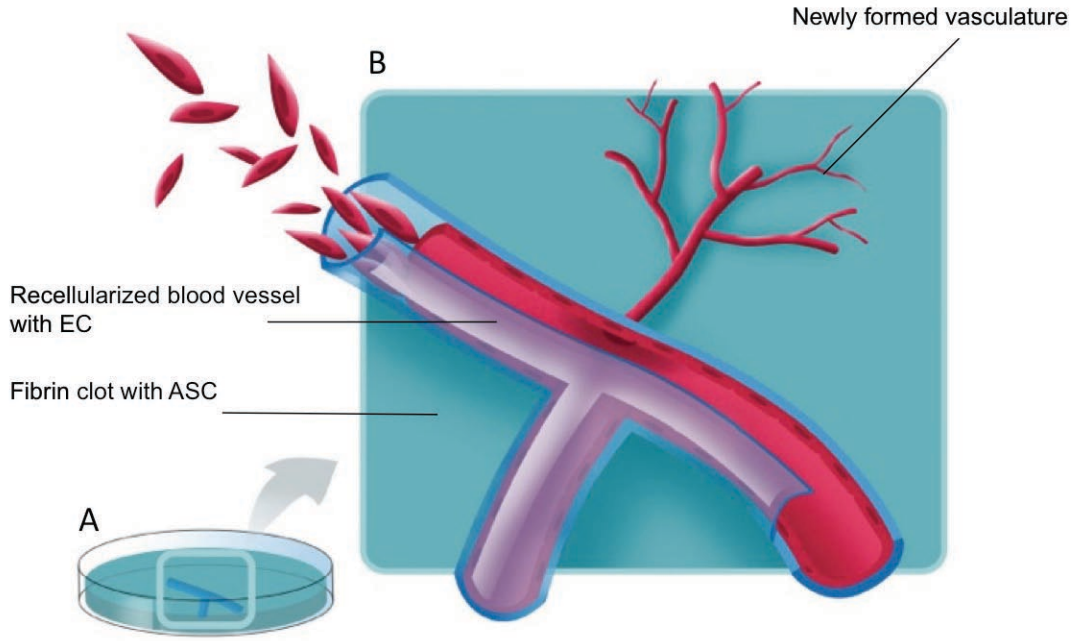

Figure 6: Graphical concept of the dual level approach to create prevascularized scaffolds for tissue engineering. A decellularized small diameter blood vessel is recellularized with endothelial cells (ECs) and embedded into a fibrin matrix with adipose-tissue derived stromal cells (ASCs) to support their ability to form new micro vascular structures. (A) Overview of the blood vessel embedded in the fibrin matrix. (B) Magnification to provide insight to new formation of a vasculature.

3 Material and Methods

3.1 Placenta harvesting and preparation

The approval for the use of this material collected by the Red Cross Hospital, Linz was given by the ethics committee of Upper Austria and informed consent was obtained from the donors. During caesarian section births the placenta was extracted. Then the placental vasculature was rinsed through the umbilical vein and arteries with Phosphate Buffered Saline solution (PBS) supplemented with additional heparin (50 IU/ml) and antibiotics - 1% penicillin/streptomycin. After the removal of the blood from the vessels, the whole placenta was frozen at -20°C until further processing. All donors were serologically tested (HIV, HBV, HCV) before the material was released for further use.

3.2 Decellularization process to prepare vascular grafts

Multiple methods were utilized to determine the most appropriate decellularization process for this tissue. The method to isolate single blood vessels out of the chorionic plate (as described in chapter 3.3) was pursued. The following two sections below give a brief overview about the methods we have attempted.

3.2.1 Whole organ decellularization

The first approach utilized the existing vasculature of the placenta to perfuse the decellularization agents through the organ. Therefore, three tubes were attached to the umbilical cord vessels and the solutions were perfused into the tissue using a peristaltic pump system. Due to a long procedural duration of 9 days, the entire process was performed at 4°C to avoid quick dissemination of possible bacterial contaminations. The perfusion rate was adjusted to 25 ml/min during the day and 3-4 ml/min during the night. Initially, the tissue was rinsed with 3 liters of PBS through the umbilical vein and arteries in two batches. One time during the day and one time over night to wash out the blood. At day 2 hypertonic and hypotonic salt solutions were perfused through the tissue to expose the cells to different osmotic pressures

followed by a PBS washing step, overnight. On day 3, a gradient of 1-3% Triton X-100 solutions, supplemented with 0.2% EDTA in PBS, was used for 3 days, with PBS rinsing overnight. After the detergent treatment, intensive washing steps followed, using PBS and PBS supplemented with 1% penicillin/streptomycin. The tissue was always perfused with 3 liters during the day and 3 liters overnight utilizing the respective solution. On day nine the decellularization process reached conclusion.

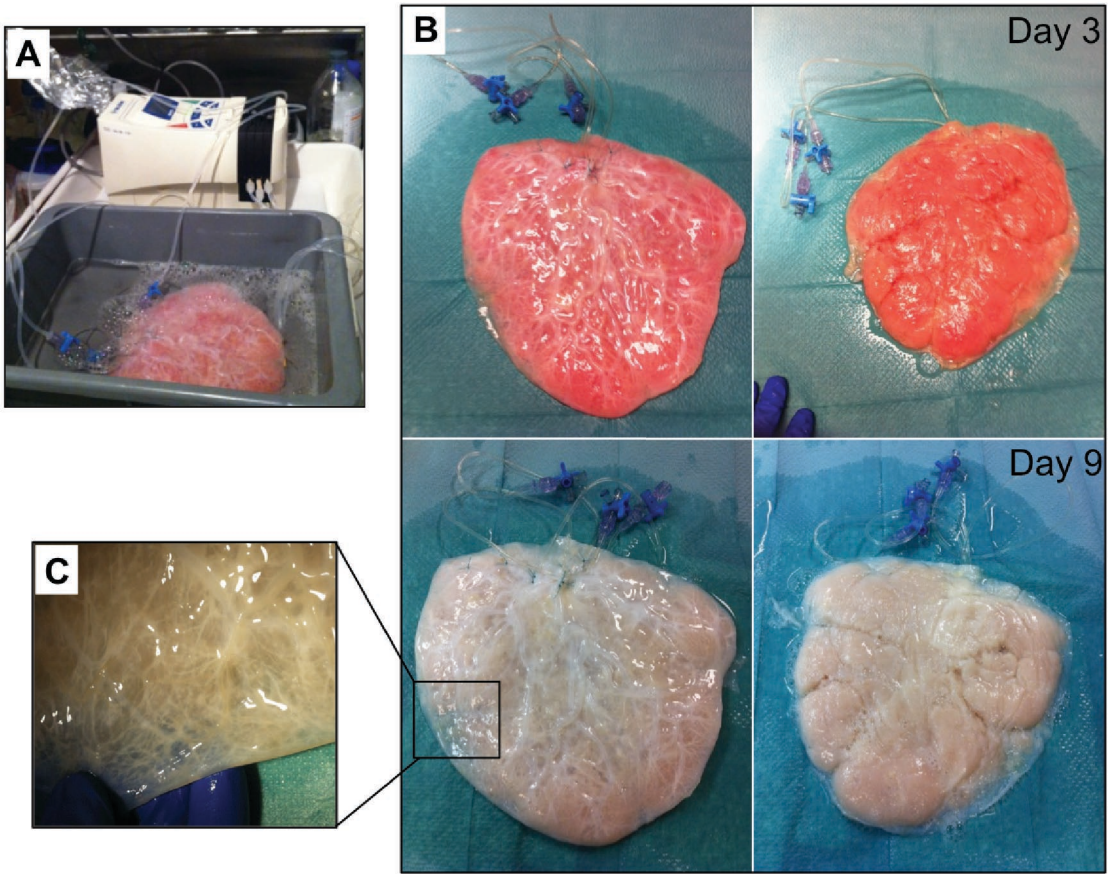

Figure 7: (A) Peristaltic pump connected to human placenta umbilical cord with perfusion tubes. (B) Top view (left) and bottom view (right) of the placenta on day 3 and day 9 of the decellularization approach. (C) Close up on the placenta tissue on day 9.

3.2.2 Chorionic plate decellularization

Separating the vasculature of the placenta chorion from the basal tissue first and then perfusing the separated tissue through the umbilical cord vessels can shorten the decellularization process. The chorion vascular tissue was placed into a self-made perfusion system and the decellularization agents were circulated. The initial pressure was measured at the inflow and adjusted between 80-120 mmHg. For each step 300 ml of the respective solution was used. The tissue was rinsed with PBS overnight. Then, osmotically active solutions were used for 2 hours each. After an additional rinsing step, 2% Triton X-100 was used for 24 hours. The tissue was rinsed with PBS and PBS supplemented with 1% penicillin/streptomycin overnight.

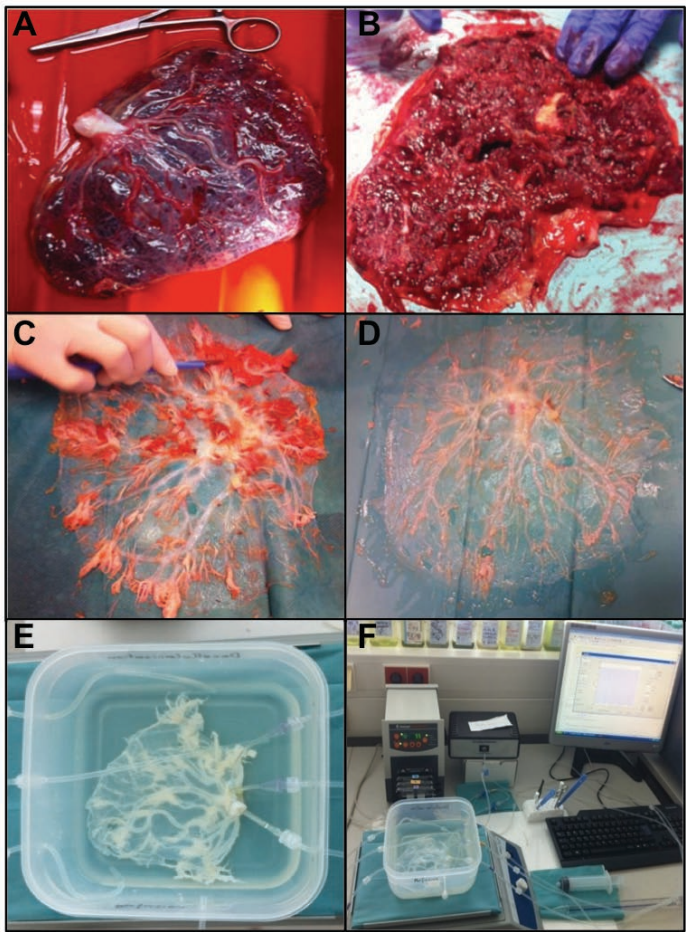

Figure 8: Preparation scheme of the chorion vasculature. (A) Placenta in top view. (B) Placenta in bottom view with the soft basal tissue facing up. (C) Peeling off the soft basal tissue from the chorion. (D) A chorion vasculature tree (E) The tissue was placed into a bowl with perfusion tubes connected to the umbilical vessels. (F) Overview of the pressure controlled perfusion system.

3.3 Single blood vessel preparation and decellularization

Before decellularization, the whole placenta was thawed and single vessel parts were isolated from the chorionic plate (Figure 9). Single arterial blood vessels, with an approximate length of 3-4 cm and with an inner diameter of 1-3 mm, were dissected, connected with a surgical thread to a 14GA BD Venflon™ (BD, Heidelberg) and stored until the following decellularization steps. The vessels were subjected to a freeze-thaw step at -80°C for 18 hours and subsequently thawed in PBS solution at room temperature (RT). The vessels were connected to a custom-made recirculating perfusion system using a peristaltic pump (Minipuls Evolution, Gilson, Middleton) for the chemical decellularization. A pressure sensor was used to measure the pulsatile perfusion and adjusted to a range of 60-80 mmHg (8000-10670 Pa). The vessels were perfused with hypertonic (1.2% NaCl) and hypotonic (0.4% NaCl) saline solutions for 30 min each to cause cell lysis. Afterwards, the samples were perfused with 1% Triton X-100 (Sigma, Vienna) and 0.02% w/w ethylene diamine tetraacetic acid (EDTA) in PBS for 24 hours at room temperature. Prior to an overnight incubation with DNase I-solution (200 IU/ml, Roche) at 4°C, the vessels were thoroughly washed with PBS for 3 hours. The DNAse I digestion was followed by several rinsing cycles with sterile PBS.

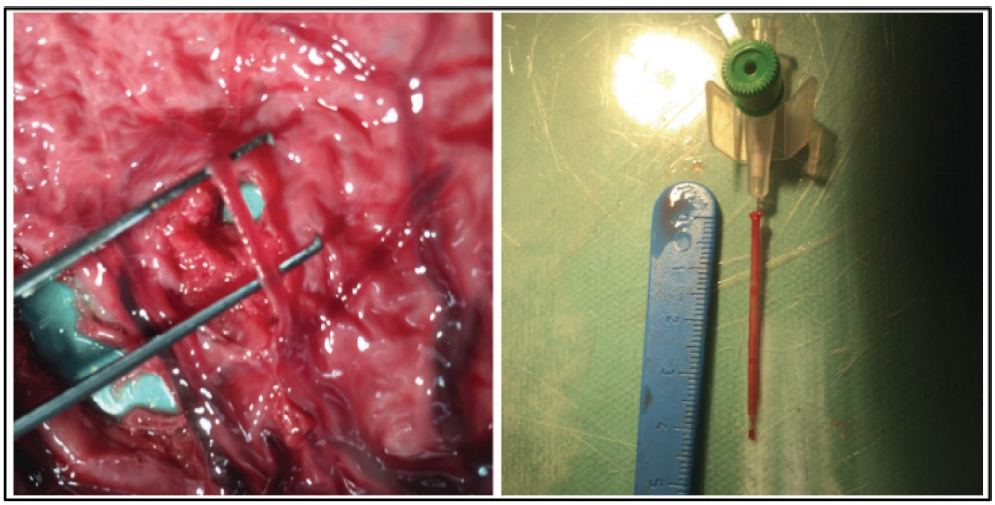

Figure 9: (A) Single arterial blood vessel isolation from placenta chorionic plate vasculature. (B) Placenta arterial blood vessel mounted on a Venflon 14GA.

3.3.1 Sterilization

For chemical sterilization of the decellularized tissue, the scaffolds were washed with a 4.8% EtOH + 0.18% (w/v) peracetic acid (PAA) aqueous solution [110], using 50 mL Falcon tubes, for 180 minutes at room temperature on a roller mixer at 30 revolutions per minute (rpm). Afterwards the vessels were rinsed with 35 ml sterile PBS 3 times for 10 min and stored in sterile PBS + 1% penicillin/streptomycin at 4°C before further use.

3.4 Characterization methods

For the quantification of the matrix components (collagen, glycosaminoglycan) and possible DNA residuals, biochemical quantification methods were used. The extract the matrix components, vascular scaffolds specimens were lyophilized, 10 mg dry ECM was weighed and digested with 3 IU/ml papain from *Papaya latex* (Sigma) in the presence of 20 mM L-Cystein (Sigma) in Papain buffer (75 mM NaCl, 27 mM Na Citrate, 0.1 M NaH_2PO_4, 15 mM EDTA, pH 6.0) at 60°C before analysis. The measured values were normalized to the dry weight of the samples.

3.4.1 Quantification of DNA residuals

The residual amounts of DNA in the decellularized scaffolds were quantified using Hoechst 33342 (Sigma). A Hoechst dye stock (10 mg/ml in dH2O) was prepared, sterilized by filtration (0.22 µm, Rotilabo, Roth, Karlsruhe) and stored at 4°C in the dark. A Hoechst dye working solution was freshly prepared and diluted with assay buffer (2 M NaCl, 50 mM NaH_2PO_4, pH 7.4) to a final concentration of 5 µg/ml. Dilutions of DNA sodium salt from calf thymus (Sigma; dissolved in ddH_2O) were used as reference. For the measurement, the samples/standards were pipetted in duplicates into 96-well black microplates (Brand, Wertheim). Then 100 µl of Hoechst working solution was added to each well, the plate was protected from light and incubated for 5 min at 37°C. After the incubation, the fluorescence was measured using an Omega POLARstar plate reader (BMG Labtech, Ortenberg) at 355 nm with a reference at 460 nm.

3.4.2 Quantification of collagen content

The collagen content of decellularized grafts and native vessel grafts was compared. Therefore the collagen was quantified using a common hydroxyproline assay as described elsewhere [111,112]. Briefly, 250 µl of papain-digested samples were put into heat resistant twist top tubes (Sorenson BioScience, Utah) and mixed with 250 µl of 12 M HCl. This results in a 6 M HCl solution which was incubated at 120°C for 20 hours for acidic hydrolyzation of the sample containing proteins. After the incubation the hydrolyzed samples were neutralized with 6 M NaOH. During the assay the standard solution was prepared by dissolving 131 mg L-hydroxyproline (Sigma) in 50 ml HCl solution, which has been neutralized with NaOH similar to the solvent matrix of the tissue sample to avoid solvent-based deviations during measurement. The L-hydroxyproline solution was further diluted (1:100) to a final concentration of 200 µM L-hydroxyproline. 60 µl of neutralized samples and of the dilution series for the standard curve were pipetted into a 96-well plate (Corning, New York). 20 µl assay buffer (0.16 M citric acid, 0.59 M sodium acetate trihydrate, 0.57 M NaOH in dH_2O, pH 6.1) and 40 µl chloramine T reagents (final conc. 15 mg/ml) were added in each well and incubated for 20 min at room temperature. After this 80 µl of 4-dimethylaminobenzaldehyde (3 M DMBA) reagent was added and incubated for 25 min at 60°C. Subsequently, the plates were immediately cooled on ice and hydroxyproline concentration was measured at 570 nm (BMG Labtech, Ortenberg). Dry weight of collagen is composed of up to 14% of hydroxyproline [113]. To determine the total collagen concentration the measured values of hydroxyproline were multiplied with a factor of 7.14.

3.4.3 Quantification of glycosaminoglycan (GAG) content

To directly measure the sulfated glycosaminoglycan (GAG) content, papain-digested samples were mixed with 1,9-dimethyl-methylene blue (DMMB, Sigma) and photometrically measured at 525 nm as described [91,114,115]. A dilution series of chondroitin sulfate C in PBS (0.5 mg/ml) was used as the standard solution. The specimens were diluted 1:40 before the measurement. 100 µl of the samples or standard dilutions were mixed with 200 µl DMMB dye

solution (46 µM DMB, 0.04 M NaCl, 0.04 M glycine in dH_2O) into flat bottom 96-well plates (Corning, New York) and extinction was measured with a plate reader (Omega, BMG Labtech, Ortenberg) at 525 nm against 590 nm as the reference wavelength.

3.4.4 Structural analysis with scanning electron microscopy

For SEM, tissue samples were fixed with 2.5% glutaraldehyde buffer solution (Merck, Darmstadt) for 2 hours at room temperature. Then the samples were dehydrated by a graded ethanol series (40%, 50%, 60%, 70%, 80%, 90%, 100%, 15 minutes each) and by increasing ethanol-hexamethyldisilazane (HMDS) series up to 100% (33%, 66%, 100% - 1 hour each) out of which the samples were air-dried. The samples were sputter coated with Pd-Au using a Polaron SC7620 sputter coater (Quorum Technologies Ltd., East Grinstead), and examined using a JEOL JSM-6510 scanning electron microscope (Jeol GmbH, Eching/Munich).

3.4.5 Histology

The samples were fixed in 4% formaldehyde solution, sodium phosphate buffered pH 6.9 (VWR) for 24 hours. Thereafter, they were washed with tap water and transferred into 50% ethanol solution for 1 hour and stored in 70% ethanol. Dehydration was completed with a further ascending series of ethanol. Then the specimens were embedded in paraffin wax, sectioned and placed on slides. Martius, Scarlet and Blue (MSB) method was chosen to stain collagen (blue), nuclei (red to black) and possible remnants of blood (fibrin red, erythrocytes yellow) (Figure 19A). Fibronectin (FN) was stained with a specific dye to evaluate the loss of this glycoprotein during the decellularization process (Figure 19B). To stain elastic fibers and nuclei an Orcein/Elastin staining was used (Figure 19C). Sections were evaluated and scanned with a light microscope (Leica DMI6000B, Leica Microsystems, Solm).

3.5 Mechanical strength testing

Two groups of vessel grafts, native and decellularized, with an outer diameter of 4 mm were radially cut into short conduits with length 7 mm. For a hoop tensile stress-strain measurement, the conduits were loaded on two steel rods and mounted in the clamps of a uniaxial mechanical testing machine (ZwickiLine, Zwick/Roell, Ulm). Specimens were tested until failure at a rate of 10 mm/min and the resulting stress-strain curves were recorded. The Young's modulus was calculated from the linear phase of the stress-strain curve of each sample.

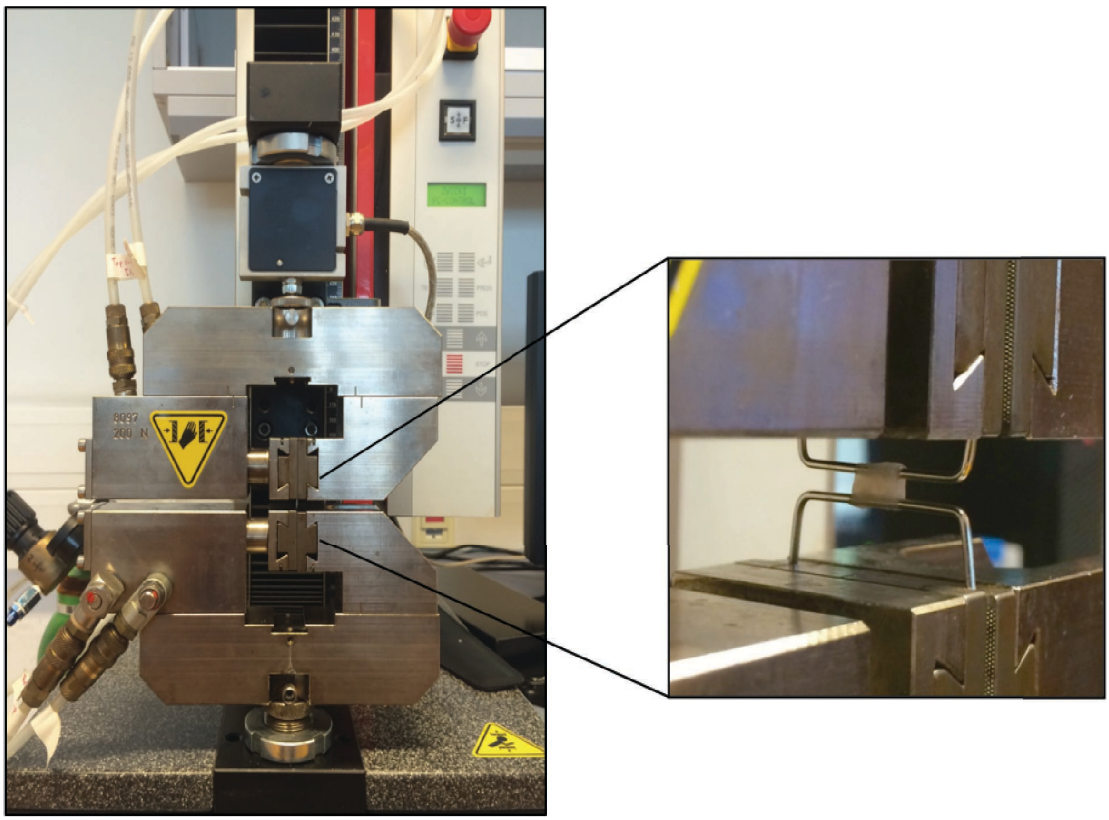

Figure 10: For mechanical testing a uniaxial mechanical testing machine (ZwickiLine, Zwick/Roell) was used. A specimen mounted on two steel rods (outer diameter 4 mm, thickness 300 µm, length 7 mm) strained until failure at 10 mm/min.

3.6 Cell isolation

Human umbilical vein endothelial cells (HUVEC) were either purchased (Lonza, Basel) or isolated as previously described [116]. For HUVEC isolation, an approximately 15 cm long piece of the umbilical cord was rinsed with PBS from the outside and through the vein to remove the blood. This was repeated until the PBS ran clear. At the same time the cord was checked for damage, e.g. needle or clamp marks. Only undamaged parts of the cord could be used for the isolation and were put into a 150 mm petri dish. One end of the cord was closed with a clamp, then the umbilical vein was filled with pre-warmed, filtered, and sterilized collagenase solution (100 mg/ml, 10-15 ml). Then the other end of the cord was clamped closed. The collagenase filled vein was transferred into a sterile pre-warmed PBS solution and incubated for 7-10 minutes at 37°C. After incubation, the cord was returned to a clean petri dish and massaged softly to allow cell detachment. The collagenase solution with the cells was removed and transferred to a 50 ml Falcon tube. An additional 20 ml EGM-2 media was flushed through the vein and collected in the 50 ml tube. In most of the cases, a small amount of red blood cell contamination occurred, which could not be prevented but doesn't have an impact on isolation. The collected cell suspension was centrifuged for 6 min at 300 g. The supernatant was aspirated carefully and the pellet was re-suspended in 1 ml EGM-2 media. The cells were plated into a human fibronectin (hFN, 2 µg/ml) coated T25 flask and incubated at 37°C and 5% CO_2. The media was changed after one and three days. When the cells were confluent; they were passaged in a 1:4 ratio and used for surface marker characterization (FACS) or stored in EGM-2 plus 10% DMSO in liquid nitrogen until further use.

3.7 Cytotoxicity and recellularization

Human endothelial cells, isolated from the umbilical cord vein (HUVEC), were seeded on the decellularized vascular scaffolds. To achieve seeding, samples of decellularized blood vessels were opened in the longitudinal direction and small pieces, 5 x 5 mm in size, were dissected (Figure 11) and placed in a 24-well plate with the luminal surfaces up.

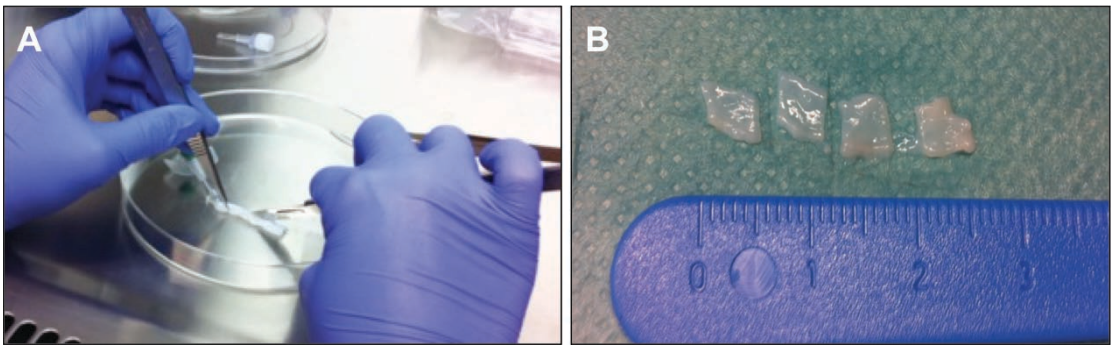

Figure 11: (A) Preparation of small vessel pieces by opening the vessel graft in longitudinal direction (B) Vascular pieces facing luminal surface up ready for recellularization

The tissue pieces were reseeded with 3 x 10^5 cells, drop-wise, on the luminal surface and pre-incubated for 30 min at 37°C, 5% CO_2 to allow optimal cell attachment before adding 1 ml endothelial cell growth medium (EGM-2, Lonza) to each well for cultivation. After 24 hours of incubation, the reseeded tissue pieces were transferred to fresh well plates. Suspension plates were used to only cultivate cells adherent to the vascular matrix and prevent adherence onto the culture plate during the recellularization. The state of recellularization was determined with live/dead staining and immunofluorescence staining after 7 days of incubation.

3.7.1 Cell viability assay

Qualitatively, the cell viability was determined with vital staining using calcein AM (Sigma) and propidium iodide (PI) as described elsewhere [117–119]. Therefore, 5 mm x 5 mm recellularized pieces (as described in 3.7) of the vessels were put into a dye solution, consisting of 3 µM Calcein AM (live) and 3 µM PI (dead) dissolved in EGM-2 expanding growth culture medium and incubated for 30 min at room temperature (RT). Samples were rinsed in PBS for 5 minutes before fluorescence was evaluated on a Leica DMI6000B epifluorescence microscope (Leica, Solms) using 492 and 517 nm filters.

3.7.2 Immunostaining CD31

For the characterization of the re-endothelialization, and to show that the cells form cell-cell contacts on the surface of the decellularized matrix, immunostaining with antibodies against CD31 was performed. The vessel pieces were fixed with 500 µl of 4% phosphate buffered formaldehyde solution for 7 hours at 4°C. After a 30 min washing step with PBS, the cells were incubated on ice with anti-CD31 antibody (1:500) (BD Biosciences, Franklin Lakes) over night. Following the incubation step, the cells were washed with ice-cold PBS/1% BSA (Bovine Serum Albumin, Lonza) solution. Directly before fluorescent microscope (Leica) analysis, the cells were additionally treated with 4,6-diamidin-2-phenylindol (DAPI) staining solution (Sigma) for one hour and rinsed again with PBS/1% BSA solution before measurement.

3.7.3 Cell surface marker characterization with flow cytometry

The expression levels of typical endothelial cell markers (CD31, CD 146, CD61, VE-Cadherin, VEGFR-2, Tie-2) were evaluated to show homogeneity of endothelial cell population after cell isolation from umbilical cord vein. Moreover, the surface marker expressions of endothelial cells cultivated on a 3D scaffold were identified. Therefore, decellularized tissue pieces were reseeded with primary endothelial cells as described in 3.7. For the control groups, 10^4 cells were seeded in each well of a 2 µg/ml human fibronectin (hFN) coated 24-well plate and incubated for 7 days, similar to the cells seeded on the tissue matrix. After one week of cultivation the cells were detached using pre-warmed accutase solution (BD Bioscience, Franklin Lakes). The cell suspensions from 8 slices were pooled and transferred to a 15 ml Falcon tube for centrifugation. Then the cell suspensions were centrifuged at 300 x g for 5 min and the cell pellets were resuspended in PBS containing 1% BSA. The antibodies used for flow cytometry analysis were either fluorescein isothyocyanate (FITC) – or phycoerythrin (PE) – conjugated and diluted in a 1:50 ratio in PBS/1% BSA. The antibodies were incubated for 30 min in the dark on ice, followed by two washing steps with PBS/1 % BSA (centrifugation for 5 min at 100 x g after each washing step). Finally the

samples were subjected to flow cytometry analysis, using a FACSCanto II flow cytometer (BD Biosciences, Franklyn, USA). Bound fluorescence was analyzed with FlowJo software (FlowJo, Oregon, USA).

3.8 Surface modification with heparin

For covalent immobilization of heparin molecules onto decellularized vessel matrix, a published protocol [76] was adapted. Briefly, up to four vessels were put into a 50 ml falcon tube, incubated with 40 ml solution, and placed on a roller mixer (30 rpm) at room temperature (RT). Initially with each step, the solutions were rinsed through the vessels using a 20 ml syringe before starting the incubation. First, the decellularized vessels were pretreated with 1 M hydroxylamine sulfate salt in aqueous solution and incubated for 16 h at room temperature. Then, the vessels were rinsed with dH_2O and incubated for 2-3 h. For covalent linkage, an EDC-heparin solution (8.35 mg/ml EDC + 180 IU/ml heparin sodium salt solution in 0.05 M HCL aqueous solution) with a pH adjusted to 1.5 was used and incubated for 48 h at room temperature. After heparin immobilization, the vessels were rinsed in PBS for one hour and then washed in PBS + 1% P/S for 4 hours. Finally the vessels were stored in sterile PBS and stored at 4°C until further use.

3.8.1 Staining of immobilized heparin with toluidine blue dye

Immobilization of heparin on the decellularized tissue matrix was determined using 0.01% toluidine dye solution. Heparin treated decellularized graft pieces were compared to untreated decellularized graft pieces as a control. Briefly, tissue pieces were incubated in toluidine blue buffer solution (20 mg toluidine blue dissolved in 200 ml of 50 mM tris-buffered saline (TBS), pH 4.5) under constant stirring at room temperature. The reaction proceeded for 20 minutes, followed by a 20 minutes long washing step using TBS buffer. After the washing step, tissue pieces were put side by side and compared.

3.8.2 Whole blood incubation for ROTEM analysis

For each specimen approximately 25 mg drained heparinized and/or untreated vessel graft pieces were weighed and collected in 1.5 ml tubes. Initially the tissue samples were washed with 500 µl isotonic NaCl solution for 60 min on an orbital shaker (Thermo mixer, 600 rpm, at room temperature) to remove possible unlinked heparin molecules from the tissue. Then, the NaCl solution was aspirated and the graft pieces were incubated with 500 µl citrated whole blood for 55 min under constant shaking (600 rpm, at room temperature). The blood was taken from healthy volunteers with no history of coagulopathy and collected in 9 ml citrate tubes for anti-coagulation. After incubation the blood was transferred to fresh 1.5 ml tubes for rotational thromboelastometry (ROTEM) measurement.

3.8.3 Rotational thromboelastometry (ROTEM) measurement

The coagulability of blood samples, incubated with heparinized grafts and non-heparinized grafts (as described above), was determined using the ROTEM delta Thromboelastometry System (TEM Innovations, Munich, Germany). This technology is used for detection and illustration of blood viscoelasticity and has been described before [77]. Briefly, for this detection method citrated blood is introduced into a pre-warmed cuvette and a cylindrical pin is immersed. Recalcification, by adding CaCl2 solution, initiates coagulation of the blood samples. Because there is only a gap of 1 mm between the pin and the cuvette, bridged by blood, any clot formation restricts the rotation of the pin and will be detected. The signals are converted into curves that show the moment of clotting, the mechanical quality of the formed clot and the possible onset of fibrinolysis. The analysis of the blood samples was performed according to the manufacturer´s protocol but was modified to display the influence of immobilized heparin molecules, bound to pieces of decellularized vascular tissue grafts, on whole blood coagulation performance.

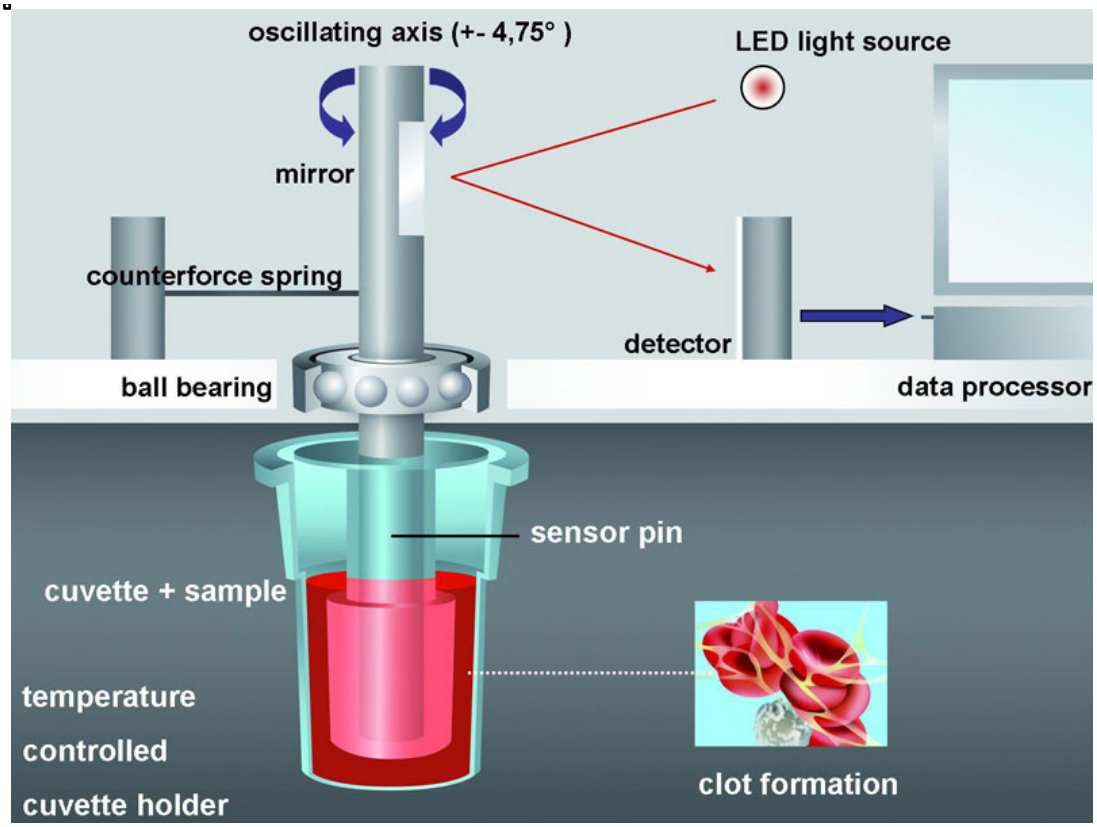

Figure 12: Principle schematic of ROTEM Thromboelastometry (TEM) detection method (source: Rotem.de). It shows the cuvette with a blood sample and the detection cascade including a LED light source reflected by a mirror on the oscillating axis of the sensor pin to create a measurable signal via the computational data processing system.

3.8.4 Clot test of whole blood

To verify the functionality of the bound heparin on the decellularized vessel grafts, vessels treated with heparin and untreated control samples were incubated with whole blood without any anti-coagulation. Therefore, the decellularized vessels were cut open longitudinally and a piece of 1 cm^2 was cut into small fragments, approximately 0.25 x 0.25 mm in size. For each sample, 8 fragments were placed into a 5 ml glass tube. Then, venous blood was taken from a healthy volunteer and 1 ml was directly pipetted into each tube. The tissue pieces were incubated on a vertical shaker (200 rpm) for 60 min at RT and visually inspected for clot formation. As a negative control whole blood was incubated without tissue fragments.

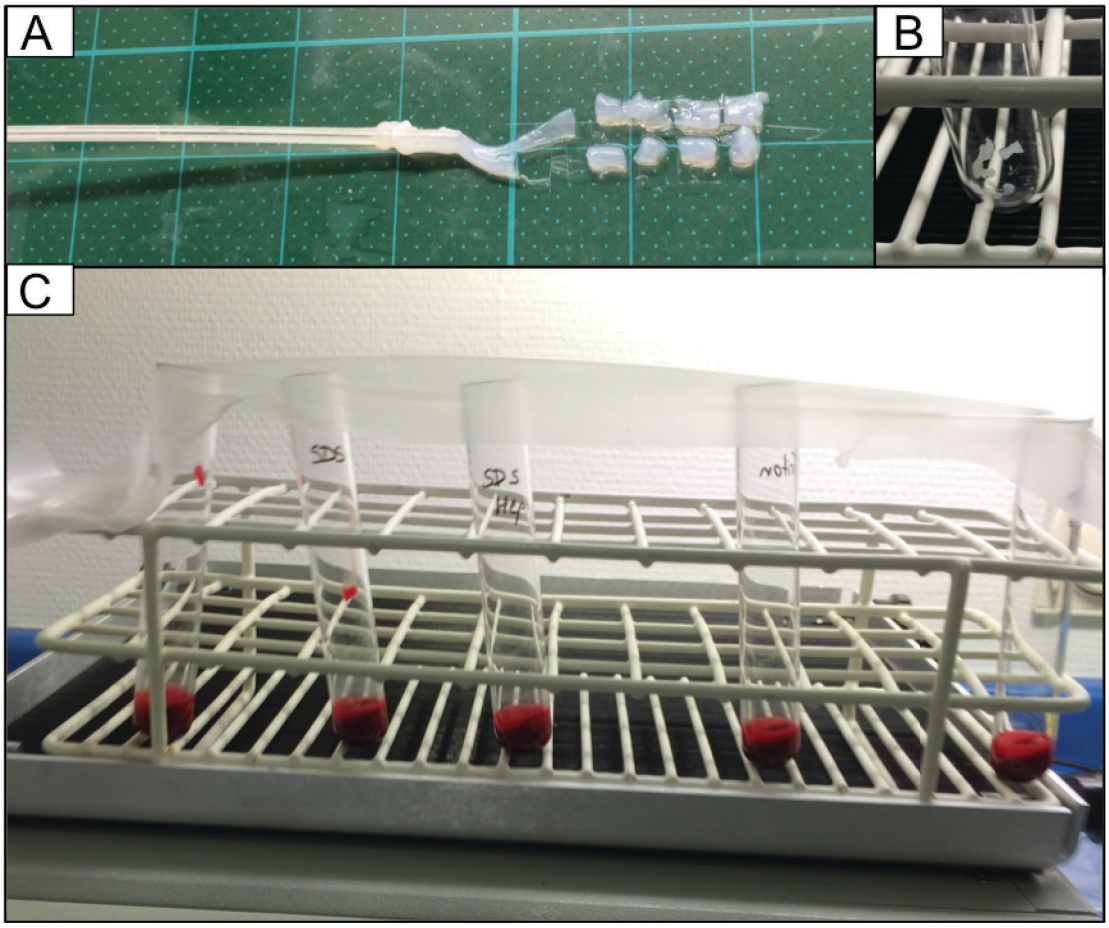

Figure 13: (A) Vessel graft on Venflon longitudinally opened and cut into small fragments (0.25 x 0.25 mm). (B) Vascular tissue fragments in a 5 ml glass tube ready for incubation. (C) Glass tubes on an orbital shaker filled with tissue fragments and 1 ml whole blood during incubation at 200 rpm at RT. The test was stopped after one our and the tubes were visually inspected for clot formation.

3.9 Preliminary study for prevascularization “dual level” approach

Before reseeding the decellularized vascular grafts were opened in a longitudinal direction and cut into small pieces 5 x 5 mm in size. The luminal surfaces of the pieces were reseeded with GFP expressing HUVEC (2 x 10^5 cells/piece) and incubated for 4 days at standard cell culture conditions. On day 4, the pieces were embedded into a fibrin matrix (5 mg fibrinogen/ml) mixed with ASCs to initiate a 3D co-culture system. The experimental groups used were: EC only on the reseeded tissue pieces embedded into a fibrin clot without additional cells, EC on the reseeded tissue pieces embedded with ASCs (1 x 10^5 cells/clot) seeded into the clot. The fibrin gel components (Baxter, Vienna, Austria) were pre-warmed to room temperature and diluted (4 U/ml thrombin 1:10 in calcium chloride (1 µM $CaCl_2$). The clots were poured on round cover- slips with a diameter of 15 mm, which were put into a 12-well plate. Cells, fibrinogen and thrombin (0.2 U/ml) were mixed to fibrin gels to at a final concentration of 2.5 mg/ml. Depending on the condition, the clot was mixed with 1x10^5 ASCs or not. After covering the reseeded tissue slices the gels of the clot were polymerized at 37 °C for 30 min. Then, the wells were filled with 1 ml EGM-2 medium each and incubated up to 14 days. Using a fluorescence microscope the GFP labeled ECs and possible vasculogenesis into the fibrin matrix was observed.

3.10 Quality control of the collagen from the placenta

Lyophilized placental collagen powder, isolated during an ongoing doctoral thesis by colleague Johannes Hackethal, was used for structural analysis, biocompatibility and viability assays of hepatic primary cells. The collagen was isolated by *pepsin digestion and precipitation* and provided for further experiments. The method has been described before [97]. The presented study only focused on the characterization of the collagen. Purity and protein conformation was determined by CD spectroscopy and an *in vitro* biocompatibility test was performed with primary hepatocytes.

3.10.1 Structural analysis using CD spectroscopy

Electronic circular dichroism (ECD) spectra were recorded (Chirascan, Applied Photophysics, Leatherhead, UK) in the far UV-region (190–240 nm) for secondary structure determination. Therefore lyophilized powder of isolated collagen type I and type III was dissolved in 0.1 M acetic acid with a final collagen concentration of 0.5 mg/ml. Human collagen I and III and rat tail collagen I/III (Sigma) were used as reference. Before measuring, the samples were put on an axial shaker for 15 minutes at 1000 rpm to ensure complete dissolution. The spectral bandwidth of the instrument was set to 3 nm and the scan speed was 10 s nm^{-1}. For temperature control the instrument was equipped with a Peltier element. The spectra were recorded at 25 °C with a path length of 1 mm. Temperature mediated unfolding was monitored at 197 nm between 25°C and 60°C (final temperature in the cuvette) with a continuous increase of temperature (1 °C min^{-1}). A wavelength scan of the sample was performed at 60 °C with the same settings as described above. The sample was cooled down to 25°C and another wavelength scan was performed to test the degree of reversible unfolding of collagen. For data analysis and conversion the Microcal origin software was used.

3.10.2 Cytotoxicity of placental collagen and cell viability

Primary rat hepatocytes were isolated from rat liver by collagenase digestion, followed by density gradient centrifugation using Ficoll [120]. The cells were seeded on human placenta collagen type I/III coated 24 well tissue culture plates. Therefore, prior to cell seeding collagen powder was dissolved in sterile PBS to a final concentration of 0.5 mg/ml and adjusted to pH 7.4. For coating, each well was filled with 200 µl collagen solution and dried inside the laminar hood. Afterwards the coated well plates were sterilized using UV light for 30 min. Then the coated wells were seeded with primary rat hepatocytes at a density of $2x10^5$ cells per well, using Dulbecco's Modified Eagles Medium (DMEM) low glucose medium (5% fetal calf serum (FCS), 1% glutamin, 1% P/S and 100 nM insulin (Huminsulin Lilly, Vienna, Austria) at 37°C and 5% CO_2 for 7 days. Gelatin (0.5 mg/ml) coated TCP were used as control, seeded with a similar number of cells per well at the same conditions.

3.10.3 Immunophenotyping of cultured primary hepatocytes

After 5 days of incubation, rat hepatocytes seeded on human placenta collagen coated tissue culture plates were stained with a mouse monoclonal antibody against cytokeratin 18 (CK18) (Millipore, Austria). The cells were washed with PBS/1% BSA once and fixated with 4% phosphate buffered formaldehyde solution (pH 6.9) for 15 min on ice. After this, the cells were washed three times with PBS/1% BSA followed by one minute incubation with 1% Triton-X100 for permeabilization of cell membranes, followed by another washing step with PBS/1% BSA. The hepatocytes were incubated with a primary CK18 antibody (1:100 dilution in PBS/1% BSA) for 60 min at RT. The cells were washed twice with PBS/1% BSA before adding the secondary antibody with another 60 min incubation at RT. Afterwards an additional staining was performed using DAPI (4',6-diamidino-2-phenylindole) solution (1µg/ml in PBS/1% BSA for 10 min at RT) to visualize the nuclei of the cells. After a final washing step the cells were covered with PBS/1% BSA in preparation for fluorescence microscopy (Leica DMI6000B, Leica Microsystems, Solm).

3.11 Statistical analysis

All calculations were performed using GraphPad software (GraphPad software, Inc., San Diego). Normal distribution of data was tested with the Kolmogorov–Smirnov test. One-way analysis of variance followed by Tukey´ s post hoc test was used to conduct statistical significance. P-values below 0.05 were considered statistically significant. All graphs in this study are shown as mean +/- standard deviation (SD).

4 Results

Of the different approaches attempted for decellularization, only the approach with isolated single blood vessels was utilized and the related detailed results are given below. A successful decellularization of single blood vessels isolated from human placenta tissue was confirmed by DNA staining and quantification methods. Furthermore, the preservation of collagen and glycosaminoglycans in the decellularized tissue was investigated. Tissue ultrastructure and histology was studied and the results are enclosed, as well as the mechanical properties. The decellularized samples were further studied regarding cytotoxicity and its suitability for reseeding with endothelial cells. Flow cytometry analysis confirmed a natural expression of typical endothelial cell surface marker genes by the endothelial cells reseeded onto decellularized vascular tissue after one week of incubation. The formation of an endothelial cell monolayer was visualized by staining of a platelet endothelial cell adhesion molecule (CD31). Vessels were prepared for a “dual-level” vascularization tests as well as for in vivo vascular grafts. It was possible to reduce the thrombogenicity by heparin immobilization onto the tissue surface, which was confirmed by in vitro blood coagulation tests.

Another goal of this study was to characterize pure human collagen, isolated from the soft tissue part of the placenta (basal tissue). The results showed high purity and a natural secondary structure of the collagen proteins, through the formation of triple helical conformations. Good *in vitro* applicability with no cytotoxic effects of the collagen was demonstrated. Therefore, primary hepatocytes were cultivated on collagen coated tissue culture plates and the retention of the natural phenotype was confirmed using a cytokeratin 18 (CK18) antibody staining.

4.1 Effective decellularization

For a quick evaluation of the decellularization procedure, a propidium iodide (PI) staining was performed to detect possible DNA residuals on the tissue. The use of a pressure controlled pulsatile pump system to perfuse the detergents through the vessels increased cell removal compared to a static system. In tissues treated with perfusion during decellularization, no detectable DNA residues could be visualized using the PI fluorescence DNA dye staining. In contrast, the control group tissue samples treated with an analogous decellularization protocol but without pulsatile perfusion, showed substantial amounts of remaining DNA fragments (Figure 14).

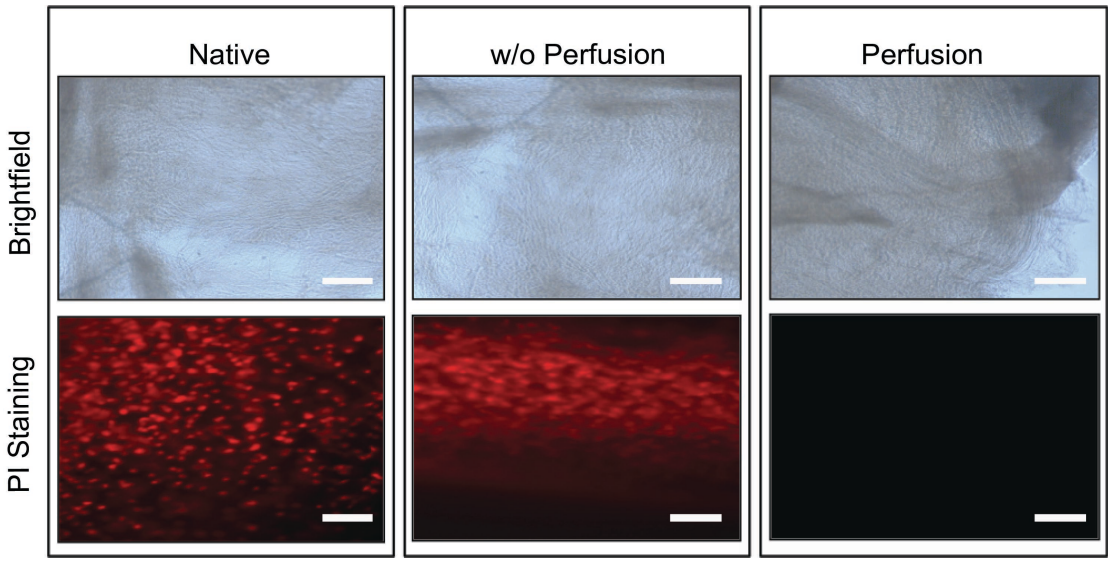

Figure 14: Comparison of native tissue and decellularized tissue using two different methods of exposure of the tissue to the decellularization agents. With the perfusion protocol all cells were removed from the tissue. However, in the tissues treated without perfusion, DNA remnants were detected (scale bars are 200 µm in size). Propidium iodide (PI) staining was used to stain possible DNA remnants in the tissues. The tissue was incubated with 3 µM PI solution for 20 minutes on ice before the images were taken. Both decellularization protocols are the same with regards to the chemicals used and the exposure times, but differ in the utilization of pulsatile perfusion. Without perfusion, the vessel tissue is floating within the reagents while with perfusion the reagents are perfused through the lumen of the vessels [121].

4.1.1 DNA reduction in decellularized tissues

Hoechst 33342 DNA staining dye was used for DNA quantification on decellularized and native tissue samples. These measurements strengthened the results from histology and PI staining, indicating successful removal of cells. In contrast to native tissue, which contained 5.74 ± 0.31 µg DNA per mg dry weight (n = 6), the decellularized tissue samples showed a significant decrease of DNA content to 0.34 ± 0.01 µg DNA per mg dry weight (n = 6).

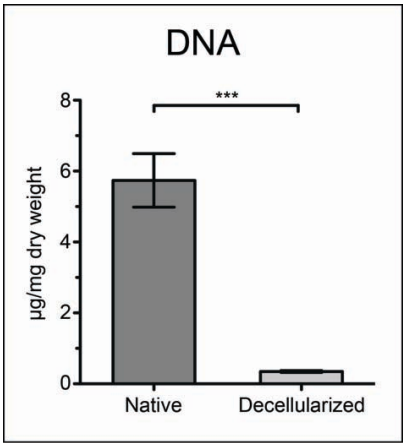

Figure 15: Quantitative determination of DNA in native and decellularized tissue samples. Data is expressed as mean values ± SD. DNA quantification showed a significant reduction of DNA content in the decellularized tissues. (n = 6, *** $p < 0.0001$) [121].

4.1.2 Preservation of collagen structures

To determine the possible loss of collagen as a result of the decellularization process, a hydroxyproline quantification assay was performed. The results, shown in Figure 16, indicate a preservation of collagen within the processed tissue. Comparing the collagen content of non-treated and decellularized samples, no significant differences could be measured. The non-treated tissue samples and decellularized samples showed a collagen content of 152.1 ± 21.8 µg per mg dry weight and 194.8 ± 15.31 µg per mg dry weight of collagen (n = 6), respectively.

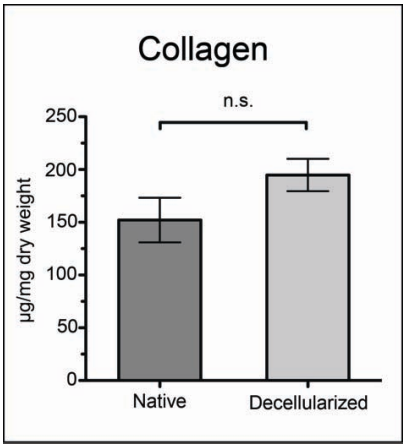

Figure 16: Quantitative determination of collagen in native and decellularized tissue samples. Data is expressed as mean values ± SD. Collagen quantification using hydroxyproline assay shows collagen content (µg/ml) (n= 6, n.s. not significant) [121].

4.1.3 Preservation of glycosaminoglycans (GAGs)

The amount of GAGs per mg of dry weight of the human vessel tissue before and after decellularization was 39.36 ± 3.83 µg per mg dry weight (n = 3) and 11.73 ± 0.66 µg per mg dry weight (n = 3), respectively. There was a significant difference in the GAG content of the fresh tissue compared to that of the decellularized tissue, indicating that approximately 30% of the GAG content could be preserved after the process.

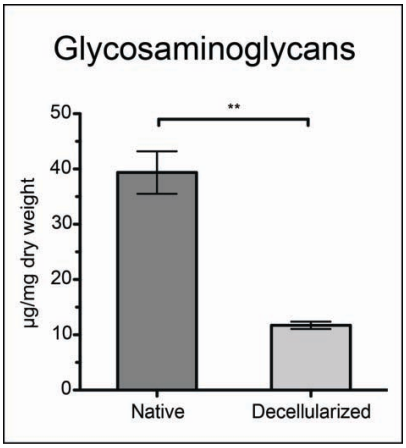

Figure 17: Quantitative determination of DNA, collagen, and glycosaminoglycans (GAG) in native and decellularized tissue samples. Data is expressed as mean values ± SD. GAG quantification shows a significant reduction with a GAG conservation of nearly 30% in the decellularized tissue (** $p < 0.001$) [121].

4.1.4 Visualization of preserved ultrastructure with SEM

Micrographs using scanning electron microscopy (SEM) allowed observation that the collagen fibers in the decellularized blood vessel were maintained, but cells were removed. Single collagen fibers were identified and appeared to be intact. No cell remnants or cellular debris was detected. In contrast, the tissue surface of the native tissue appeared covered with cells (Figure 18).

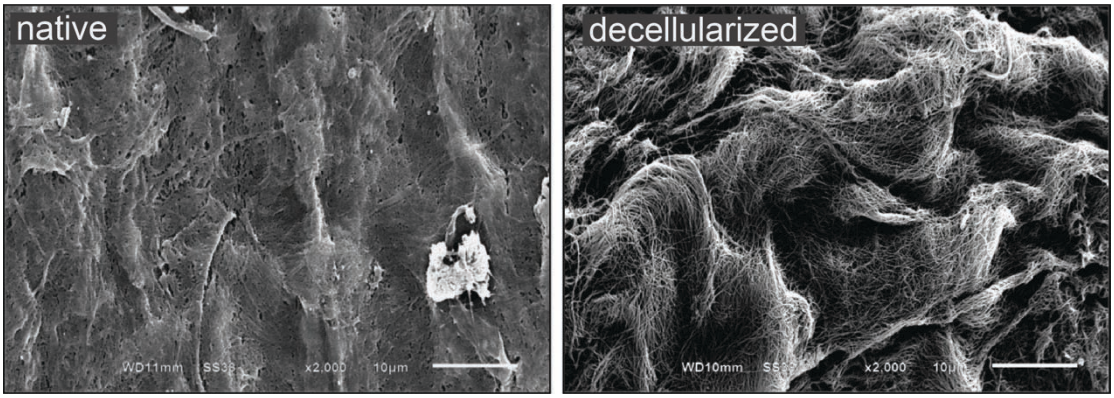

Figure 18: Scanning electron microscopy shows a preservation of the native hierarchical fiber structures in the decellularized tissues. In the decellularized tissue single collagen fibers can be identified and appear to be intact, without any cell remnants or cellular debris (scale bar 10 µm) [121].

4.1.5 Histology

A histological examination confirmed the complete decellularization of the placenta tissue. In contrast to the untreated controls, no cellular residues were detected in the decellularized vessels by Martius, Scarlet Blue (MSB) staining (Figure 19A). Furthermore, MSB staining confirmed the conservation of collagenous structures within the decellularized samples. Utilizing a specific fibronectin staining, no fibronectin could be detected in tissues after decellularization (Figure 19B). Moreover, performing an Orcein staining did not give any signal for elastin, either in native or in decellularized tissues (Figure 19C).

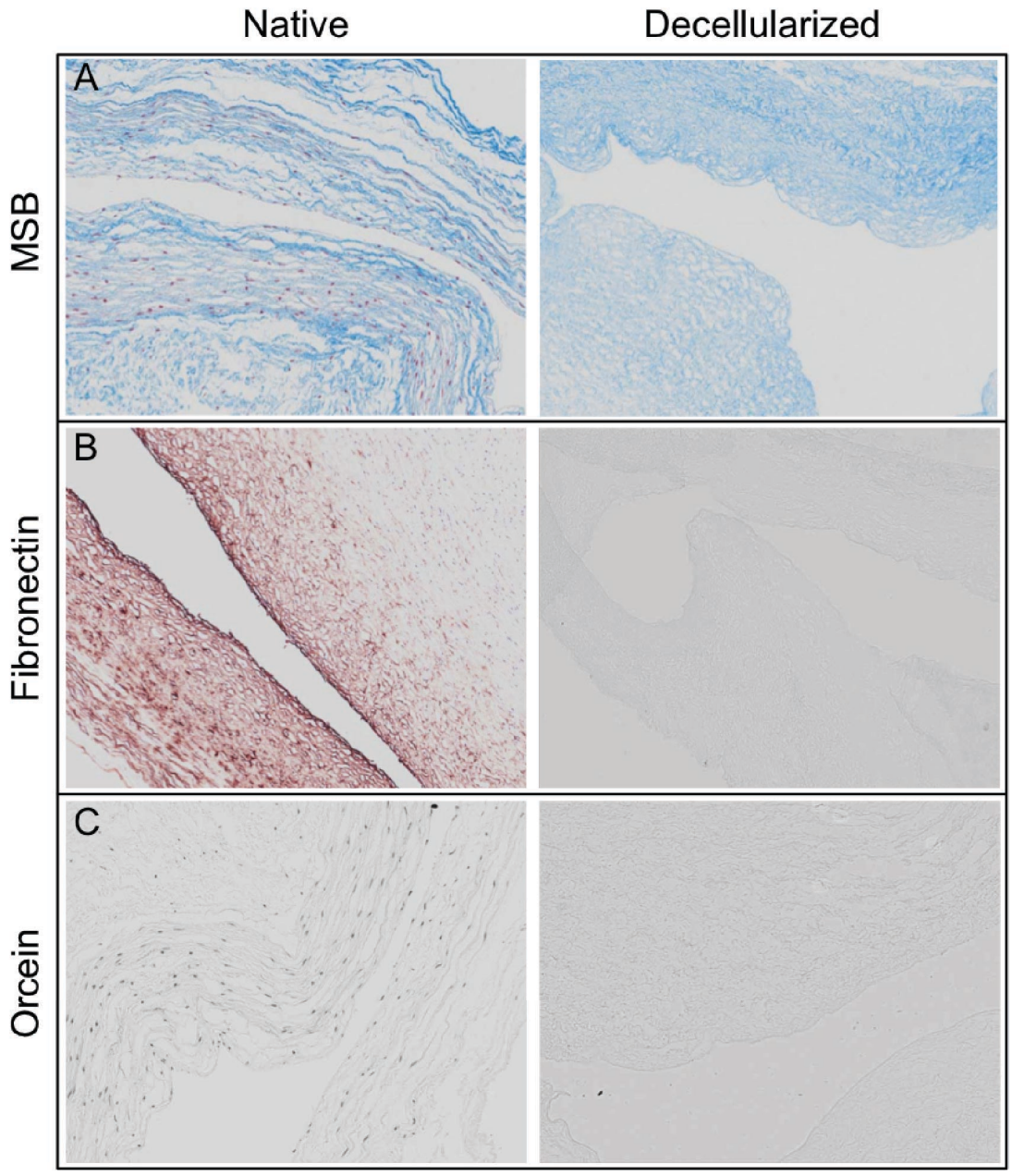

Figure 19: (A) MSB staining confirms the conservation of collagenous structures (blue) within the decellularized samples. No cellular residues (red dots) can be detected in the decellularized tissue samples. (B) Fibronectin could only be detected in samples of native tissue. There was no signal for fibronectin in decellularized tissues. (C) Elastin could not be detected in any tissue sample using an orcein/elastin staining method.

4.1.6 Mechanical properties

To determine mechanical properties of the decellularized vessels and the native controls, respective specimens were strained to failure. A preservation of 59% of the initial strength could be observed. In detail, mechanical testing revealed a significant decrease in maximum tensile strength Fmax [N] from the native tissue F_{max} = 6.83 ± 2.01 N to decellularized structures F_{max} = 4.04 ± 0.79 N (Figure 20).

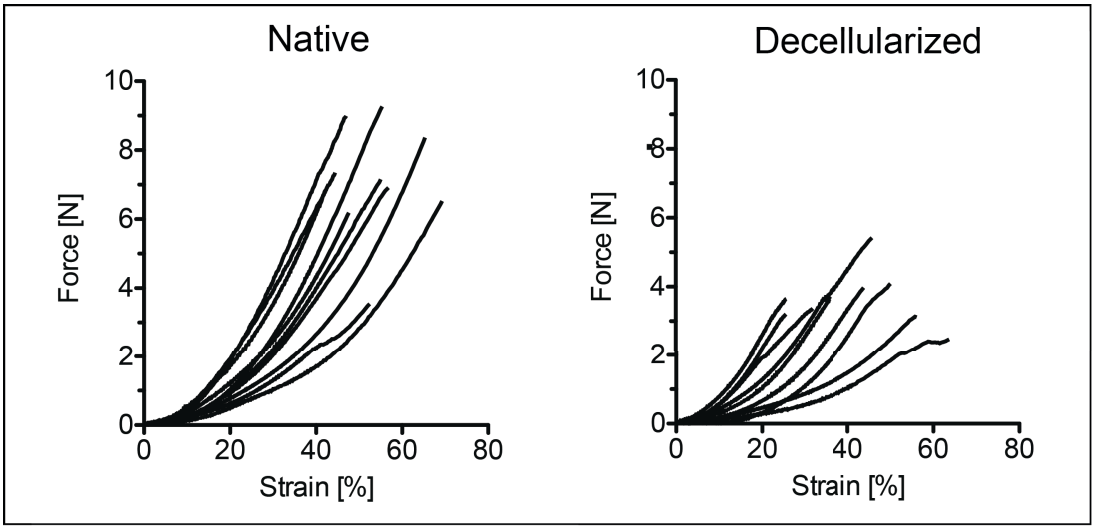

Figure 20: Stress-strain curves of native and decellularized vessels. Test specimen were mounted on two steel rods (outer diameter 4 mm, thickness 300 µm, length 7 mm) strained until failure at 10 mm/min [121].

Similarly to the straining curves, the value of the Young´s modulus (E) was reduced from native tissue to decellularized tissue with native tissue having an E = 5.36 ± 0.78 MPa and the decellularized tissue E = 3.65 ± 0.93 MPa. This corresponds to a loss of stiffness of approximately 32%. The deformation (ε) at F_{max} was ε = 54.21 ± 7.89% for the native specimens (n=9) compared to ε = 42.44 ± 12.04% for the decellularized group (Figure 21). The theoretical maximal internal pressure the vessel can withstand before mechanical failure was calculated using Barlow's formula. The theoretical burst pressure obtained using the measured ultimate tensile strength, wall thickness and outer diameter was 3185 ± 915 mmHg for the native vessels and 2056 ± 455 mmHg for the decellularized vessels.

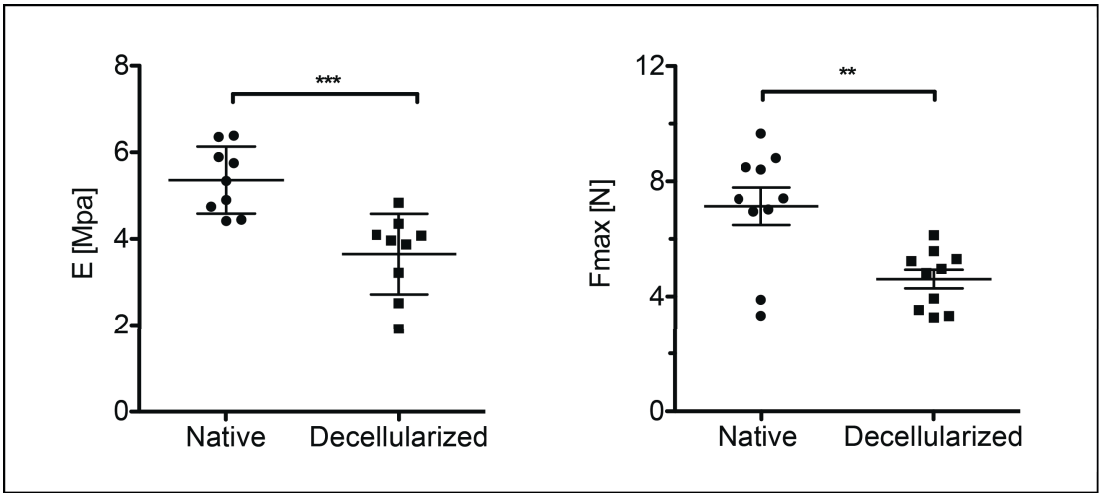

Figure 21: (left) Young's modulus (*** $p < 0.0006$) and (right) maximal force at failure F_{max} (** $p < 0.0026$) at failure [121].

4.1.7 No cytotoxicity of decellularized graft material

Residuals from chemicals, used during the decellularization process, could have a toxic effect. To show no cytotoxic effect of the material, endothelial cells (HUVEC) were seeded on the decellularized tissues and incubated for 7 days at 37°C and 5% CO_2. After recellularization, the cells started to adhere and spread on the materials immediately. On day 4, a Calcein AM staining confirmed the viability of the reseeded cells. To visualize possible dead cells a propidium iodide (PI) staining was used. No dead cells could be detected. Therefore, we observed a 100% viability of reseeded cells after one week of incubation.

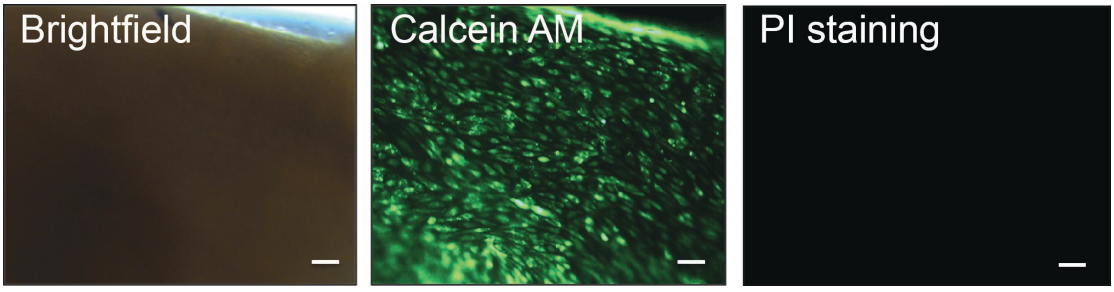

Figure 22: Endothelial cells reseeded to the surface of the acellular scaffolds and stained with Calcein AM and Propidium Iodide (PI) resulting in live cells (middle panel) green and dead cells (right panel) red. PI does not give any signal in the recellularized tissue samples (scale bars 200 µm) [121].

Endothelial cells naturally form a monolayer on vascular tissue surfaces. To confirm cell-cell contacts between the endothelial cells, the reseeded cells were stained with a specific antibody for platelet endothelial cell adhesion molecules (CD31, PECAM-1). The figure below shows a monolayer of endothelial cells reseeded on the decellularized tissue (Figure 23).

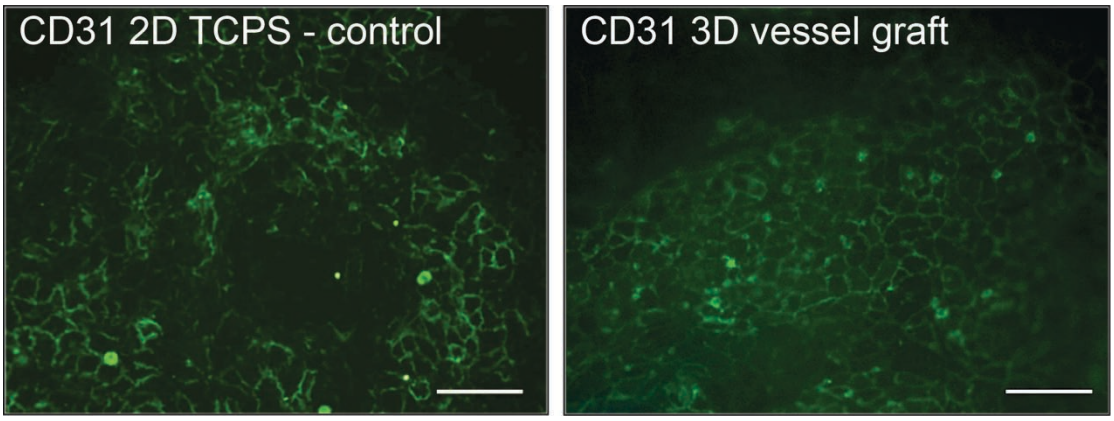

Figure 23: To visualize a monolayer formation by cell-cell contacts between endothelial cells a staining of platelet endothelial cell adhesion molecules (PECAM-1) – CD31 was performed. (left panel) Endothelial cells seeded on tissue culture plate surface as a control. (right panel) Endothelial cells seeded on acellular blood vessel lumen (vessel graft) (scale bars are 200 µm) [121].

4.1.8 Endothelial cell marker expression after 3D seeding

In order to prove that endothelial surface marker expression does not change after seeding on the decellularized scaffold, endothelial cells were reseeded on decellularized vessel matrices and incubated for 7 days in EGM-2 growth medium. As a control, cells seeded on tissue culture well plates were used. After incubation the endothelial cells were subjected to flow cytometry. For this experiment cells from two different single donors and pooled donor cells (Sigma) were used. The observed cells were positive for specific endothelial cell markers (CD31, VE-Cadherin, CD61, CD146, Tie-2, VEGFR2). The results, as shown in Figure 24, are representative from four independent experiments.

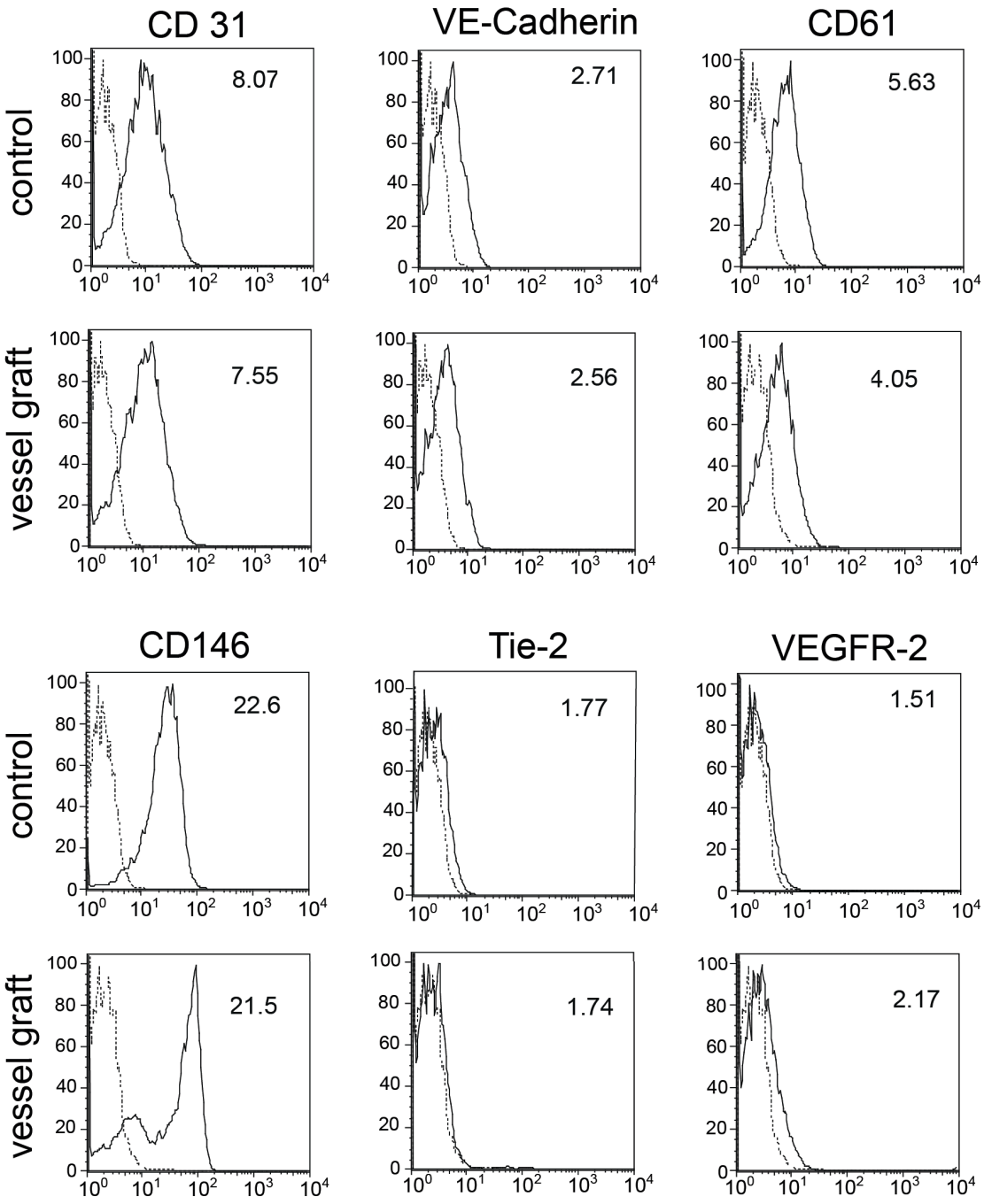

Figure 24: Expression of endothelial cell marker genes (CD31, VE-Cadherin, CD61, CD146, Tie-2, VEGFR-2) did not change of HUVECs reseeded on acellular vascular graft pieces after one week of incubation. Endothelial cells cultivated on culture plates were used as control. Representative histograms were chosen for four independent experiments. Cells from two different single donors and pooled donor cells were used [121].

4.2 Anticoagulant effect of surface heparinization

Two different in vitro experiments were used to determine the anti-coagulant effect of heparin bound to decellularized vessel grafts. To demonstrate the presence of a significant amount of covalently linked heparin molecules on the decellularized tissue surface, toluidine blue dye reacted with heparin on scaffold surfaces.

4.2.1 Immobilized heparin detected with toluidine blue dye

Heparin molecules were linked to decellularized vascular tissue surfaces using EDC crosslinking chemistry as described in 3.8. Incubation of heparinized vascular grafts with 0.01% toluidine dye solution (50 mM TRIS buffer, pH 4.5) was used to visualize a successful heparin linkage to the tissue. Representative images are shown to demonstrate binding of toluidine blue dye to heparin on treated decellularized grafts. Toluidine dye was washed off from untreated decellularized grafts during following rinsing step.

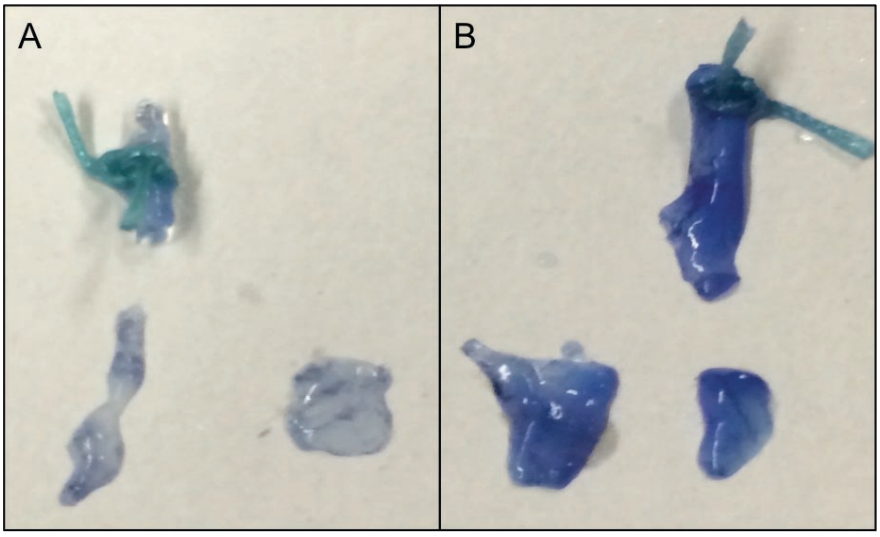

Figure 25: Decellularized vascular tissue grafts connected to tubes with surgical thread were cut open in the longitudinal direction and incubated for 20 min incubation with 0.01% toluidine dye solution. After a 20 minute washing step, (A) toluidine blue dye was washed off from untreated decellularized grafts. (B) Toluidine blue dye bound to immobilized heparin on decellularized grafts.

4.2.2 Rotation thromboelastometry showed impact on clotting time

The ROTEM data showed an inhibition of the blood coagulation of re-calcified blood samples pre-incubated with heparinized vessel grafts. The following parameters were calculated from ROTEM data. Untreated blood samples, without contact to decellularized tissue during initial incubation (Zero Ctr), showed normal clot formation with a clotting time (CT) of 504.3 ± 35.24 seconds. A comparable CT-value of 436 ± 23.67 seconds was observed in blood samples incubated with untreated tissue pieces. Blood samples incubated with heparin bound tissue did not show clot formation in 60 min.

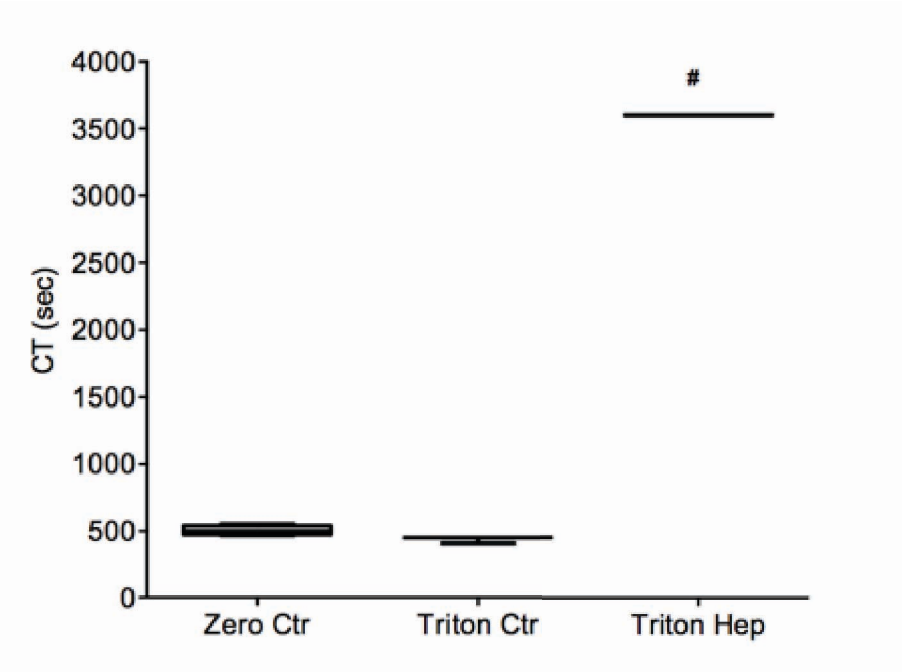

Figure 26: Graft pieces were incubated with 400 µl citrated whole blood for 55 min under constant shaking (600 rpm at RT). After incubation the blood was used for rotational thromboelastometry (ROTEM) measurement. At Zero Ctr blood only was incubated, the Triton Ctr was incubated with untreated decellularized vessel graft pieces and the Triton Hep was incubated with heparin treated decellularized vessel graft pieces. The clotting time (CT) value shows the beginning of clot formation in seconds. Blood incubated with heparin treated vessel graft pieces did not show any clot formation within 60-minute duration of the test (#).

4.2.3 Antithrombotic effect of heparinized grafts

A second experimental setup confirmed the anti-thrombogenic effect of heparinized grafts after direct incubation of fresh venous whole blood. In this experiment a visual examination for clot formation of whole blood was performed. All controls, blood only (Zero Ctr) and Triton X control (Decell Ctr), formed clots with an average clot time of approximately 15 minutes, as an exact clot time could not be measured with this setup. In contrast whole blood incubated with heparin treated vessels (Decell Hep) did not form clots during the 60-minute period of the experiment. This indicates that the heparin molecules covalently linked to the decellularized vessel grafts are anti-thrombotic. The experiment was performed in duplicates for untreated tissue control and heparinized groups and a single zero control with blood only.

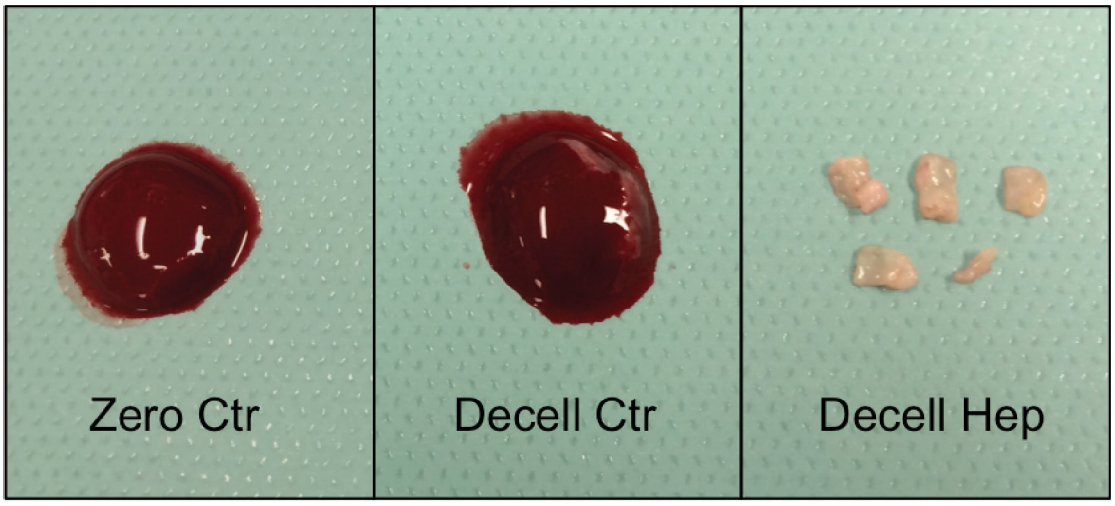

Figure 27: Blood clots of venous whole blood after incubation in glass tubes for 60 min at room temperature under constant shaking. Blood only (Zero Ctr) and blood incubated with decellularized untreated vessel graft fragments (Decell Ctr) formed stable clots during incubation. Blood incubated with fragments of decellularized heparin linked vessel grafts did not form clots (Decell Hep).

4.3 Dual level approach - preliminary study

At day 4 after recellularization of the vascular tissue a confluent cell monolayer could be observed. These homogeneously repopulated scaffolds were brought into our co-culture system and further incubated for up to 14 days at standard cell culture conditions. Recellularized tissues, embedded in a fibrin matrix with ASCs, showed vascular tube formation. Microtubes sprouted into the surrounding fibrin matrix. Between day 12 and day 14 no significant changes of the sprouts could be observed. As a control recellularized tissue pieces, embedded into a fibrin matrix without ASCs, did not start to sprout but remained in monolayer shape.

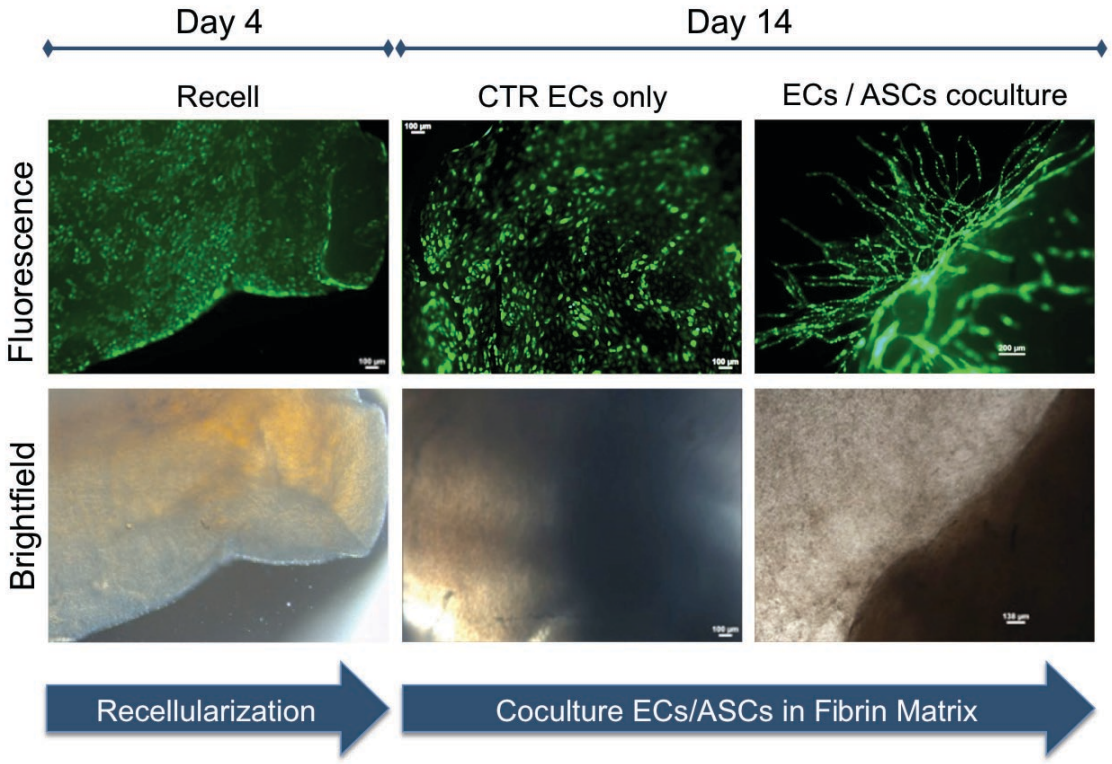

Figure 28: The decellularized tissue was successfully recellularized with endothelial cells (ECs), which displayed vascular tube formation from the scaffold in co-culture with ASCs.

4.4 Small diameter vascular graft for preclinical study

Dr. Helga Bergmeister from the Medical University of Vienna - Department of Biomedical Research, performed a pilot *in vivo* study. A 1.5 cm long decellularized and heparin treated arterial graft from human placenta chorion was implanted into a rat, replacing a piece of the aorta abdominalis. After anastomosis no additional bleeding of the graft was observed. The grafts showed good surgical applicability and sufficient mechanical strength. Based upon these preliminary results a preclinical study to further evaluate biocompatibility and functionality of the grafts is scheduled. A similar technique, but using decellularized umbilical artery grafts, has been described before [47].

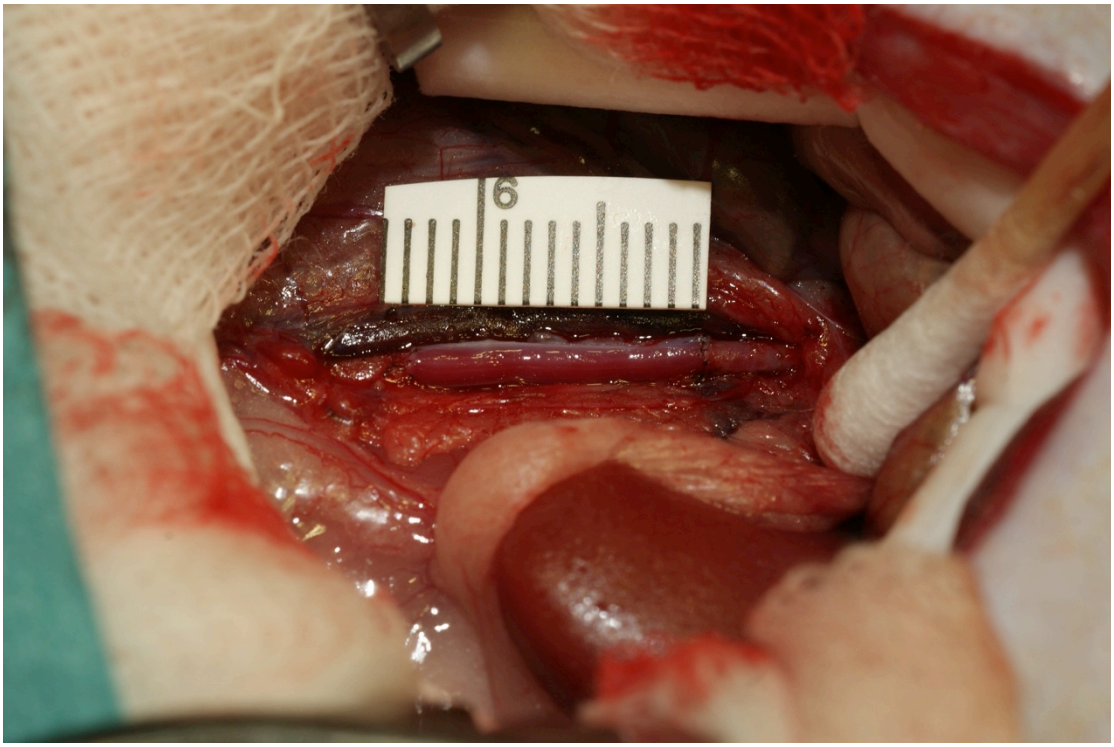

Figure 29: The picture shows a 1.5 cm long vascular graft after anastomosis to the aorta abdominalis of a rat. A good suitability of the transplant could be confirmed. No bleeding from the graft was observed.

4.5 Placenta collagen - structural analysis and cytotoxicity

Collagen isolated from human placenta matrix was characterized with CD-Spectroscopy and tested for possible cytotoxic effects by seeding primary hepatocytes on collagen coated tissue culture plates.

4.5.1 Circular dichroism

CD spectroscopy was used to determine the integrity of collagenous triple-helix and solubility of collagen samples isolated from human placenta tissue. A positive peak at 223 nm and a negative peak at 197 nm are observed for all collagen solutions used. The human placenta collagen showed a similar spectrum compared to reference samples of rat-tail collagen and human collagen type I and III (Sigma). Samples of 7 representative isolations were measured and compared to reference samples (Figure 30).

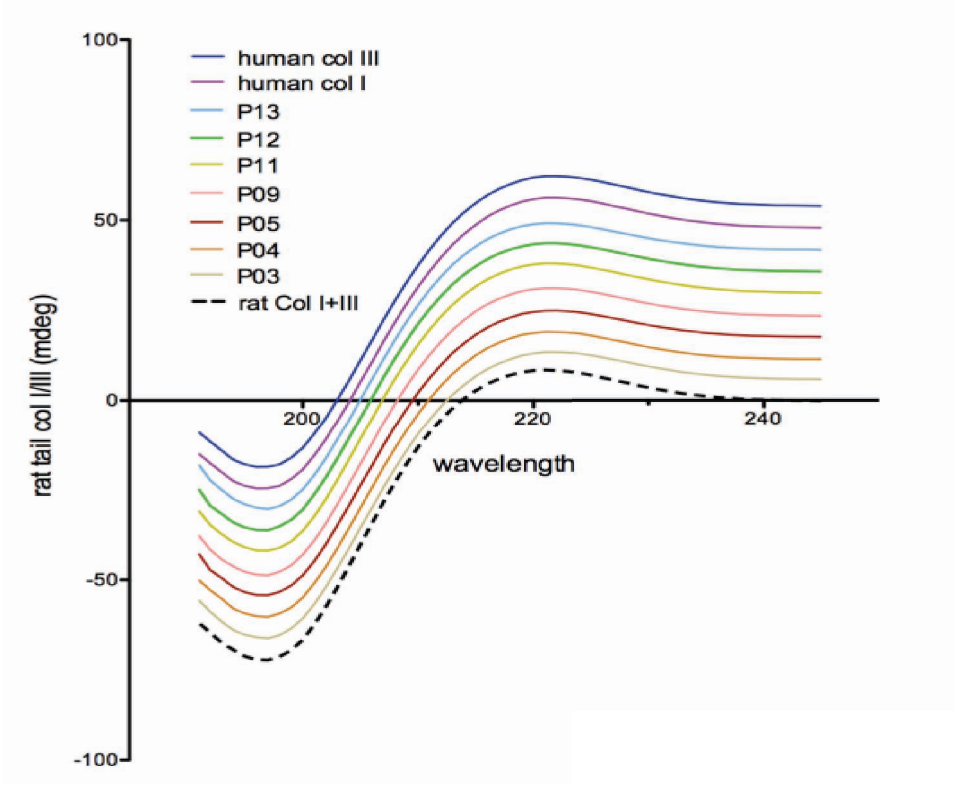

Figure 30: The positive peak at 221 nm and the negative peak at 197 nm are indicative for collagen triple helix formation. The dashed curve displays the original position of all measurements and the rat-tail collagen I/III control. The other measurements were shifted by adding 5 millidegree (mdeg) more to each sample.

4.5.2 Collagen coating supports primary cells adherence

Primary hepatocytes, seeded on coated tissue culture plates showed a higher attachment rate on placental collagen-coated wells compared to cells seeded on gelatin-coated wells. Hence, by using placental collagen coated well plates for cell cultivation, a primary culture of rat hepatocytes could be established. Furthermore, primary rat hepatocytes, seeded on placental collagen-coated wells, showed a representative phenotype for hepatocytes with the presence of CK18 on intact cell surfaces. This has been confirmed by anti-CK18 antibody staining.

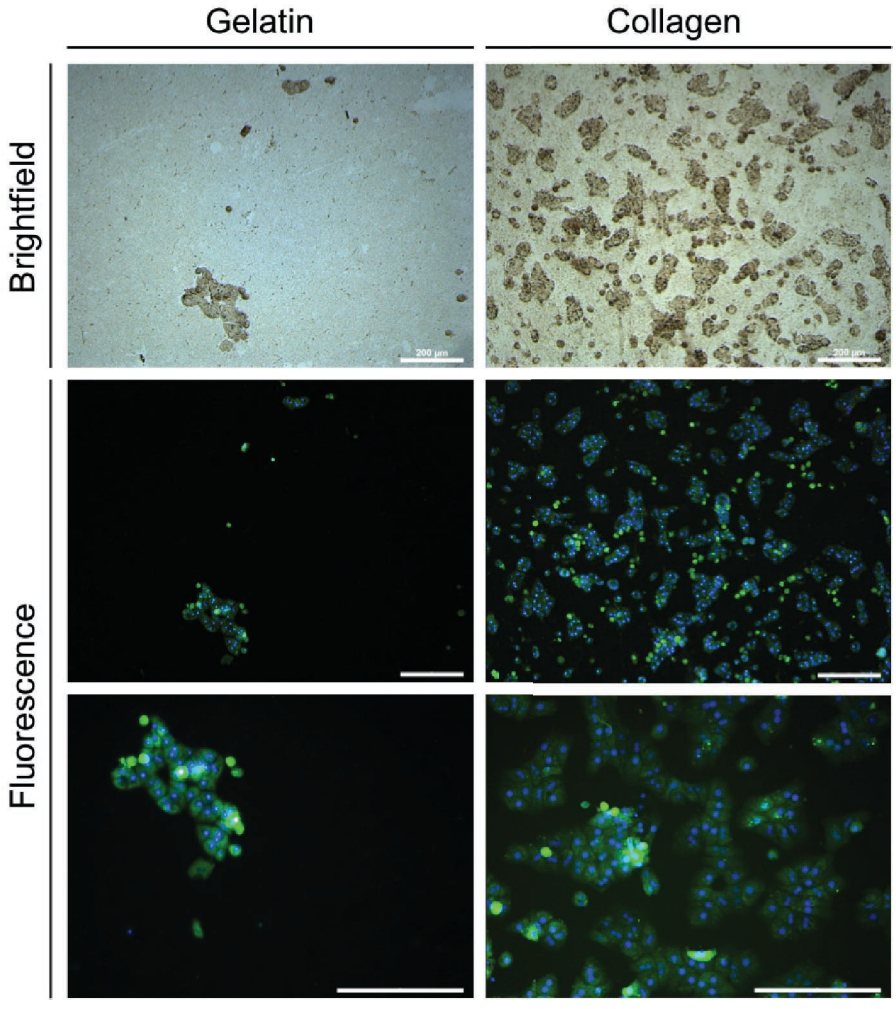

Figure 31: Brightfield and fluorescence microscopic images of primary rat hepatocytes. Placental collagen coated wells were supportive for cell attachment in contrast to gelatin coated well plates. Cultivated rat hepatocytes exhibited typical morphology and a hepatic phenotype was confirmed by CK18 antibody staining on day 6 of cultivation.

5 Discussion

The present study was designed to demonstrate the potential of the human placenta as an origin for human tissue-based material. A lack of decent human tissue sources, easy of availability in amount and quality, are often the hallmarks of decellularized tissue for tissue engineering and regenerative medicine [122,123]. The most important finding in this work was that placental vascular structures could be utilized by establishing a sufficient decellularization process. Therefore, vascular structures were isolated from the placenta chorion to be processed and potentially used as small diameter vascular grafts (SDVG) or as a basis of novel prevascularization strategies.

Besides great accessibility of the tissue, the use of human placenta as a source for biomaterials could be beneficial due to its origin and special qualities. In reviewing the literature, there is evidence that suggests more immature collagen contains fewer molecular cross-links compared to collagen structures of tissue from adult individuals. This feature should promote a rapid degradation and remodeling of the tissue in an in vivo situation. Therefore, it is a conceivable theory that fetal or neonatal tissues promote a more robust and constructive tissue remodeling than tissues from adult donors [42]. However, it was somewhat surprising that no elastic fibers were detected in arteries isolated from the placenta chorion. Performing an Orcein staining, which is sensitive for elastic fibers, did not produce any signal for elastin, either in native or in decellularized tissues (Figure 19C). Prior studies of the placental tissue have noted that no histologic markers are present that differentiate veins from arteries in histologic sections of placenta tissue and that arteries possess no elastica [79]. However, the actual positive or negative effects of these specific properties are not totally clear yet and have to be explored further.

Arteries isolated from the chorionic vasculature can be selected to have an inner diameter below 1 mm. Indeed, the length without branches of each isolated vessel is highly dependent on the donor tissue. Therefore, vessels with an average length of 4 cm can be isolated from the placenta chorion. However, in some cases, isolation of single vessels with an approximate inner

diameter of 1.4 to 2 mm and a length over 8 cm without branches, was possible. The anatomy of a monozygotic placenta can offer longer blood vessels without branches, due to its size. In 2009, there was a study about the isolation and decellularization of umbilical cord arteries [47]. The experiments showed that an isolated segment of an umbilical artery could reach a length of over 20 cm without branches. This is a clear advantage of the umbilical cord to be used as small diameter graft for bypass surgery. However, the umbilical artery always has a relatively large inner diameter of 4.5-5.5 mm. This is much bigger than the inner diameter of small diameter blood vessels isolated from the chorionic plate. Therefore decellularized arteries isolated from the human placenta chorion might be a promising material to develop vascular prostheses for smaller grafts with an inner diameter below 2 millimeters.

5.1 Decellularization protocol

In the present study we investigated different ways to gain vascular structures out of placental tissue. We have performed perfusions of the whole organ, the chorionic plate, and single blood vessels. Indeed, the placenta tissue provides a complete vasculature that allows transport of the decellularization chemicals throughout the tissue. However, the decellularization process is highly dependent upon tissue characteristics and density [62]. During our preliminary experiments, we observed that the whole organ approach requires longer exposure to chemicals, higher volumes of the chemical solutions and longer rinsing times compared to a single blood vessel decellularization. Therefore, we decided to focus on establishing a single blood vessel decellularization protocol to keep the process short in time with low concentrations of chemicals used.

The described decellularization protocol is based on the combination of a freeze-thaw (-80°C/RT) step, a short osmotic pressure treatment, with hypotonic and hypertonic salt solutions, and a chemical detergent step using 1% Triton X-100. The chemical decellularization step was performed with a computer controlled pulsatile flow perfusion of the reagents through the vessel structures. This has enabled successful decellularization of the vascular tissue using low concentrations of the detergent Triton X-100 and short

exposure times in contrast to a non-perfusion decellularization process, which had limited success. Using a pulsatile perfusion system, the exposure time of the Triton X-100 could be reduced from 48 to 24 hours compared to previously published decellularization studies [124,125]. In fact, tissue after a static decellularization process in a non-perfused control group still contained DNA fragments and cell remnants detected using a propidium iodide (PI) staining (Figure 14). A reduction of chemical exposure time can be important due to the fact that the concentration and choice of detergent for decellularization may influence the preservation of important structural and biochemical components [62].

Triton X-100 is a non-ionic detergent, which is known to be less effective than ionic detergents such as sodium dodecyl sulfate (SDS), but may be used for thin tissue structures for successful decellularization. To facilitate a rapid removal of cells, even from dense tissues, SDS may be used to yield a functional bioscaffold [126,127]. However, there are reports that ionic detergents like SDS tend to damage extracellular matrix (ECM) components, in particular, they denature proteins and cause severe structural alterations resulting in impaired mechanical and biocompatibility properties [128–130]. These alterations in the ultrastructure of the matrix [131] or residual of the detergent [132] can impair cellular repopulation of the matrix. Moreover, there have been reports that the use of SDS requires intense washing steps to prevent toxic effects due to residues [132]. These findings suggest that the use of Triton X-100 during our decellularization process was a reasonable choice to produce fully decellularized thin vascular tissue matrices.

However, it is important to bear in mind that a decellularization process is always associated with structural alterations. The effects on the extracellular matrix (ECM) and its components are dependent on the methods and chemicals used in the process. In the present study, histology and electron microscopy confirmed a full decellularization. However, our results also showed removal of some ECM components during decellularization. The amount of GAGs within the tissue was reduced to one third of the native tissue. But no significant reduction in collagen content could be detected

between the native and the decellularized vascular grafts using fluorescence quantification methods. In contrast, a trend towards increasing collagen values was observed after decellularization. Since the values were normalized to the dry weight of the samples, this mirrors the loss of cell mass and soluble proteins in the tissue.

Consequently, our decellularization process using Triton X-100 as detergent in combination with a pulsatile perfusion is suitable for an effective removal of cellular elements while preserving major components of the extracellular matrix.

5.2 Cytocompatibility of decellularized vascular tissue

In this study we used human umbilical vein endothelial cells for examination of cell-tissue compatibility. Once seeded onto the luminal surface of decellularized vessel graft pieces, endothelial cells provided endothelialization and maintained phenotypical characteristics and cell specific expression patterns, shown by a CD31 staining. CD31, also called platelet-adhesion molecule (PECAM-1), is a specific membrane bound protein of endothelial cells [133]. An additional viability staining, using Calcein AM and propidium iodide dye, showed a high viability of cells reseeded to the decellularized matrix. This strongly indicates a lack of toxic effects from possible residues of the chemicals used during the decellularization process.

Our results suggest that recellularization before implantation of the graft is possible. Benefits of cell seeding to improve graft functionality and promote patency and longevity of vascular grafts have been demonstrated before [134,135]. However, applications, including cell-seeding techniques, are associated with potentially high costs and often require several weeks or months of preparation. The development of cell-free off-the-shelf vascular grafts with good implantation qualities would be desirable. In particular, a recent study successfully showed re-endothelialization and remodeling of acellular tissue-engineered grafts in a large animal model [136]. According to the investigation heparin and vascular endothelial growth factor was bound to the tissue surface to functionalize the grafts prior to implantation.

5.3 Surface modification with heparin

In an attempt to create functionalized, cell-free vascular grafts, heparin molecules were covalently linked to the graft surface of our decellularized vessels. Following the immobilization method described previously, [76] an initial treatment with hydroxylamine sulfate creates secondary amide groups by the amination of the carboxylic groups of collagen. This provides additional binding sites for a covalent linkage of EDC-activated heparin molecules onto the pretreated collagen surface. Experiments to determine the effect of heparin-linked small diameter vascular grafts (SDVG) on whole blood coagulation have been performed in this study to possibly predict a successful outcome of an *in vivo* application of the graft. One method was adapted from a previous study using a similar protocol for graft heparinization [76]. With this method, an antithrombotic effect by direct incubation of whole blood with heparin-linked SDVG was shown (Figure 26). One disadvantage of this measurement method is the interpretation of the results. A non-visual determination makes it easier to measure exact time points of blood coagulation. Therefore, thromboelastometry was used to establish an *in vitro* functional test to measure exact time to clot formation time of whole blood.

Viscoelastic measurements of blood, such as thromboelastometry (ROTEM) are well established as a point-of-care technique in clinical diagnostics [137]. They are used to determine the real-time kinetics of clot initiation and clot formation. Beside clinical applications, ROTEM measurements also can be used for *in vivo* and *in vitro* experimental research [138,139]. One additional advantage of this method is a small sample volume of 300 µl blood per measurement. This allows the use of blood from one single donor for a wide range of measurements and eliminates the possible influence of donor variations. A similar application of ROTEM, compared to our approach, has been reported before [78]. In this previous study, ROTEM was used to evaluate the influence of nonmulberry silk biomaterials on blood coagulation. Indeed, an incubation of citrated blood with insoluble biomaterials can activate or deactivate blood coagulation components.

The results of this study demonstrated that heparin treated SDVG have an antithrombotic effect on whole blood using ROTEM. Our observations of an anticoagulative effect of heparin linked vascular graft pieces on whole blood are in agreement with an earlier conclusion that surface-immobilized heparin effectively triggers the intrinsic blood coagulation pathway and inhibits the initial contact activation enzymes by an antithrombin-mediated mechanism [101]. In previous studies it has been suggested that a chemical attachment allows the active site of heparin to remain available for binding antithrombin III even after surface immobilization [140]. However, a proper washing treatment of the tissue to remove the activating reagents is important to prevent potential toxic effect in the recipient [141]. The thromboelastic measurements, among other characterization techniques, should provide a guidance to prevent post-implant complications. A staining of the vascular grafts using toluidine blue dye showed immobilized heparin on the grafts (Figure 25). Complete coverage of heparin on the grafts is important due to the fact that heparin free spots on the surface could initiate thrombosis in clinical application.

Several reports have shown that heparin also can act as binding site for potent molecules in graft functionalization [142,143]. A graft modification with heparin bound vascular endothelial growth factor (VEGF), could be used to attract endothelial cells and enhance angiogenesis [101].

5.4 Prevascularization – a “dual-level” approach

The current study adds evidence to a possible combination of decellularized vascular tissue with endothelial cell based prevascularization strategies, here described as dual-level approach. We could show that endothelial cells reseeded onto acellular vascular matrix pieces form vessel-like structures when cultured with adipose tissue derived stromal cells (ASC) in fibrin gels (Figure 27). This dual-level approach should add strengths of cell-based and scaffold-based strategies. By providing a larger vascular network for the endothelial cells to integrate with, we want to support their ability to form new microvascular structures from the decellularized vessel.

The aim of the study was to demonstrate the cytocompatibility of the vascular matrix after decellularization and to show that it is suitable to support vascular tube formation of endothelial cells within a 3D co-culture system [144]. We used small pieces of the vascular matrix to pretest our hypothesis. The use of decellularized tubular structures for the dual-level approach requires more complex, upfront recellularization strategies [68] and will be addressed in future studies.

According to our observations, it could be argued that the tube formation of the endothelial cells is due to close physical interaction between the EC and ASC, as described in previous studies [29] rather than being induced by the acellular scaffold. However, the findings raise intriguing questions regarding a functional connection between the vascular sprouts and the decellularized scaffold matrix. In future studies, it might be possible to address these questions by using decellularized tubular grafts in combination with a perfusion bioreactor system.

5.5 Placenta substances for tissue engineering

Another objective of this study was to validate isolated collagen's native protein secondary structure and to show that there is no cytotoxic effect of human collagen isolated from human placental soft tissue on seeded cells. A native conformation of proteins is inevitable for its stability and functionality [37]. Therefore, a triple helical conformation of pure collagen extracted from human placenta tissue was examined by acquisition of circular dichroism (CD) spectra. Clear peaks, with a positive band at 221 nm and a negative band at 197 nm, confirmed that the native protein structures could be maintained during isolation [145]. The isolated collagen was compared to commercially available collagen products from other tissue sources and showed similar quality (Figure 29). Despite these promising results, questions remain. Future studies on thermo stability and refolding of denatured proteins could give insight on the behavior of the proteins, which is essential to its natural function [146]. Furthermore, an *in vitro* experiment gave first insight on excellent cytocompatibility of the isolated collagen. A cell culture approach of seeding primary hepatocytes on collagen coated tissue culture plates confirmed that

there were no toxic chemical residues from the extraction in the final collagen product.

Prior studies have noted the importance of collagen-based biomaterials, for example as 3D scaffold for cell cultures [147], or in applications for wound healing [148]. As any other material which should be used for medical applications, the placenta collagen had to undergo mandatory screening for toxicity [149] and cell-matrix interactions. Therefore, primary hepatocytes were seeded onto collagen coated well plates. We decided to use this cell type due to the fact that primary hepatocytes are anchorage-dependent cells. Cell maintenance and cell functions are dependent on adhesion of the cells to a suitable surface [150]. Moreover, a previous study described a collagen-based cell culture system suitable to create a primary hepatocyte culture model for aging studies [151]. Our results showed good biocompatibility and biofunctionality of the tested material. We observed an enhanced adhesion of primary hepatocytes on collagen-coated surfaces compared to gelatin-coated plates *in vitro*. The presence of specific surface marker proteins, cytokeratin 18 (CK18), confirmed the hepatic phenotype of the cells in culture.

6 Conclusion and Outlook

This study demonstrates the potential of human placenta material for applications in the field of tissue engineering and regenerative medicine. We demonstrated an effective method to isolate, decellularize, and preserve small diameter vessel grafts from the human placenta chorion. Due to a distinctive vasculature of the human placenta chorion, blood vessels within a wide range of inner diameter can be obtained from this tissue. In fact, it is possible to isolate single arteries down to an inner diameter of 1 mm and an average length of 4-5 cm. Therefore, to utilize these available arteries a decellularization protocol and detailed characterization methods were established. The results showed that the architecture and quality of the vascular scaffolds promotes recellularization. Human endothelial cells reseeded to acellular tissue pieces showed biocompatibility and no toxic effects from chemical residues after decellularization. In support of our dual-level prevascularization approach endothelial cells homogeneously reseeded to the blood vessel pieces showed new blood vessel formation in a 3D co-culture system. Nevertheless, further research is required to establish functional connection of the vascular sprouts to the scaffold matrix, for example by establishing a bioreactor system for adequate reendothelialization and perfusion of tubular blood vessel structures.

This work has enhanced our knowledge of the importance of having sufficient small diameter vascular grafts for clinical use. A surface modification, using chemicals to covalently bind heparin molecules to the collagenous matrix of the vascular grafts, should create the possibility to directly use the SDVG without a previous re-endothelialization. In cases of regenerative biomaterial therapies, cell-free materials can often be used “off the shelf” and are less expensive than cell-based biomaterials. An *in vivo* application of the acellular grafts will be the next step to show the suitability of this material for medical applications in human regenerative medicine.

Beside the use of placental vascular structures, pure collagen isolated from human placental soft tissue was characterized for its secondary structure using circular dichroism spectra. Primary hepatocytes were seeded on

collagen-coated plates and demonstrated a supportive environment and cytocompatibility of the isolated collagen.

This thesis should open a discussion about the wide range of possibilities for the use of placenta tissue in tissue engineering and regenerative medicine. Dependent on the objectives, different parts of the placenta tissue can be isolated and processed. Future research should therefore concentrate on the investigation of possible applications for this potent human material source.

The core data of this thesis could successfully be published in September 2015 in Acta Biomaterialia, a monthly peer-reviewed journal covering research in the field of biomedical and biomaterial science. The paper is provided in the annex.

Bibliography

[1] Eurostat. Eurostat regional yearbook 2014. http://ec.europa.eu/eurostat/

[2] Katari R, Peloso A, Orlando G. Tissue Engineering and Regenerative Medicine: Semantic Considerations for an Evolving Paradigm. Front Bioeng Biotechnol 2015;2:1–6.

[3] Nerem RM. Tissue engineering: the hope, the hype, and the future. Tissue Eng 2006;12:1143–50.

[4] Ravi M, Paramesh V, Kaviya SR, Anuradha E, Solomon FDP. 3D Cell Culture Systems: Advantages and Applications. J Cell Physiol 2015;230:16–26.

[5] Selim M, Bullock AJ, Blackwood KA, Chapple CR, Macneil S. Developing biodegradable scaffolds for tissue engineering of the urethra. BJU Int 2011;107:296–302.

[6] Mozaffarian D, Benjamin EJ, Go a. S, Arnett DK, Blaha MJ, Cushman M, et al. Heart Disease and Stroke Statistics--2015 Update: A Report From the American Heart Association. vol. 131. 2015.

[7] Huang AH, Niklason LE. Engineering of arteries in vitro. Cell Mol Life Sci 2014;71:2103–18.

[8] Teebken OE, Haverich A. Tissue engineering of small diameter vascular grafts. Eur J Vasc Endovasc Surg 2002;23:475–85.

[9] Chlupá J. Blood Vessel Replacement : 50 years of Development and Tissue Engineering Paradigms in Vascular Surgery 2009;58.

[10] Yow K-H, Ingram J, Korossis S a., Ingham E, Homer-Vanniasinkam S. Tissue engineering of vascular conduits. Br J Surg 2006;93:652–61.

[11] Dahl SLM, Blum JL, Niklason LE. Bioengineered Vascular Grafts: Can We Make Them Off-the-Shelf? Trends Cardiovasc Med 2011;21:83–9.

[12] Kakisis JD, Liapis CD, Breuer C, Sumpio BE. Artificial blood vessel: The Holy Grail of peripheral vascular surgery. J Vasc Surg 2005;41:349–54.

[13] Grainger DW. The Williams dictionary of biomaterials. Mater Today 1999;2:29.

[14] Hubbell JA. Bioactive biomaterials ok.pdf 1999:123–9.

[15] Heness G, Ben-Nissan B. Innovative bioceramics. Mater Forum 2004;27:104–14.

[16] Parida P, Behera A, Mishra SC. Classification of Biomaterials used in Medicine. Int J Adv Appl Sci 2012;1:125–9.

[17] Janik H, Marzec M. A review: Fabrication of porous polyurethane scaffolds. Mater Sci Eng C 2015;48:586–91.

[18] Lutolf MP, Hubbell J a. Synthetic biomaterials as instructive extracellular microenvironments for morphogenesis in tissue engineering. Nat Biotechnol 2005;23:47–55.

[19] Allen R a, Seltz LM, Jiang H, Kasick RT, Sellaro TL, Badylak SF, et al. Adrenal extracellular matrix scaffolds support adrenocortical cell proliferation and function in vitro. Tissue Eng Part A 2010;16:3363–74.

[20] Cheng N-C, Estes BT, Awad HA, Guilak F. Chondrogenic differentiation of adipose-derived adult stem cells by a porous scaffold derived from native articular cartilage extracellular matrix. Tissue Eng Part A 2009;15:231–41.

[21] Ross E a, Williams MJ, Hamazaki T, Terada N, Clapp WL, Adin C, et al. Embryonic stem cells proliferate and differentiate when seeded into kidney scaffolds. J Am Soc Nephrol 2009;20:2338–47.

[22] Valentin JE, Turner NJ, Gilbert TW, Badylak SF. Functional skeletal muscle formation with a biologic scaffold. Biomaterials 2010;31:7475–84.

[23] Parekh A, Mantle B, Banks J, Swarts JD, Badylak SF, Dohar JE, et al. Repair of the tympanic membrane with urinary bladder matrix. Laryngoscope 2009;119:1206–13.

[24] Burch PT, Kaza AK, Lambert LM, Holubkov R, Shaddy RE, Hawkins J a. Clinical performance of decellularized cryopreserved valved allografts compared with standard allografts in the right ventricular outflow tract. Ann Thorac Surg 2010;90:1301–5.

[25] Rice RD, Ayubi FS, Shaub ZJ, Parker DM, Armstrong PJ, Tsai JW. Comparison of surgisis??, AlloDerm??, and Vicryl Woven Mesh?? grafts for abdominal wall defect repair in an animal model. Aesthetic Plast Surg 2010;34:290–6.

[26] Brown AC, Barker TH. Fibrin-based biomaterials: Modulation of macroscopic properties through rational design at the molecular level. Acta Biomater 2014;10:1502–14.

[27] Ahmed T a E, Dare E V, Hincke M. Fibrin: a versatile scaffold for tissue engineering applications. Tissue Eng Part B Rev 2008;14:199–215.

[28] Barsotti MC, Felice F, Balbarini A, Di Stefano R. Fibrin as a scaffold for cardiac tissue engineering. Biotechnol Appl Biochem 2011;58:301–10.

[29] Rohringer S, Hofbauer P, Schneider KH, Husa AM, Feichtinger G, Peterbauer-Scherb A, et al. Mechanisms of vasculogenesis in 3D fibrin matrices mediated by the interaction of adipose-derived stem cells and endothelial cells. Angiogenesis 2014;17:921–33.

[30] Boyle J. Molecular biology of the cell, 5th edition by B. Alberts, A. Johnson, J. Lewis, M. Raff, K. Roberts, and P. Walter. vol. 36. 2008.

[31] Mouw JK, Ou G, Weaver VM. Extracellular matrix assembly: a multiscale deconstruction. Nat Rev Mol Cell Biol 2014;15:771–85.

[32] Hoganson DM, Owens GE, O'Doherty EM, Bowley CM, Goldman SM, Harilal DO, et al. Preserved extracellular matrix components and retained biological activity in decellularized porcine mesothelium. Biomaterials 2010;31:6934–40.

[33] Chun SY, Lim GJ, Kwon TG, Kwak EK, Kim BW, Atala A, et al. Identification and characterization of bioactive factors in bladder submucosa matrix. Biomaterials 2007;28:4251–6.

[34] Hynes RO. The extracellular matrix: not just pretty fibrils. Science 2009;326:1216–9.

[35] Badylak SF, Freytes DO, Gilbert TW. Extracellular matrix as a biological scaffold material: Structure and function. Acta Biomater 2009;5:1–13.

[36] Parenteau-Bareil R, Gauvin R, Berthod F. Collagen-based biomaterials for tissue engineering applications. Materials (Basel) 2010;3:1863–87.

[37] Shoulders MD, Raines RT. Collagen Structure and Stability. Annu Rev Biochem 2010:929–58.

[38] Kleinman HK, Klebe RJ, Martin GR. Role of collagenous matrices in the adhesion and growth of cells. J Cell Biol 1981;88:473–85.

[39] Pieper JS, Van Wachem PB, Van Luyn MJ a, Brouwer L a., Hafmans T, Veerkamp JH, et al. Attachment of glycosaminoglycans to collagenous matrices modulates the tissue response in rats. Biomaterials 2000;21:1689–99.

[40] Badylak SF. The extracellular matrix as a biologic scaffold material. Biomaterials 2007;28:3587–93.

[41] Gilbert TW. Strategies for tissue and organ decellularization. J Cell Biochem 2012;113:2217–22.

[42] Badylak SF. Decellularized allogeneic and xenogeneic tissue as a bioscaffold for regenerative medicine: Factors that influence the host response. Ann Biomed Eng 2014;42:1517–27.

[43] Bernard MP, Myers JC, Chu M, Ramirez F, Eikenberry EF, Prockop DJ. Structure of a cDNA for the Procw2 Chain 1983;2:1139–45.

[44] Kleinman HK, Philp D, Hoffman MP. Role of the extracellular matrix in morphogenesis. Curr Opin Biotechnol 2003;14:526–32.

[45] Keatch RP, Schor AM, Vorstius JB, Schor SL. Biomaterials in regenerative medicine: engineering to recapitulate the natural. Curr Opin Biotechnol 2012;23:579–82.

[46] Mangold S, Schrammel S, Huber G, Niemeyer M, Schmid C, Stangassinger M, et al. Evaluation of decellularized human umbilical vein (HUV) for vascular tissue engineering - comparison with endothelium-denuded HUV. J Tissue Eng Regen Med 2015;9:13–23.

[47] Gui L, Muto A, Chan SA, Breuer CK, Niklason LE. Development of decellularized human umbilical arteries as small-diameter vascular grafts. Tissue Eng Part A 2009;15:2665–76.

[48] Wilshaw S-P, Rooney P, Berry H, Kearney JN, Homer-Vanniasinkam S, Fisher J, et al. Development and characterization of acellular allogeneic arterial matrices. Tissue Eng Part A 2012;18:471–83.

[49] Gao Y, Liu F, Zhang L, Su X, Liu JY, Li Y. Acellular blood vessels combined human hair follicle mesenchymal stem cells for engineering of functional arterial grafts. Ann Biomed Eng 2014;42:2177–89.

[50] Pellegata AF, Asnaghi MA, Stefani I, Maestroni A, Maestroni S, Dominioni T, et al. Detergent-enzymatic decellularization of swine blood vessels: insight on mechanical properties for vascular tissue engineering. Biomed Res Int 2013;2013:918753.

[51] Dahl SLM, Koh J, Prabhakar V, Niklason LE. Decellularized native and engineered arterial scaffolds for transplantation. Cell Transplant 2003;12:659–66.

[52] Grandi C, Baiguera S, Martorina F, Lora S, Amistà P, Dalzoppo D, et al. Decellularized bovine reinforced vessels for small-diameter tissue-engineered vascular grafts. Int J Mol Med 2011;28:315–25.

[53] Amiel GE, Komura M, Shapira O, Yoo JJ, Yazdani S, Berry J, et al. Engineering of blood vessels from acellular collagen matrices coated with human endothelial cells. Tissue Eng 2006;12:2355–65.

[54] Pellegata AF, Adelaide Asnaghi M, Zonta S, Zerbini G, Mantero S. A novel device for the automatic decellularization of biological tissues. Int J Artif Organs 2012;35:191–8.

[55] Quint C, Kondo Y, Manson RJ, Lawson JH, Dardik A, Niklason LE. Decellularized tissue-engineered blood vessel as an arterial conduit. Proc Natl Acad Sci U S A 2011;108:9214–9.

[56] Azhim a., Yamagami K, Muramatsu K, Morimoto Y, Tanaka M. The use of sonication treatment to completely decellularize blood arteries: A pilot study. Proc Annu Int Conf IEEE Eng Med Biol Soc EMBS 2011:2468–71.

[57] Dall'Olmo L, Zanusso I, Di Liddo R, Chioato T, Bertalot T, Guidi E, et al. Blood Vessel-Derived Acellular Matrix for Vascular Graft Application. Biomed Res Int 2014;2014:1–9.

[58] Assmann A, Delfs C, Munakata H, Schiffer F, Horstkötter K, Huynh K, et al. Acceleration of autologous in vivo recellularization of decellularized aortic conduits by fibronectin surface coating. Biomaterials 2013;34:6015–26.

[59] Ott HC, Matthiesen TS, Goh S-K, Black LD, Kren SM, Netoff TI, et al. Perfusion-decellularized matrix: using nature's platform to engineer a bioartificial heart. Nat Med 2008;14:213–21.

[60] Jungebluth P, Moll G, Baiguera S, Macchiarini P. Tissue-Engineered Airway: A Regenerative Solution. Clin Pharmacol Ther 2012;91:81–93.

[61] De Kock J, Ceelen L, De Spiegelaere W, Casteleyn C, Claes P, Vanhaecke T, et al. Simple and quick method for whole-liver decellularization: a novel in vitro three-dimensional bioengineering tool? Arch Toxicol 2011;85:607–12.

[62] Crapo PM, Gilbert TW, Badylak SF. An overview of tissue and whole organ decellularization processes. Biomaterials 2011;32:3233–43.

[63] Zilla P, Human P, Bezuidenhout D. Bioprosthetic heart valves: the need for a quantum leap. Biotechnol Appl Biochem 2004;40:57–66.

[64] Zhou M, Liu Z, Liu C, Jiang X, Wei Z, Qiao W, et al. Tissue engineering of small-diameter vascular grafts by endothelial progenitor cells seeding heparin-coated decellularized scaffolds. J Biomed Mater Res - Part B Appl Biomater 2012;100 B:111–20.

[65] Smart NJ, Bryan N, Hunt J a. A scientific evidence for the efficacy of biologic implants for soft tissue reconstruction. Colorectal Dis 2012;14 Suppl 3:1–6.

[66] Spark JI, Yeluri S, Derham C, Wong YT, Leitch D. Incomplete cellular depopulation may explain the high failure rate of bovine ureteric grafts. Br J Surg 2008;95:582–5.

[67] Courtman DW, Errett BF, Wilson GJ. The role of crosslinking in modification of the immune response elicited against xenogenic vascular acellular matrices. J Biomed Mater Res 2001;55:576–86.

[68] Villalona G a, Udelsman B, Duncan DR, McGillicuddy E, Sawh-Martinez RF, Hibino N, et al. Cell-seeding techniques in vascular tissue engineering. Tissue Eng Part B Rev 2010;16:341–50.

[69] Gui L, Boyle MJ, Kamin YM, Huang AH, Starcher BC, Miller C a, et al. Construction of tissue-engineered small-diameter vascular grafts in fibrin scaffolds in 30 days. Tissue Eng Part A 2014;20:1499–507.

[70] Santos MI, Reis RL. Vascularization in Bone Tissue Engineering: Physiology, Current Strategies, Major Hurdles and Future Challenges. Macromol Biosci 2010;10:12–27.

[71] Rahmany MB, Van Dyke M. Biomimetic approaches to modulate cellular adhesion in biomaterials: A review. Acta Biomater 2013;9:5431–7.

[72] Yang H, Tan Q, Zhao H. Progress in various crosslinking modification for acellular matrix. Chin Med J 2014;127:3156–64.

[73] Kapadia MR, Popowich DA, Kibbe MR. Modified Prosthetic Vascular Conduits. Circulation 2008;117:1873–82.

[74] Deanfield JE, Halcox JP, Rabelink TJ. Endothelial function and dysfunction: Testing and clinical relevance. Circulation 2007;115:1285–95.

[75] Ren X, Feng Y, Guo J, Wang H, Li Q, Yang J, et al. Surface modification and endothelialization of biomaterials as potential scaffolds for vascular tissue engineering applications. Chem Soc Rev 2015;44:5680–742.

[76] Conklin BS, Richter ER, Kreutziger KL, Zhong DS, Chen C. Development and evaluation of a novel decellularized vascular xenograft. Med Eng Phys 2002;24:173–83.

[77] Theusinger OM, Nürnberg J, Asmis LM, Seifert B, Spahn DR. Rotation thromboelastometry (ROTEM®) stability and reproducibility over time. Eur J Cardio-Thoracic Surg 2010;37:677–83.

[78] Kundu B, Schlimp CJ, Nürnberger S, Redl H, Kundu SC. Thromboelastometric and platelet responses to silk biomaterials. Sci Rep 2014;4:4945.

[79] Benirschke K. Remarkable placenta. Clin Anat 1998;11:194–205.

[80] Gray H. Anatomy of the Human Body. 1919.

[81] Wang Y. Vascular Biology of the Placenta. Colloq Ser Integr Syst Physiol From Mol to Funct 2010;2:1–98.

[82] Silini AR, Cargnoni A, Magatti M, Pianta S, Parolini O. The Long Path of Human Placenta, and Its Derivatives, in Regenerative Medicine. Front Bioeng Biotechnol 2015;3.

[83] Trelford JD, Hanson FW, Anderson DG, Mendel V. Wound healing and the amniotic membrane. J Med 1975;6:383–8.

[84] Dhall K. Amnion graft for treatment of congenital absence of the vagina. Br J Obstet Gynaecol 1984;91:279–82.

[85] Bose B. Burn wound dressing with human amniotic membrane. Ann R Coll Surg Engl 1979;61:444–7.

[86] Gruss JS, Jirsch DW. Human amniotic membrane: a versatile wound dressing. Can Med Assoc J 1978;118:1237–46.

[87] Buck DW, Khalifeh M, Redett RJ. Plastic surgery repair of abdominal wall and pelvic floor defects. Urol Oncol 2007;25:160–4.

[88] Moore JE, Dua HS, Page a B, Irvine a D, Archer DB. Ocular surface reconstruction in LOGIC syndrome by amniotic membrane transplantation. Cornea 2001;20:753–6.

[89] Lindenmair A, Nürnberger S, Stadler G, Meinl A, Hackl C, Eibl J, et al. Intact human amniotic membrane differentiated towards the chondrogenic lineage. Cell Tissue Bank 2014;15:213–25.

[90] Faulk WP, Matthews R, Stevens PJ, Bennett JP, Burgos H, Hsi BL. Human amnion as an adjunct in wound healing. Lancet 1980;1:1156–8.

[91] Wilshaw S, Sc B, Kearney JN, Ph D, Fisher J, Ingham E. Production of an Acellular Amniotic Membrane Matrix for Use in Tissue Engineering 2006;12:2117–29.

[92] Flynn L, Semple JL, Woodhouse K a. Decellularized placental matrices for adipose tissue engineering. J Biomed Mater Res A 2006;79:359–69.

[93] Kakabadze A, Kakabadze Z. Prospect of Using Decellularized Human Placenta and Cow Placentome for Creation of New Organs: Targeting the Liver (Part I: Anatomic Study). Transplant Proc 2015;47:1222–7.

[94] Cabrera-Crespo J, Goncalves VM, Martins EA, Grellet S, Lopes AP, Raw I. Albumin purification from human placenta. Biotechnol Appl Biochem 2000;31 (Pt 2):101–6.

[95] Risteli L, Timpl R. Isolation and characterization of pepsin fragments of laminin from human placental and renal basement membranes. Biochem J 1981;193:749–55.

[96] Moscatelli D, Presta M, Rifkin DB. Purification of a factor from human placenta that stimulates capillary endothelial cell protease production, DNA synthesis, and migration. Proc Natl Acad Sci U S A 1986;83:2091–5.

[97] Quteish D, Singh G, Dolby a. E. Development and testing of a human collagen graft material. J Biomed Mater Res 1990;24:749–60.

[98] Greenfield NJ. Using circular dichroism spectra to estimate protein secondary structure. Nat Protoc 2006;1:2876–90.

[99] Kanungo I, Fathima NN, Jonnalagadda RR, Nair BU. Go natural and smarter: fenugreek as a hydration designer of collagen based biomaterials. Phys Chem Chem Phys 2015;17:2778–93.

[100] Lovett M, Lee K, Edwards A, Kaplan DL. Vascularization strategies for tissue engineering. Tissue Eng Part B Rev 2009;15:353–70.

[101] Cabric S, Sanchez J, Johansson U, Larsson R, Nilsson B, Korsgren O, et al. Anchoring of vascular endothelial growth factor to surface-immobilized heparin on pancreatic islets: implications for stimulating islet angiogenesis. Tissue Eng Part A 2010;16:961–70.

[102] Zhang N, Richter A, Suriawinata J, Harbaran S, Altomonte J, Cong L, et al. Elevated Vascular Endothelial Growth Factor Production in Islets Improves Islet Graft Vascularization. Diabetes 2004;53:963–70.

[103] Laschke MW, Harder Y, Amon M, Martin I, Farhadi J, Ring A, et al. Angiogenesis in tissue engineering: breathing life into constructed tissue substitutes. Tissue Eng 2006;12:2093–104.

[104] Laschke MW, Vollmar B, Menger MD. Inosculation: connecting the life-sustaining pipelines. Tissue Eng Part B Rev 2009;15:455–65.

[105] Cheng G, Markenscoff P, Zygourakis K. A 3D hybrid model for tissue growth: The interplay between cell population and mass transport dynamics. Biophys J 2009;97:401–14.

[106] Laschke MW, Menger MD. Vascularization in Tissue Engineering: Angiogenesis versus Inosculation. Eur Surg Res 2012;48:85–92.

[107] Kokemueller H, Spalthoff S, Nolff M, Tavassol F, Essig H, Stuehmer C, et al. Prefabrication of vascularized bioartificial bone grafts in vivo for segmental mandibular reconstruction: experimental pilot study in sheep and first clinical application. Int J Oral Maxillofac Surg 2010;39:379–87.

[108] Rivron NC, Liu J, Rouwkema J, De Boer J, Van Blitterswijk CA. Engineering vascularised tissues in vitro. Eur Cells Mater 2008;15:27–40.

[109] Tremblay P-LL, Hudon V, Berthod F, Germain L, Auger F a. Inosculation of tissue-engineered capillaries with the host's vasculature in a reconstructed skin transplanted on mice. Am J Transplant 2005;5:1002–10.

[110] Hodde J, Hiles M. Virus safety of a porcine-derived medical device: Evaluation of a viral inactivation method. Biotechnol Bioeng 2002;79:211–6.

[111] Kheir E, Stapleton T, Shaw D, Jin Z, Fisher J, Ingham E. Development and characterization of an acellular porcine cartilage bone matrix for use in tissue engineering. J Biomed Mater Res A 2011;99:283–94.

[112] Edwards CA, O'Brien WD. Modified assay for determination of hydroxyproline in a tissue hydrolyzate. Clin Chim Acta 1980;104:161–7.

[113] Colgrave ML, Allingham PG, Jones A. Hydroxyproline quantification for the estimation of collagen in tissue using multiple reaction monitoring mass spectrometry. J Chromatogr A 2008;1212:150–3.

[114] Farndale RW, Buttle DJ, Barrett AJ. Improved quantitation and discrimination of sulphated glycosaminoglycans by use of dimethylmethylene blue. Biochim Biophys Acta 1986;883:173–7.

[115] Mirsadraee S, Wilcox HE, Korossis S a, Kearney JN, Watterson KG, Fisher J, et al. Development and characterization of an acellular human pericardial matrix for tissue engineering. Tissue Eng 2006;12:763–73.

[116] Petzelbauer P, Bender JR, Wilson J, Pober JS. Heterogeneity of dermal microvascular endothelial cell antigen expression and cytokine responsiveness in situ and in cell culture. J Immunol 1993;151:5062–72.

[117] Decherchi P, Cochard P, Gauthier P. Dual staining assessment of Schwann cell viability within whole peripheral nerves using calcein-AM and ethidium homodimer. J Neurosci Methods 1997;71:205–13.

[118] Tas J, Westerneng G. Fundamental aspects of the interaction of propidium diiodide with nuclei acids studied in a model system of polyacrylamide films. J Histochem Cytochem 1981;29:929–36.

[119] Zhou S, Cui Z, Urban J. Dead cell counts during serum cultivation are underestimated by the fluorescent live/dead assay. Biotechnol J 2011;6:513–8.

[120] Shen L, Hillebrand A, Wang DQ-H, Liu M. Isolation and primary culture of rat hepatic cells. J Vis Exp 2012:1–4.

[121] Schneider KH, Aigner P, Holnthoner W, Monforte X, Nuernberger S, Ruenzler D, et al. Decellularized human placenta chorion matrix as a favorable source of small-diameter vascular grafts. Acta Biomater 2016;29:125–34.

[122] Ikada Y. Challenges in tissue engineering. J R Soc Interface 2006;3:589–601.

[123] Amini AR, Laurencin CT, Nukavarapu SP. Bone tissue engineering: recent advances and challenges. Crit Rev Biomed Eng 2012;40:363–408.

[124] Narita Y, Kagami H, Matsunuma H, Murase Y, Ueda M, Ueda Y. Decellularized ureter for tissue-engineered small-caliber vascular graft. J Artif Organs 2008;11:91–9.

[125] Zou Y, Zhang Y. Mechanical evaluation of decellularized porcine thoracic aorta. J Surg Res 2012;175:359–68.

[126] Syed O, Walters NJ, Day RM, Kim H-W, Knowles JC. Evaluation of decellularization protocols for production of tubular small intestine submucosa scaffolds for use in oesophageal tissue engineering. Acta Biomater 2014;10:5043–54.

[127] Baraki H, Tudorache I, Braun M, Höffler K, Görler A, Lichtenberg A, et al. Orthotopic replacement of the aortic valve with decellularized allograft in a sheep model. Biomaterials 2009;30:6240–6.

[128] Seddon AM, Curnow P, Booth PJ. Membrane proteins, lipids and detergents: Not just a soap opera. Biochim Biophys Acta - Biomembr 2004;1666:105–17.

[129] Mancuso L, Gualerzi a, Boschetti F, Loy F, Cao G. Decellularized ovine arteries as small-diameter vascular grafts. Biomed Mater 2014;9:045011.

[130] Samouillan V, Dandurand-Lods J, Lamure a., Maurel E, Lacabanne C, Gerosa G, et al. Thermal analysis characterization of aortic tissues for cardiac valve bioprostheses. J Biomed Mater Res 1999;46:531–8.

[131] Gratzer PF, Harrison RD, Woods T. Matrix alteration and not residual sodium dodecyl sulfate cytotoxicity affects the cellular repopulation of a decellularized matrix. Tissue Eng 2006;12:2975–83.

[132] Cebotari S, Tudorache I, Jaekel T, Hilfiker A, Dorfman S, Ternes W, et al. Detergent decellularization of heart valves for tissue engineering: Toxicological effects of residual detergents on human endothelial cells. Artif Organs 2010;34:206–10.

[133] Delisser HM, Baldwin HS, Albelda SM. Platelet Endothelial Cell Adhesion Molecule 1 (PECAM-1/CD31): A Multifunctional Vascular Cell Adhesion Molecule. Trends Cardiovasc Med 1997;7:203–10.

[134] Kristin J Pawlowski, Stanley E. Rittgers, Steven P. Schmidt GLB. ENDOTHELIAL CELL SEEDING OF POLYMERIC VASCULAR GRAFTS. Front Biosci 9, 2004:370–7.

[135] Hashi CK, Zhu Y, Yang G-Y, Young WL, Hsiao BS, Wang K, et al. Antithrombogenic property of bone marrow mesenchymal stem cells in nanofibrous vascular grafts. Proc Natl Acad Sci U S A 2007;104:11915–20.

[136] Koobatian MT, Row S, Smith R, Koenigsknecht C, Stelios T, Swartz DD. Successful Endothelialization and Remodeling of a Cell-Free Small-Diameter Arterial Graft in a Large Animal Model. Biomaterials 2015;76:344–58.

[137] Schöchl H. b, Solomon C., Voelckel W. Thromboelastometry in the perioperative setting. Netherlands J Crit Care 2010;14:23–31.

[138] Schöchl H, Solomon C, Schulz A, Voelckel W, Hanke A, Van Griensven M, et al. Thromboelastometry (TEM) findings in disseminated intravascular coagulation in a pig model of endotoxinemia. Mol Med 2011;17:266–72.

[139] Zipperle J, Schlimp CJ, Holnthoner W, Husa AM, Nürnberger S, Redl H, et al. A novel coagulation assay incorporating adherent endothelial cells in thromboelastometry. Thromb Haemost 2013;109:869–77.

[140] Dan, Liao, Xinwen, Wang, Peter H. Lin, Qizhi Yao CC. Covalent linkage of heparin provides a stable anti-coagulation surface of decellularized porcine arteries. J Cell Mol Med 2009;13:2736–43.

[141] Khor E. Methods for the treatment of collagenous tissues for bioprostheses. Biomaterials 1997;18:95–105.

[142] Ye X, Wang H, Zhou J, Li H, Liu J, Wang Z, et al. The effect of Heparin-VEGF multilayer on the biocompatibility of decellularized aortic valve with platelet and endothelial progenitor cells. PLoS One 2013;8:e54622.

[143] Zhou M, Liu Z, Wei Z, Liu C, Qiao T, Ran F, et al. Development and validation of small-diameter vascular tissue from a decellularized scaffold coated with heparin and vascular endothelial growth factor. Artif Organs 2009;33:230–9.

[144] Holnthoner W, Hohenegger K, Husa A, Muehleder S, Meinl A, Peterbauer-scherb A, et al. Adipose-derived stem cells induce vascular tube formation of outgrowth endothelial cells in a fi brin matrix 2012.

[145] Usha R, Ramasami T. Structure and conformation of intramolecularly cross-linked collagen. Colloids Surfaces B Biointerfaces 2005;41:21–4.

[146] Kelly SM, Jess TJ, Price NC. How to study proteins by circular dichroism. Biochim Biophys Acta - Proteins Proteomics 2005;1751:119–39.

[147] Chevallay B, Herbage D. Collagen-based biomaterials as 3D scaffold for cell cultures: applications for tissue engineering and gene therapy. Med Biol Eng Comput 2000;38:211–8.

[148] Chattopadhyay S, Raines RT. Review collagen-based biomaterials for wound healing. Biopolymers 2014;101:821–33.

[149] Ramshaw JAM, Peng YY, Glattauer V, Werkmeister JA. Collagens as biomaterials. J Mater Sci Mater Med 2009;20:S3–8.

[150] Kataropoulou M, Henderson C, Grant MH. Metabolic studies of hepatocytes cultured on collagen substrata modified to contain glycosaminoglycans. Tissue Eng 2005;11:1263–73.

[151] Shenvi S V, Dixon BM, Petersen Shay K, Hagen TM. A rat primary hepatocyte culture model for aging studies. Curr Protoc Toxicol 2008;Chapter 14:Unit 14.7.

[152] Lorand L, Graham RM. Transglutaminases: crosslinking enzymes with pleiotropic functions. Nat Rev Mol Cell Biol 2003;4:140–56.

[153] Karp G. Cell and Molecular Biology: Concepts and Experiments. 2008.

7 Abbreviations

ASC	Adipose tissue derived stromal cells
BSA	Bovine serium albumin
CK18	Cytokeratin 18
CT	Clotting time
CVD	Cardiovascular diseases
DMB	1,9-dimethyl-methylene blue
DMBA	Dimethylaminobenzaldehyde
ECD	Electronic circular dichroism
ECM	Extracellular Matrix
EC	Endothelial cells
EDC	Ethylcarbodiimide hydrochloride
EDTA	Ethylendiaminetetraacetic acid
EGM	Endothelial cell growth medium
FACS	Fluorescence-activated cell sorting
FITC	Fluorescein isothyocyanate
FN	Fibronectin
GAG	Glycosaminoglycans
HMDS	Ethanol-hexamethyldisilazane
HUVEC	Human umbilical vein endothelial cells
P/S	Penicillin/streptomycin
PAA	Paracetic acid
PBS	Phosphate buffered saline
PE	Phycoerythrin
PECAM-1	Platelet endothelial cell adhesion molecule
PI	Propidium iodide
ROTEM	Rotational thromboelastometry
RT	Room temperature
SDS	Sodium dodecyl sulfate
SDS	Sodium deoxycholate
SDVG	Small diameter vascular grafts
TEM	Thromboelastometry
TEVG	Tissue engineered vascular grafts
VEGF	Vascular endothelial growth factor

8 Appendix

Decellularized human placenta chorion matrix as a favorable source of small-diameter vascular grafts

Acta Biomaterialia (2015),
http://dx.doi.org/10.1016/j.actbio.2015.09.038

Acta Biomaterialia 29 (2016) 125–134

Contents lists available at ScienceDirect

Acta Biomaterialia

journal homepage: www.elsevier.com/locate/actabiomat

Decellularized human placenta chorion matrix as a favorable source of small-diameter vascular grafts

Karl Heinrich Schneider [a,b,*], Petra Aigner [a,b,c], Wolfgang Holnthoner [a,b], Xavier Monforte [b,c], Sylvia Nürnberger [b,d,e], Dominik Rünzler [b,c], Heinz Redl [a,b], Andreas Herbert Teuschl [b,c]

[a] Ludwig Boltzmann Institute for Experimental and Clinical Traumatology/AUVA Research Center, Vienna, Austria
[b] Austrian Cluster for Tissue Regeneration, Vienna, Austria
[c] Department of Biochemical Engineering, University of Applied Sciences Technikum Wien, Vienna, Austria
[d] Bernhard Gottlieb University Clinic of Dentistry, Universitätsklinik für Zahn-, Mund- und Kieferheilkunde Ges.m.b.H, Vienna, Austria
[e] Medical University of Vienna, Department of Trauma Surgery, Vienna, Austria

ARTICLE INFO

Article history:
Received 28 April 2015
Received in revised form 21 August 2015
Accepted 28 September 2015
Available online 30 September 2015

Keywords:
Decellularized matrix
Human placenta
Vascular grafts
Recellularization

ABSTRACT

Biomaterials based on decellularized tissues are increasingly attracting attention as functional alternatives to other natural or synthetic materials. However, a source of non-cadaver human allograft material would be favorable. Here we establish a decellularization method of vascular tissue from cryopreserved human placenta chorionic plate starting with an initial freeze–thaw step followed by a series of chemical treatments applied with a custom-made perfusion system. This novel pulsatile perfusion set-up enabled us to successfully decellularize the vascular tissue with lower concentrations of chemicals and shorter exposure times compared to a non-perfusion process. The decellularization procedure described here lead to the preservation of the native extracellular matrix architecture and the removal of cells. Quantitative analysis revealed no significant changes in collagen content and a retained glycosaminoglycan content of approximately 29%. In strain-to-failure tests, the decellularized grafts showed similar mechanical behavior compared to native controls. In addition, the mechanical values for ultimate tensile strength and stiffness were in an acceptable range for *in vivo* applications. Furthermore, biocompatibility of the decellularized tissue and its recellularizationability to serve as an adequate substratum for upcoming recellularization strategies using primary human umbilical vein endothelial cells (HUVECs) was demonstrated. HUVECs cultured on the decellularized placenta vessel matrix performed endothelialization and maintained phenotypical characteristics and cell specific expression patterns. Overall, the decellularized human placenta vessels can be a versatile tool for experimental studies on vascularization and as potent graft material for future *in vivo* applications.

Statement of significance

In the US alone more than 1 million vascular grafts are needed in clinical practice every year. Despite severe disadvantages, such as donor site morbidity, autologous grafting from the patient's own arteries or veins is regarded as the gold standard for vascular tissue repair. Besides, strategies based on synthetic or natural materials have shown limited success. Tissue engineering approaches based on decellularized tissues are regarded as a promising alternative to clinically used treatments to overcome the observed limitations. However, a source for supply of non-cadaver human allograft material would be favorable. Here, we established a decellularization method of vascular tissue from the human placenta chorionic plate, a suitable human tissue source of consistent quality. The decellularized human placenta vessels can be a potent graft material for future *in vivo* applications and furthermore might be a versatile tool for experimental studies on vascularization.

* Corresponding author at: Ludwig Boltzmann Institute for Experimental and Clinical Traumatology/AUVA Research Center, Donaueschingenstrasse 13, 1200 Vienna, Austria.
E-mail address: karl.schneider@trauma.lbg.ac.at (K.H. Schneider).

http://dx.doi.org/10.1016/j.actbio.2015.09.038
1742-7061/

1. Introduction

In the US alone more than 1 million vascular grafts are needed in clinical practice every year [1]. Currently, autologous grafting from the patient's own arteries or veins is regarded as the gold standard for vascular tissue repair. However, this method has several disadvantages as it requires multiple surgical procedures including procedures on healthy tissue [2]. In addition, in almost 30% of the cases, the necessary amounts of autologous material may not be available [3,4]. As an alternative, vascular prostheses based on synthetic polymers such as polyethylene terephthalate (PET) and expanded polytetrafluoroethylene (ePTFE) are used in clinics. In particular, small-caliber grafts with an inner diameter below 5 mm have limited success due to reported adverse healing reactions, including surface thrombogenicity [5,6].

Biomaterials based on decellularized tissues are increasingly attracting attention as a functional alternative to other natural or synthetic materials [7,8] because these decellularized materials are naturally derived and inherently support various cell functions. For instance, proteins of the extracellular matrix and the arrangement of tissue fibers have been proven to support cell migration and proliferation, including gene expression and cell–cell interactions [9–11]. Despite these obvious advantages, tissue engineering approaches using decellularized material are often limited due to batch-to-batch variations of the accessible allograft raw material [12]. Furthermore, the less favorable use of xenografts may elicit significant immune response in the recipient due to differences in the primary structure of the residual proteins in the ECM [13,14]. We hypothesize that the vasculature of the human placenta, in particular the placental chorionic plate, has great potential as a material source for human vascular allografts for a wide range of inner diameter sizes. Human placenta, an organ which develops jointly from the mother and the baby during pregnancy, is generally discarded after birth. According to the U.S. census figures from 2013, there were more than 3.9 million births in the United States [15]. Therefore, the placenta is likely to be the most easily accessible raw material of human tissue with consistent quality and without additional harm to the donor [16].

In this study, we established a method to obtain efficiently decellularized small-diameter (<4 mm) vessel grafts isolated from the human placental chorionic plate. The decellularization process, in general a combination of mechanical, chemical and enzymatic approaches, has to be accompanied by adequate analytics [17,18] to guarantee the effectiveness of the process and thus the characteristics of the final structure. Consequently, the removal of cells and cellular debris and the conservation of the decellularized tissue matrix in terms of composition and ultrastructure, were evaluated by histology, scanning electron microscopy analysis and an array of biochemical quantification methods. Moreover, biocompatibility of the decellularized tissue and its ability to serve as an adequate substrate for recellularization strategies using primary endothelial cells were shown. This indicates that this biomaterial could be a versatile tool for experimental studies on vascularization and a potent graft material for future *in vivo* applications.

2. Materials and methods

2.1. Materials

If not indicated otherwise, all reagents were purchased from Sigma–Aldrich (Vienna, Austria) and are of analytical grade. All antibodies were obtained from BD Biosciences (Franklin Lakes, USA). Endothelial cell growth medium and bovine fetal calf serum (FCS) were bought from Lonza (Lonza, Basel, Switzerland).

2.2. Harvesting of human placenta

The ethics committee of Upper Austria gave approval for the use of this material collected by the Red Cross Hospital, Linz and informed consent was obtained from the donors. After the extraction of the placenta during caesarian section births, the placental vasculature was rinsed through the umbilical vein and arteries with Phosphate Buffered Saline solution (PBS) supplemented with additional heparin (50 IU/ml) and antibiotics (1% penicillin/streptomycin). After removal of the blood from the vessels, the whole placenta was frozen at −20 °C until further processing. All donors were serologically tested (HIV, HBV, HCV).

2.3. Preparation and decellularization of human vascular scaffolds from the placenta chorion

Prior to the decellularization of the placenta vessels, the whole placenta was thawed and single vessel parts, with an approximate length of 3–4 cm and with an inner diameter of 2–3 mm, were isolated from the chorionic plate with one end of the harvested vessel connected with a surgical thread to a 14GA BD Venflon™ (BD, Heidelberg) for the following perfusion steps. Then the vessels were subjected to a freeze–thaw step at −80 °C for 18 h and subsequently thawed in PBS solution at room temperature (RT). For the chemical decellularization, the vessels were connected with the Venflon to a custom-made recirculating perfusion system using a peristaltic pump (Minipuls Evolution, Gilson, Middleton) (Fig. 1A). The pulsatile perfusion was measured by a pressure sensor and adjusted to a range of 60–80 mmHg (8000–10,670 Pa). The vessels were perfused with hypertonic (1.2% NaCl) and hypotonic (0.4% NaCl) saline solutions for 30 min each to cause cell lysis by osmotic pressure. Afterwards, the samples were perfused with 1% Triton X-100 (Sigma, Vienna) and 0.02% w/w ethylenediaminetetraacetic acid (EDTA) in PBS for 24 h at room temperature. Before incubation in DNase I-solution (200 IU/ml, Roche) over night at 4 °C, the vessels were thoroughly washed with PBS for 3 h. For chemical sterilization, after several rinsing cycles in sterile PBS, the scaffolds were washed with 0.1% (w/v) peracetic acid (PAA) solution at pH 7.0, as described by Lomas et al. [19], in a 50 mL Falcon tube for 3 h at room temperature on a roller mixer (Type, Firma, Stadt, Land) at 30 rotations per minute (rpm). Finally the vessels were rinsed with 35 ml sterile PBS 3 times for 10 min and stored in sterile PBS at 4 °C before further use.

2.4. Quantification of matrix components, DNA residuals and statistics

Biochemical quantification methods were used to quantify DNA, glycosaminoglycan (GAG), and its collagen contents. All vascular scaffolds specimens were lyophilized, 10 mg dry ECM was weighed and digested with 3 IU/ml papain from *Papaya latex* (Sigma) in the presence of 20 mM L-Cystein (Sigma) in Papain buffer (75 mM NaCl, 27 mM Na Citrate, 0.1 M NaH_2PO_4, 15 mM EDTA, pH 6.0) at 60 °C before analysis. The measured values were normalized to the dry weight of the samples.

2.4.1. DNA quantification

To quantify the residual amounts of DNA on the decellularized scaffolds, Hoechst 33342 (Sigma) was used to quantify the remaining DNA. A Hoechst dye stock (10 mg/ml in dH_2O) was prepared, sterilized by filtration (0.22 μm, Rotilabo, Roth, Karlsruhe) and stored at 4 °C in the dark. Prior to each assay the working dye solutions were freshly prepared and diluted with assay buffer (2 M NaCl, 50 mM NaH_2PO_4, pH 7.4) to a final concentration of 5 μg/ml. Dilutions of DNA sodium salt from calf thymus (Sigma; dissolved in ddH_2O) were used to generate a standard curve. The samples/standards were pipetted in duplicates into 96-well black

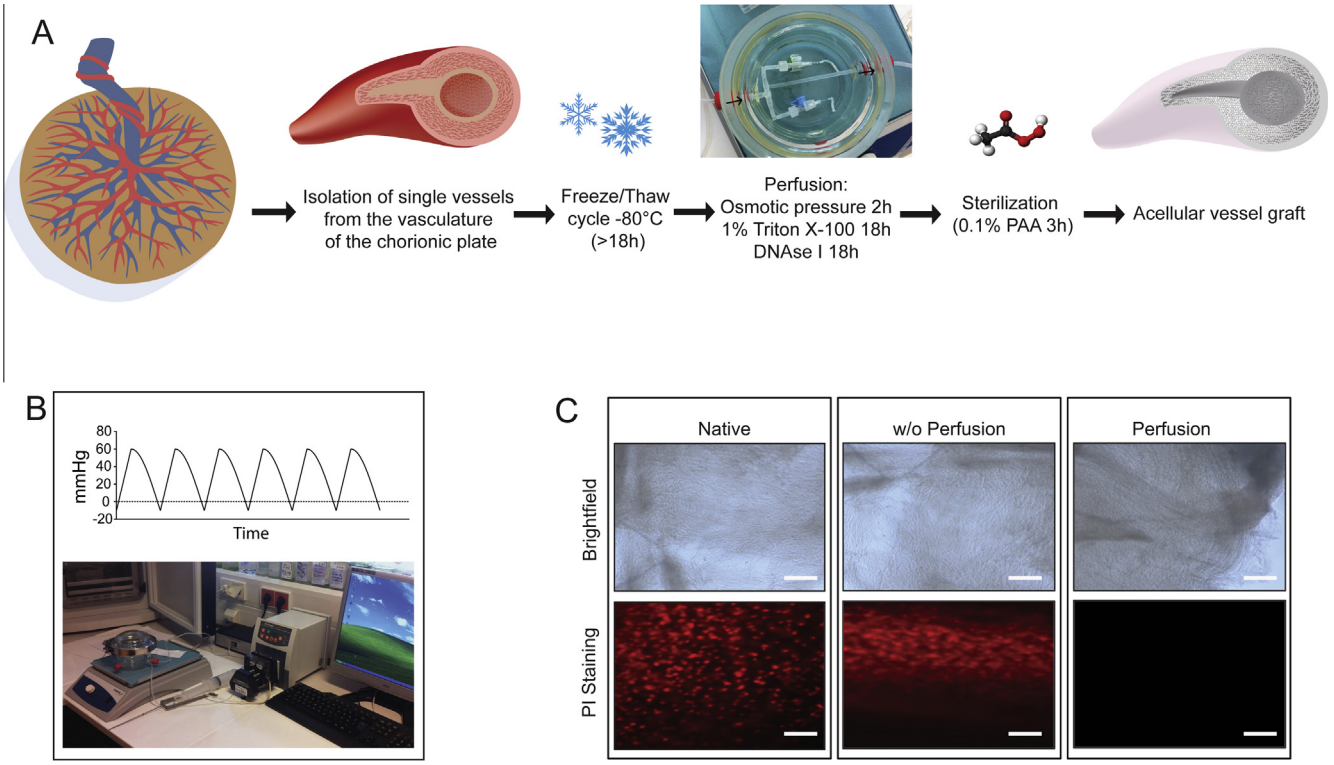

Fig. 1. Perfusion based decellularization approach to generate acellular vessel grafts with perfusion setup, and initial efficiency control using DNA staining. (A) Decellularization process: After the separation of a single blood vessel from the placenta chorionic vasculature, the decellularization protocol begins with a freezing step. Followed by pulsatile perfusion of the chemicals through the blood vessels and a final sterilization step using PAA 0.1% adjusted to pH 7.4 produced a sterile acellular vessel graft. (B) The upper panel shows a representative pressure curve during perfusion decellularization with a maximum pressure of 60–80 mmHg. The lower panel shows the perfusion setup including peristaltic pump and perfusion glass chamber. (C) Comparison of native tissue and decellularized tissue using two different methods of exposure of the tissue to the decellularization agents. Both decellularization protocols are the same with regards to the chemicals used and the times exposed, but differ in the utilization of pulsatile perfusion. At one method the vessel tissue is floating within the reagents and at the other method the reagents are perfused through the lumen of the vessels. With the perfusion protocol all cells were removed from the tissue. However, in the tissues treated without perfusion, DNA remnants were detected (scale bars are 200 μm). Propidium Iodide (PI) staining was used to stain possible DNA remnants in the tissues. The tissue was incubated with 3 μM PI solution for 20 min on ice before the images were taken.

microplate (Brand, Wertheim). Then 100 μl of Hoechst working solution was added to each well, the plate was protected from light and incubated for 5 min at 37 °C under constant shaking on an orbital shaker. After the incubation the fluorescence was measured using an Omega POLARstar plate reader (BMG Labtech, Ortenberg) at 355 nm with a reference at 460 nm wavelengths.

2.4.2. Collagen quantification

To compare the collagen content of the decellularized grafts with native vessel grafts, the collagens were quantified using a common hydroxyproline assay as described elsewhere [20,21]. Briefly, 200–250 μl solution of papain-digested samples were put into heat resistant twist top tubes (Sorenson BioScience, Utah) and mixed with the same volume of 12 M HCl to result in a final concentration of 6 M HCl. The solution was incubated at 120 °C for 20 h for acidic hydrolyzation. The hydrolyzed samples were then neutralized with 6 M NaOH. To avoid deviation of the measurements, the standard solution was prepared by dissolving 131 mg L-hydroxyproline (Sigma) in 50 ml of HCl solution, which had been neutralized with 6 M NaOH (similar to the solvent matrix of the tissue sample) and further diluted (1:100) to a final concentration of 200 μM hydroxyproline. 60 μl of neutralized samples and of the dilution series for the standard curve were pipetted into a 96-well plate (Corning, New York). In each well, 20 μl assay buffer (0.16 M citric acid, 0.59 M sodium acetate trihydrate, 0.57 M NaOH in dH_2O, pH 6.1) and 40 μl chloramine T reagents (final conc. 15 mg/ml) were added and incubated for 20 min at room temperature. Thereafter 80 μl of 4-dimethylaminobenzaldehyde (3 M DMBA) reagent was added and incubated for 25 min at 60 °C. Subsequently, the plates were immediately cooled on ice and hydroxyproline concentration was measured at 570 nm (BMG Labtech, Ortenberg). To determine the total collagen concentration the measured values of hydroxyproline were multiplied with a factor of 7.14.

2.4.3. Glycosaminoglycan quantification

To directly measure the sulfated glycosaminoglycan (GAG) content, papain-digested samples were stained with 1,9-dimethylmethylene blue (DMB, Sigma) and photometrically measured at 525 nm as described [22–24]. A dilution series of chondroitin sulfate C in PBS (0.5 mg/ml) was used as the standard solution. The specimens were diluted 1:40 before the measurement. 100 μl of the samples or standard dilutions were mixed with 200 μl DMB dye solution (46 μM DMB, 0.04 M NaCl, 0.04 M Glycine in dH_2O) into flat bottom 96-well plates (Corning, New York) and extinction was measured with a plate reader (Omega, BMG Labtech, Ortenberg) at 525 nm against 590 nm as the reference wavelength.

2.4.4. Histological analysis

The samples were fixed in 4% formaldehyde solution, buffered pH 6.9, (VWR) for 24 h. Thereafter, they were washed with tap water and transferred into 50% ethanol solution for 1 h and stored in 70% ethanol. Dehydration was competed with a further ascending series of alcohol. Then the specimens were embedded in paraffin

wax, sectioned and placed on slides. The Martius, Scarlet and Blue (MSB) method was chosen to stain collagen (blue), nuclei (red to black) and possible remnants of blood (fibrin red, erythrocytes yellow). Sections were evaluated and scanned with a light microscope (Leica DMI6000B, Leica Microsystems, Solm).

2.4.5. Scanning electron microscopy (SEM)

For SEM, tissue samples were fixed with 2.5% glutaraldehyde (Merck, Darmstadt) for 2 h at room temperature. Then the samples were dried by a graded ethanol series (40%, 50%, 60%, 70%, 80%, 90%, 100%, 15 min each) and by increasing ethanol–hexamethyldisi lazane (HMDS) series up to 100% (33%, 66%, 100% – 1 h each). The samples were sputter coated with Pd–Au using a Polaron SC7620 sputter coater (Quorum Technologies Ltd., East Grinstead), and examined using a JEOL JSM-6510 scanning electron microscope (Jeol GmbH, Eching/Munich).

2.5. Mechanical testing

Two groups of vessel grafts, native and decellularized, with an outer diameter of 4 mm were radially cut into short conduits with length 7 mm. For a hoop tensile measurement, the conduits were loaded on two steel rods and mounted in clamps of a uniaxial mechanical testing machine (ZwickiLine, Zwick/Roell, Ulm). Specimens were tested until failure at a rate of 10 mm/min and the resulting stress–strain curves were recorded. The resisting area of the grafts was calculated to obtain the Young's modulus from the linear phase of the stress–strain curve of each sample.

2.6. Cell isolation

HUVECs were either purchased (Lonza, Basel) or isolated as previously described [25].

2.7. Endothelial cell seeding and biocompatibility

Human endothelial cells, isolated from the umbilical cord vein (HUVECs), were used to reendothelialize the decellularized vascular scaffolds. Samples of decellularized blood vessels were opened in the longitudinal direction and small pieces, 5 × 5 mm in size, were cut out and placed in a 24-well plate with the luminal surfaces up. The tissue pieces were reseeded with 3 × 105 cells, drop-wise, on the luminal surface and pre-incubated for 30 min at 37 °C, 5% CO_2 to allow optimal cell attachment before adding 1 ml endothelial cell growth medium (EGM-2, Lonza) to each well for cultivation. After 24 h of incubation the reseeded tissue pieces were transferred to fresh well plates. Suspension plates were used to only cultivate adherent cells to the vascular matrix and prevent adherence onto the culture plate during the recellularization. The state of recellularization was determined with live/dead staining and immunofluorescence staining after 7 days of incubation.

2.8. Live/dead cell viability and immunostaining

Qualitatively, the cell viability was determined with vital staining using calcein AM (Sigma) and Propidium Iodide (PI) as described elsewhere [26–28]. Therefore, 5 mm × 5 mm decellularized pieces (as described in 2.7) of the vessels were put into a dye solution, consisting of 3 μM Calcein AM (live) and 3 μM PI (dead) dissolved in EGM-2 expanding growth culture medium and incubated for 30 min at room temperature (RT). Samples were rinsed in PBS for 5 min before fluorescence was evaluated on a Leica DMI6000B epifluorescence microscope (Leica, Solms) using 492 and 517 nm filters. For the characterization of the reendothelialization, and to show that the cells form cell–cell contacts on the surface of the decellularized matrix, immunostaining, with antibodies against CD31, was performed. The vessel pieces were fixed with 500 μl of 4% phosphate buffered formaldehyde solution for 7 h at 4 °C. After a 30 min washing step with PBS, the cells were incubated on ice with anti-CD31 antibody (BD Biosciences, Franklin Lakes) over night. Following the incubation step, the cells were washed with ice cold PBS/1% BSA (Bovine Serum Albumin, Lonza) solution. Directly before fluorescent microscope (Leica) analysis, the cells were additionally treated with 4,6-diamidin-2-phenylindol (DAPI) staining solution (Sigma) for 1 h and rinsed again with PBS/1% BSA solution before measurement.

2.9. Endothelial marker expression analysis with flow cytometry

The expression levels of typical endothelial cell markers (CD31, CD 146, CD61, VE-Cadherin, VEGFR-2, Tie-2) were determined after reseeding the vessel matrix with endothelial cells isolated from the two different sources. The decellularized tissues pieces were reseeded with primary endothelial cells as described above. For the control groups 10^4 cells were seeded to each well of a 2 μg/ml fibronectin (hFN) coated 24-well plate and incubated for 7 days, similar to the cells seeded on the tissue matrix. After 1 week of cultivation the cells were detached using prewarmed Accutase solution (BD Bioscience, Franklin Lakes). Afterwards the cell suspensions pooled from 8 slices were transferred to a 15 ml Falcon tube for centrifugation. For flow cytometry analysis the cell suspensions were centrifuged at 300×*g* for 5 min and the cell pellets were resuspended in PBS containing 1% BSA. The antibodies used were either fluorescein isothiocyanate (FITC) – or phycoerythrin (PE) – conjugated and diluted in a 1:50 ratio in PBS/1% BSA. The antibodies were incubated for 30 min in the dark on ice, followed by two washing steps with PBS/1% BSA (centrifugation for 5 min at 100×*g* force after each washing step). Finally the samples were subjected to flow cytometry analysis, using a FACSCanto II flow cytometer (BD Biosciences, Franklyn, USA). Bound fluorescence was analyzed with FlowJo software (FlowJo, Oregon, USA).

2.10. Statistical analysis

All calculations were performed using GraphPad software (GraphPad software, Inc., San Diego). Normal distribution of data was tested with the Kolmogorov–Smirnov test. One-way analysis of variance followed by Tukey's post hoc test was used to conduct statistical significance. *p*-Values below 0.05 were considered statistically significant. All graphs in this study are shown as mean +/− standard deviation (SD).

3. Results

3.1. Successful decellularization of vascular tissue from human placenta chorion with a pulsatile flow perfusion system

In order to quickly evaluate a successful decellularization protocol, a PI staining was performed to detect possible DNA residuals on the tissue. The pressure controlled pulsatile perfusion of the detergents through the vessels increased cell removal and led to a simultaneous reduction of the exposure time with a 1% concentration of Triton X-100. The PI fluorescence DNA dye staining of vascular tissue samples, treated with the adapted perfusion system, showed no detectable DNA residues after decellularization. In contrast, tissue samples of a control group, treated with an analogous decellularization protocol of ours, but without pulsatile perfusion, left substantial amounts of remaining DNA fragments, indicating incomplete decellularization (Fig. 1C).

3.1.1. Quantification of residual DNA confirmed reduction of DNA in decellularized samples

Quantification of DNA on decellularized and native tissue samples, using Hoechst 33342 dye, strengthened the previous results from histology and PI staining indicating successful removal of the cells. In contrast to native tissue, which contained 5.74 ± 0.31 μg DNA per mg dry weight (n = 6), the decellularized tissue samples showed a significant decrease of DNA content to 0.34 ± 0.01 μg DNA per mg dry weight (n = 6) (Fig. 2A, left panel).

3.1.2. Collagen preservation after decellularization

To determine the possible loss of collagen as a result of the decellularization process, a hydroxyproline quantification assay was performed. The results, shown in Fig. 2A (middle panel), indicate preservation of collagen within the processed tissue. There were no significant differences in collagen content between the non-treated and decellularized samples. Non-treated tissue samples and decellularized samples showed a collagen content of 152.1 ± 21.8 μg per mg dry weight and

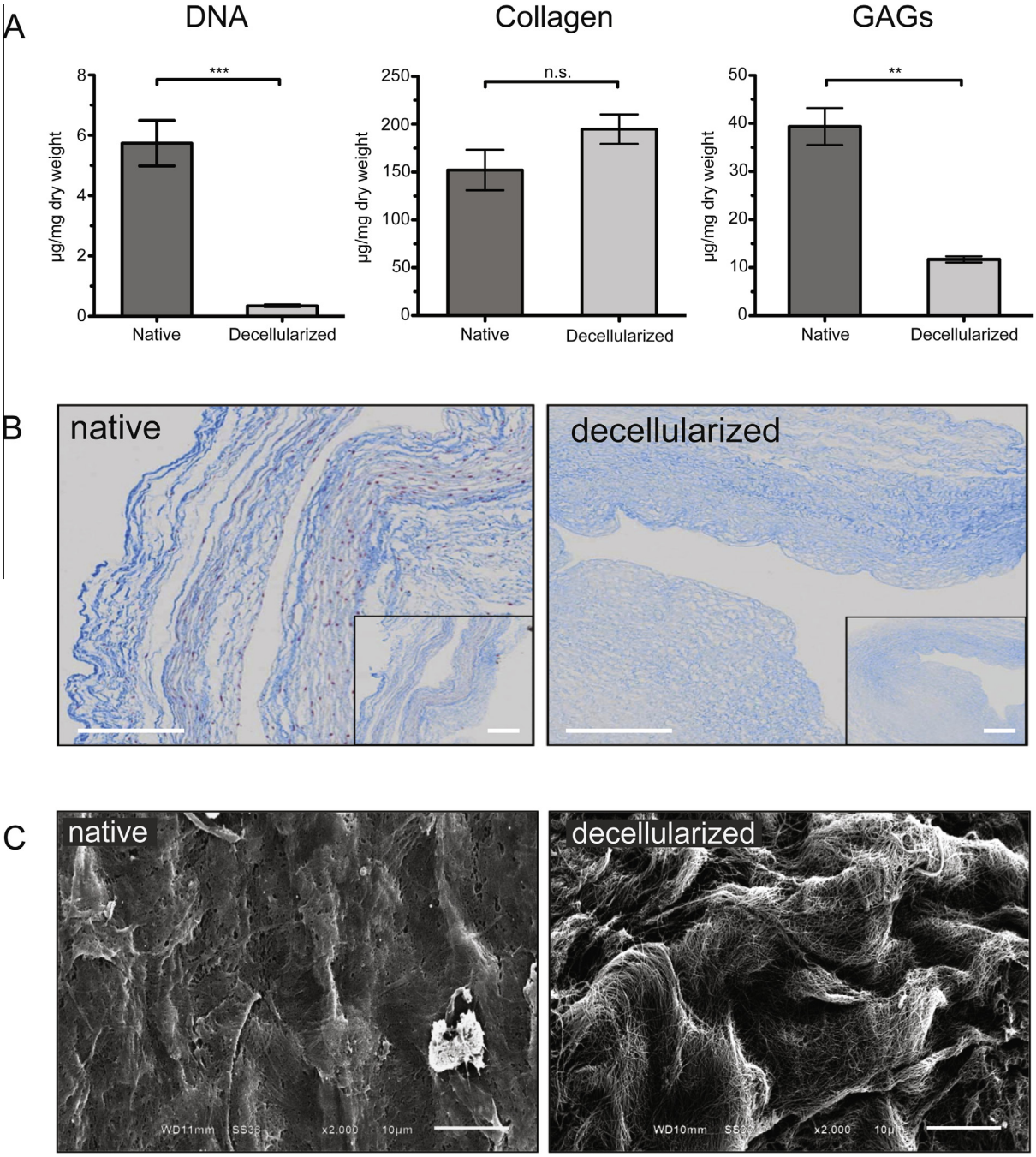

Fig. 2. (A) Quantitative determination of DNA, collagen, and glycosaminoglycans (GAG) in native and decellularized tissue samples. Data is expressed as mean values ± SD. (A, left panel) DNA quantification shows a significant reduction of DNA content in the decellularized tissues. (n = 6, $^{***}p < 0.0001$). (A, middle panel) Collagen quantification using hydroxyproline assay shows collagen content (μg/ml) (n = 6, n.s. not significant). (A right panel) GAG quantification shows a significant reduction with a GAG conservation of 29% in the decellularized tissue ($^{**}p < 0.001$). (B) MSB staining confirms the conservation of collagenous structures (blue) within the decellularized samples. No cellular residues (red dots) can be detected in the decellularized tissue samples (scale bars are 200 μm). (C) Scanning electron microscopy show a preservation of the native hierarchical fiber structures in the decellularized tissues. In the decellularized tissue single collagen fibers can be identified and appear to be intact, without any cell remnants or cellular debris (scale bars are 10 μm). (For interpretation of the references to color in this figure legend, the reader is referred to the web version of this article.)

A Test Set-up

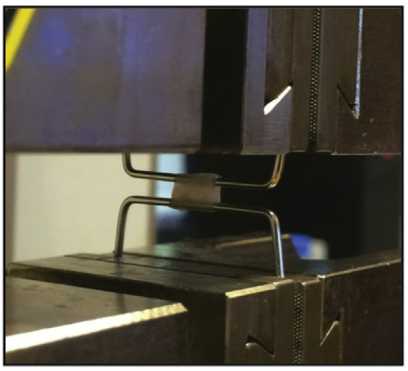

Mechanical properties

	Native	Decellularized
F_{max} [N]	6.83 ± 2.01	4.04 ± 0.79
Young modulus (E) [Mpa]	5.36 ± 0.78	3.65 ± 0.93
Deformation at F_{max} (ε) [%]	54.21 ± 7.89	42.44 ± 12.04
Theoretical Burst Strength [mmHg]	3185 ± 915	2056 ± 455

B Straining curves

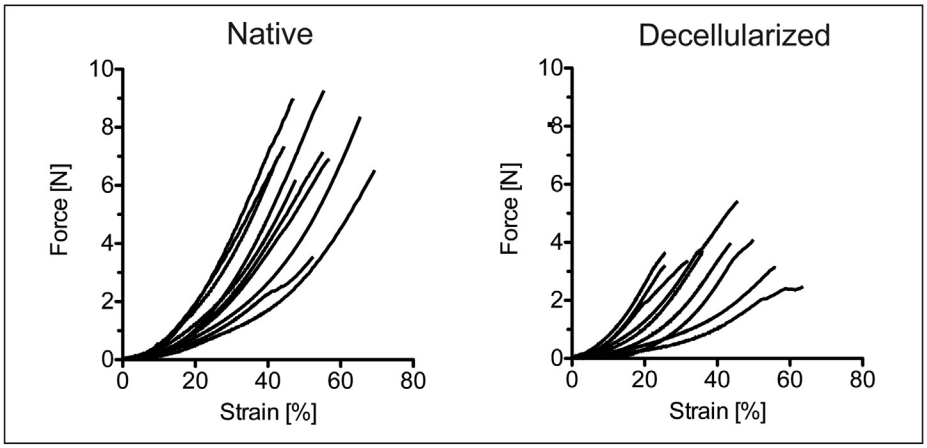

C Young`s modulus (E) and F_{max} at failure

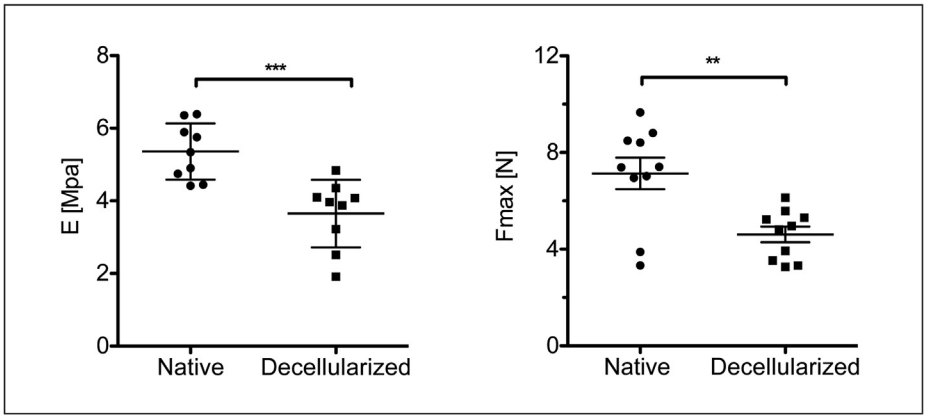

Fig. 3. Mechanical testing results: (A, left panel) test specimen mounted on two steel rods (outer diameter 4 mm, thickness 300 μm, length 7 mm) strained until failure at 10 mm/min. (A, right panel) Table: mechanical properties. The theoretical burst pressure was calculated using Barlow's equation. (B) stress–strain curves of native and decellularized vessels. (C, left) Young's modulus ($^{***}p < 0.0006$) and (C, right) F_{max} ($^{**}p < 0.0026$).

194.8 ± 15.31 μg per mg dry weight of collagen ($n = 6$), respectively.

3.1.3. Conserved glycosaminoglycan content

The amount of GAGs per mg of dry weight of the human vessel tissue before and after decellularization was 39.36 ± 3.83 μg per mg dry weight ($n = 3$) and 11.73 ± 0.66 μg per mg dry weight ($n = 3$), respectively. There was a significant difference in the GAG content of the fresh tissue compared to that of the decellularized tissue, indicating that approximately 30% of the GAG content could be preserved after the process (Fig. 2A, right panel).

3.1.4. Preservation of fibrous ultrastructure and removal of cellular components

A histological examination confirmed the complete decellularization of the placenta tissue. In contrast to the untreated controls,

no cellular residues were detected in the decellularized vessels by Martius, Scarlet Blue (MSB) staining. Furthermore, MSB staining confirmed the conservation of collagenous structures within the decellularized samples (Fig. 2B). SEM analysis micrographs showed the preservation of the native hierarchical fiber structures in the decellularized tissues. In the decellularized tissue, single collagen fibers could be identified and appeared to be intact. No cell remnants or cellular debris were detectable (Fig. 2C).

3.2. Mechanical testing

To characterize the mechanical properties (summarized in Fig. 3) of the decellularized vessels and the native controls, respective specimens were strained to failure. Mechanical testing revealed a significant decrease in maximum tensile strength F_{max} [N] from the native tissue $F_{max} = 6.83 \pm 2.01$ N to decellularized structures $F_{max} = 4.04 \pm 0.79$ N (Fig. 3). This roughly corresponds to a preservation of 59% of initial strength. Similarly, the Young modulus was reduced from native tissue to decellularized tissue with native tissue having an $E = 5.36 \pm 0.78$ MPa and the decellularized tissue $E = 3.65 \pm 0.93$ MPa. This corresponds to a loss of stiffness of approximately 32%. The deformation (ε) at F_{max} was $\varepsilon = 54.21 \pm 7.89\%$ for the native specimens ($n = 9$) compared to $\varepsilon = 42.44 \pm 12.04\%$ for the decellularized group (Fig. 3). The theoretical maximal internal pressure the vessel can withstand before mechanical failure was calculated using Barlow's formula. The theoretical burst pressure obtained using the measured ultimate tensile strength, wall thickness and outer diameter was 3185 ± 915 mmHg for the native vessels and 2056 ± 455 mmHg for the decellularized vessels.

3.3. Biocompatibility and reseeding efficiency

For biocompatibility testing of the decellularized vascular tissues, the vessels were seeded with endothelial cells (EC) and incubated for 7 days at 37° C and 5% CO_2. In Fig. 4A, pictures of fluorescent cells on the decellularized tissues are shown. Cells started to adhere and spread on the materials immediately. Calcein AM stainings confirmed the viability of the reseeded cells. Additionally, cell–cell contacts between the endothelial cells seeded on the decellularized tissue could be detected by CD31 staining (Fig. 4B).

3.4. Endothelial marker expression

The data shown in Fig. 4C is representative for four independent experiments. Cells from two different single donors and pooled donor cells (Sigma) were used. In order to prove that endothelial surface marker expression does not change after seeding on the decellularized scaffold, endothelial cells were reseeded on decellularized vessel matrices and incubated for 7 days in EGM-2 growth medium. As a control, cells seeded on tissue culture well plates were used. After incubation the endothelial cells were subjected to flow cytometry. The cells were positive for specific endothelial cell markers (VE-Cadherin, CD31, CD61, CD146, Tie-2, VEGFR2).

4. Discussion

In this study we show for the first time the decellularization of vessel grafts isolated from the human placental chorionic plate for prospective use in novel tissue engineering approaches and regenerative medicine (e.g. 3D cell cultivation or small diameter vessel replacement). Our protocol is based on the combination of an initial freeze–thaw (−80 °C) step, a short osmotic pressure treatment step with a hypertonic salt solution and a chemical disruption step using 1% Triton X-100. Perfusion is applied through the lumen of the vessels via a custom-made pressure-controlled perfusion system. The choice of detergent for decellularization and adding mechanical agitation may also influence the preservation of important structural and biochemical components [7]. Strong ionic detergents such as SDS facilitate rapid removal of cells from dense tissues and can yield a functional bioscaffold [29,30]. However, there are reports that ionic detergents tend to damage ECM components, in particular denature proteins, and cause severe structural alterations resulting in impaired mechanical and biocompatibility properties [31–33]. There are reports that either alterations in the ultrastructure of the matrix [34] or residual concentrations of the detergent [35] impair cellular repopulation of the matrix. It has been reported that the use of SDS requires intense washing steps to prevent toxicological effects [35]. Therefore, we decided to use 1% Triton X-100 as a non-ionic detergent with the goal of producing acellular vascular grafts with less alterations of the ultrastructure and no toxic effects on repopulated cells. The effectiveness of Triton X-100 to disrupt cell membranes during decellularization processes has been reported previously [36,37]. The perfusion set-up enabled us to use lower concentrations of the detergent with shorter exposure times compared to non-perfusion processes. In contrast to previously published decellularization studies, which used 1% Triton X-100, the exposure time of the detergent could be reduced from 48 to 24 h due to the perfusion system [38,39]. In fact, after static decellularization process in a non-perfused control group DNA fragments and cell remnants could still be detected using a PI staining (shown in Fig. 1C). However, the new protocol utilizing a pulsatile perfusion of chemicals through the vessels led to an effective removal of cellular components while maintaining the major structures of the ECM. A full decellularization was confirmed by histology and electron microscopy. Moreover, no significant difference in collagen content could be detected between the native and the decellularized vascular grafts using fluorescence quantification methods. In contrast, a trend towards increasing collagen values was observed after decellularization. Since the values were normalized to the dry weight of the samples, this mirrors the loss of cell mass and soluble proteins in the tissue. Triton X-100 is less effective than SDS, but also causes fewer disruptions of the ECM and its components. Hence, Triton X-100 is more suitable to remove cells from thin tissues than from complex and thick tissues. Nevertheless, every cell removal agent will alter ECM components. Compared to native tissue, the amount of GAGs within the tissue was reduced to one third during the decellularization process.

Mechanical properties were determined by recording stress–strain profiles to compare decellularized grafts to native tissue. Although a reduction in both stiffness and ultimate tensile strength could be observed, the theoretical burst pressure values (approx. 2000 mmHg) calculated for the vascular grafts after decellularization but before recellularization, were in an acceptable range for *in vivo* situations. In contrast to our decellularized graft, other tissue engineered constructs require a long maturation time to reach appropriate burst strength [40–42]. For instance, in a study of L'Heureux et al. in which tissue engineered blood vessels are constructed by vascular smooth muscle cells, an incubation/cultivation time of 7 weeks is needed to reach burst strength values comparable to our readily usable decellularized grafts [43]. Our proposed decellularization process leads to vascular grafts possessing the suitable mechanical strength for grafting without any cost- and time-intensive *ex vivo* maturation steps. This opens up the possibility for "off-the-shelf" small diameter vessel grafts. In this respect, the possibility for long-term storage of the decellularized vessels grafts is also an important point in future clinical scenarios. A possible cryopreservation of the decellularized tissue would be beneficial. In previous studies, the storage of vascular tissue at −80 °C did not show negative effects on ultrastructure or mechan-

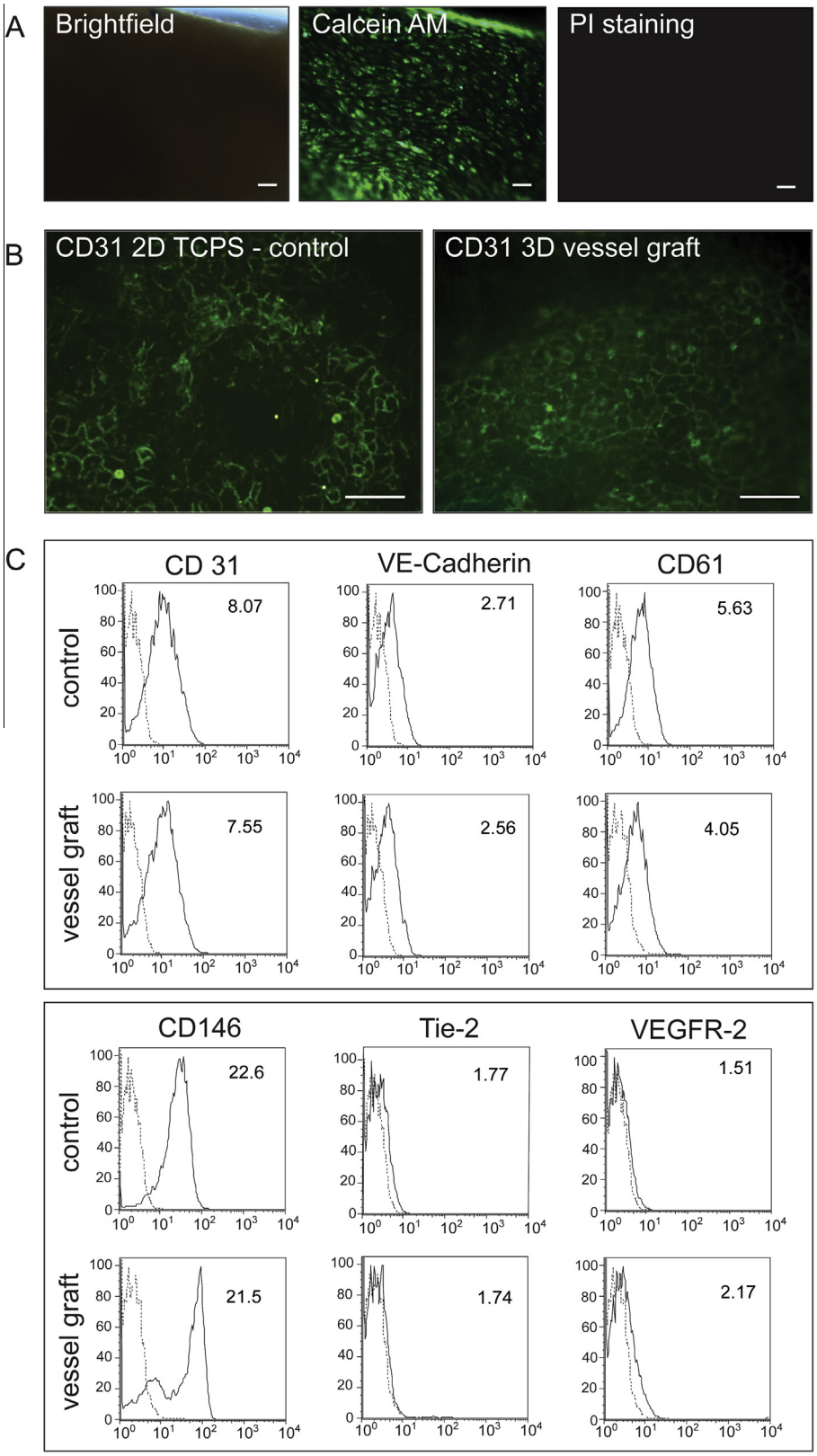

Fig. 4. (A) Endothelial cells reseeded to the surface of the acellular scaffolds and stained with Calcein AM and Propidium Iodide (PI) resulting in live cells (A, middle panel) green and dead cells (A, right panel) red. PI does not give any signal in the decellularized tissue samples (scale bars are 200 μm). (B) To visualize the formation of cell–cell contacts between endothelial cells a staining of platelet endothelial cell adhesion molecules (PECAM-1) – CD31 was performed. (B, left) Endothelial cells seeded on tissue culture plate surface (control). (B, right) Endothelial cells seeded on acellular blood vessel lumen (vessel graft) (scale bars are 200 μm). (C) Endothelial cell marker expression (CD31, VE-Cadherin, CD61, CD146, Tie-2, VEGFR-2) of HUVECs after recellularization of the scaffolds (vessel grafts) was confirmed after 1 week of incubation. HUVECs cultivated for 1 week on tissue culture plate were used as control. The data is representative of four independent experiments. Cells from two different single donors and pooled donor cells were used. (For interpretation of the references to color in this figure legend, the reader is referred to the web version of this article.)

ical properties [44,45]. Having in mind that our decellularization protocol includes a freezing step we hypothesize that a cryopreservation of our acellular vessel tissue is possible. The choice of source tissue for naturally derived biomaterials can be quite challenging. It can be obtained from either animal-derived tissue (xenografts) or human-derived tissue (homograft). However, due to limited availability of human-derived tissue and the risk of transmission of non-human animal pathogens, a suitable human tissue source of consistent quality is desired. Since the placenta can be obtained regularly in hospitals, it can be considered the easiest accessible human tissue source of healthy donors for the preparation of decellularized vessel grafts in different sizes and branching patterns on a large scale. So far placenta tissue, in particular the amnion, is widely used in research, including primary cell and stem cell isolation, and in clinics, for example in ophthalmology and wound treatment [23,46–49]. Due to the placenta's function connecting the developing fetus to the mother, this organ is mainly composed of fetal elements [16]. Vascular grafts of the chorionic plate should therefore trigger minimal immune response after decellularization [50,51]. Only a few studies reported the use of the chorionic plate and its vascular structures. For instance, Flynn et al. in 2006 described the decellularization of intact placental segments using the existing vasculature for delivering the decellularization agents into the tissue [52] and proposed the obtained placenta segments to be a potential scaffold for soft tissue augmentation. However, they did not report on vascular matrix grafts or decellularized blood vessels.

Recently, the decellularization of donor organs such as heart, jejunum, bladder, or liver has been shown to provide acellular scaffold matrix that can be seeded with appropriate cell types and support their respective specific cell functions [53–57]. Here we show biocompatibility of the decellularized vessel grafts by recellularization of the matrix with primary human endothelial cells. Once seeded onto the luminal surface of a decellularized vessel graft endothelial cells performed endothelialization and maintained phenotypical characteristics and cell specific expression patterns. Furthermore, a vital staining showed a high viability of the cells reseeded to the decellularized matrix. This strongly indicates a lack of toxic effects from residues of the chemicals used during the decellularization process.

5. Conclusion and outlook

Human placenta material has great potential to be used as source for tissue engineering and regenerative medicine purposes. We demonstrated the possibility to isolate small diameter vascular structures from the placental chorionic plate and achieved a fully decellularized vessel graft. Furthermore we proved recellularization capacity without toxic effects from possible chemical residues. This acellular matrix could also be used to investigate cell–matrix interactions in greater detail. Moreover, future planned *in vivo* studies will provide more detailed information on the suitability of these vascular grafts for vascular transplantation.

Conflict of interest

The authors have no conflict of interest to declare.

Acknowledgments

The authors thank the Red Cross Blood Transfusion Service, Linz, Upper Austria for processing and providing the placenta material. The financial support by the City of Vienna (MA27, #12-06 and MA23, #14-06) and by the seventh frame network program BIODESIGN is gratefully acknowledged.

References

[1] T. Pennel, G. Fercana, D. Bezuidenhout, A. Simionescu, T.-H. Chuang, P. Zilla, et al., The performance of cross-linked acellular arterial scaffolds as vascular grafts; pre-clinical testing in direct and isolation loop circulatory models, Biomaterials 35 (2014) 6311–6322.
[2] P. Chamiot-Clerc, X. Copie, J.F. Renaud, M. Safar, X. Girerd, Comparative reactivity and mechanical properties of human isolated internal mammary and radial arteries, Cardiovasc. Res. 37 (1998) 811–819.
[3] P.L. Faries, F.W. LoGerfo, S. Arora, M.C. Pulling, D.I. Rohan, C.M. Akbari, et al., Arm vein conduit is superior to composite prosthetic-autogenous grafts in lower extremity revascularization, J. Vasc. Surg. 31 (2000) 1119–1127.
[4] C.P. Twine, A.D. McLain, Graft type for femoro-popliteal bypass surgery, Cochrane Database Syst. Rev. 2 (2010) CD001487.
[5] J. Chlupá, Blood vessel replacement: 50 years of development and tissue engineering paradigms in vascular surgery, Physiol. Res. 58 (2009).
[6] P. Klinkert, P.N. Post, P.J. van Breslau, J.H. Bockel, Saphenous vein versus PTFE for above-knee femoropopliteal bypass. A review of the literature, Eur. J. Vasc. Endovasc. Surg. 27 (2004) 357–362.
[7] P.M. Crapo, T.W. Gilbert, S.F. Badylak, An overview of tissue and whole organ decellularization processes, Biomaterials 32 (2011) 3233–3243.
[8] T.W. Gilbert, Strategies for tissue and organ decellularization, J. Cell. Biochem. 113 (2012) 2217–2222.
[9] M.P. Bernard, J.C. Myers, M.L. Chu, F. Ramirez, E.F. Eikenberry, D.J. Prockop, Structure of a cDNA for the proα2 chain of human type I procollagen. Comparison with chick cDNA for proα2(I) identifies structurally conserved features of the protein and the gene, Biochemistry 22 (5) (1983) 1139–1145.
[10] H.K. Kleinman, D. Philp, M.P. Hoffman, Role of the extracellular matrix in morphogenesis, Curr. Opin. Biotechnol. 14 (2003) 526–532.
[11] R.P. Keatch, A.M. Schor, J.B. Vorstius, S.L. Schor, Biomaterials in regenerative medicine: engineering to recapitulate the natural, Curr. Opin. Biotechnol. 23 (2012) 579–582.
[12] M. He, A. Callanan, Comparison of methods for whole-organ decellularization in tissue engineering of bioartificial organs, Tissue Eng. Part B Rev. 19 (2013) 194–208.
[13] J.I. Spark, S. Yeluri, C. Derham, Y.T. Wong, D. Leitch, Incomplete cellular depopulation may explain the high failure rate of bovine ureteric grafts, Br. J. Surg. 95 (2008) 582–585.
[14] D.W. Courtman, B.F. Errett, G.J. Wilson, The role of crosslinking in modification of the immune response elicited against xenogenic vascular acellular matrices, J. Biomed. Mater. Res. 55 (2001) 576–586.
[15] J.a. Martin, B.E. Hamilton, S.J. Ventura, M.J. Osterman, T.J. Mathews, Births: final data for 2012, Natl. Vital Stat. Rep. 64 (2013).
[16] K. Benirschke, Remarkable placenta, Clin. Anat. 11 (1998) 194–205.
[17] D.M. Faulk, C.a. Carruthers, H.J. Warner, C.R. Kramer, J.E. Reing, L. Zhang, et al., The effect of detergents on the basement membrane complex of a biologic scaffold material, Acta Biomater. 10 (2014) 183–193.
[18] S. Xing, C. Liu, B. Xu, J. Chen, D. Yin, C. Zhang, Effects of various decellularization methods on histological and biomechanical properties of rabbit tendons, Exp. Ther. Med. 8 (2014) 628–634.
[19] R. Lomas, J. Cruse-Sawyer, C. Simpson, E. Ingham, R. Bojar, J. Kearney, Assessment of the biological properties of human split skin allografts disinfected with peracetic acid and preserved in glycerol, Burns 29 (2003) 515–525.
[20] E. Kheir, T. Stapleton, D. Shaw, Z. Jin, J. Fisher, E. Ingham, Development and characterization of an acellular porcine cartilage bone matrix for use in tissue engineering, J Biomed. Mater. Res. A 99 (2011) 283–294.
[21] C.A. Edwards, W.D. O'Brien, Modified assay for determination of hydroxyproline in a tissue hydrolyzate, Clin. Chim. Acta 104 (1980) 161–167.
[22] R.W. Farndale, D.J. Buttle, A.J. Barrett, Improved quantitation and discrimination of sulphated glycosaminoglycans by use of dimethylmethylene blue, Biochim. Biophys. Acta 883 (1986) 173–177.
[23] S. Wilshaw, B. Sc, J.N. Kearney, D. Ph, J. Fisher, E. Ingham, Production of an acellular amniotic membrane matrix for use in tissue engineering, Tissue Eng. 12 (2006).
[24] S. Mirsadraee, H.E. Wilcox, S.a. Korossis, J.N. Kearney, K.G. Watterson, J. Fisher, et al., Development and characterization of an acellular human pericardial matrix for tissue engineering, Tissue Eng. 12 (2006) 763–773.
[25] P. Petzelbauer, J.R. Bender, J. Wilson, J.S. Pober, Heterogeneity of dermal microvascular endothelial cell antigen expression and cytokine responsiveness in situ and in cell culture, J. Immunol. 151 (1993) 5062–5072.
[26] P. Decherchi, P. Cochard, P. Gauthier, Dual staining assessment of Schwann cell viability within whole peripheral nerves using calcein-AM and ethidium homodimer, J. Neurosci. Methods 71 (1997) 205–213.
[27] J. Tas, G. Westerneng, Fundamental aspects of the interaction of propidium diiodide with nuclei acids studied in a model system of polyacrylamide films, J. Histochem. Cytochem. 29 (1981) 929–936.
[28] S. Zhou, Z. Cui, J. Urban, Dead cell counts during serum cultivation are underestimated by the fluorescent live/dead assay, Biotechnol. J. 6 (2011) 513–518.
[29] O. Syed, N.J. Walters, R.M. Day, H.-W. Kim, J.C. Knowles, Evaluation of decellularization protocols for production of tubular small intestine submucosa scaffolds for use in oesophageal tissue engineering, Acta Biomater. 10 (2014) 5043–5054.
[30] H. Baraki, I. Tudorache, M. Braun, K. Höffler, A. Görler, A. Lichtenberg, et al., Orthotopic replacement of the aortic valve with decellularized allograft in a sheep model, Biomaterials 30 (2009) 6240–6246.

[31] A.M. Seddon, P. Curnow, P.J. Booth, Membrane proteins, lipids and detergents: Not just a soap opera, Biochim. Biophys. Acta – Biomembr. 1666 (2004) 105–117.
[32] L. Mancuso, a. Gualerzi, F. Boschetti, F. Loy, G. Cao, Decellularized ovine arteries as small-diameter vascular grafts, Biomed. Mater. 9 (2014) 045011.
[33] V. Samouillan, J. Dandurand-Lods, a. Lamure, E. Maurel, C. Lacabanne, G. Gerosa, et al., Thermal analysis characterization of aortic tissues for cardiac valve bioprostheses, J. Biomed. Mater. Res. 46 (1999) 531–538.
[34] P.F. Gratzer, R.D. Harrison, T. Woods, Matrix alteration and not residual sodium dodecyl sulfate cytotoxicity affects the cellular repopulation of a decellularized matrix, Tissue Eng. 12 (2006) 2975–2983.
[35] S. Cebotari, I. Tudorache, T. Jaekel, A. Hilfiker, S. Dorfman, W. Ternes, et al., Detergent decellularization of heart valves for tissue engineering: Toxicological effects of residual detergents on human endothelial cells, Artif. Organs 34 (2010) 206–210.
[36] P.M. Baptista, M.M. Siddiqui, G. Lozier, S.R. Rodriguez, A. Atala, S. Soker, The use of whole organ decellularization for the generation of a vascularized liver organoid, Hepatology 53 (2011) 604–617.
[37] M. Zhou, Z. Liu, C. Liu, X. Jiang, Z. Wei, W. Qiao, et al., Tissue engineering of small-diameter vascular grafts by endothelial progenitor cells seeding heparin-coated decellularized scaffolds, J. Biomed. Mater. Res. – Part B Appl. Biomater. 100B (2012) 111–120.
[38] Y. Narita, H. Kagami, H. Matsunuma, Y. Murase, M. Ueda, Y. Ueda, Decellularized ureter for tissue-engineered small-caliber vascular graft, J. Artif. Organs 11 (2008) 91–99.
[39] Y. Zou, Y. Zhang, Mechanical evaluation of decellularized porcine thoracic aorta, J. Surg. Res. 175 (2012) 359–368.
[40] S. Wang, X.M. Mo, B.J. Jiang, C.J. Gao, H.S. Wang, Y.G. Zhuang, et al., Fabrication of small-diameter vascular scaffolds by heparin-bonded P(LLA-CL) composite nanofibers to improve graft patency, Int. J. Nanomed. 8 (2013) 2131–2139.
[41] H. Ahn, Y.M. Ju, H. Takahashi, D.F. Williams, J.J. Yoo, S.J. Lee, et al., Engineered small diameter vascular grafts by combining cell sheet engineering and electrospinning technology, Acta Biomater. 16 (2015) 14–22.
[42] L.E. Niklason, W. Abbott, J. Gao, B. Klagges, K.K. Hirschi, K. Ulubayram, et al., Morphologic and mechanical characteristics of engineered bovine arteries, J. Vasc. Surg. 33 (2001) 628–638.
[43] N. L'Heureux, S. Pâquet, R. Labbé, L. Germain, F.a. Auger, A completely biological tissue-engineered human blood vessel, FASEB J. 12 (1998) 47–56.
[44] A.F. Pellegata, M.A. Asnaghi, I. Stefani, A. Maestroni, S. Maestroni, T. Dominioni, et al., Detergent-enzymatic decellularization of swine blood vessels: insight on mechanical properties for vascular tissue engineering, Biomed. Res. Int. 2013 (2013) 918753.
[45] B.D. Stemper, N. Yoganandan, M.R. Stineman, T.A. Gennarelli, J.L. Baisden, F.A. Pintar, Mechanics of fresh, refrigerated, and frozen arterial tissue, J. Surg. Res. 139 (2007) 236–242.
[46] H. Niknejad, H. Peirovi, M. Jorjani, A. Ahmadiani, J. Ghanavi, M. Seifalian, et al., Properties of the amniotic membrane for potential use in tissue engineering, Eur. Cell Mater. (2008).
[47] A. Lindenmair, S. Nürnberger, G. Stadler, A. Meinl, C. Hackl, J. Eibl, et al., Intact human amniotic membrane differentiated towards the chondrogenic lineage, Cell Tissue Bank. 15 (2014) 213–225.
[48] A. Banerjee, S. Nürnberger, S. Hennerbichler, S. Riedl, C.M. Schuh, A. Hacobian, et al., In toto differentiation of human amniotic membrane towards the Schwann cell lineage, Cell Tissue Bank. 15 (2014) 227–239.
[49] W.P. Faulk, R. Matthews, P.J. Stevens, J.P. Bennett, H. Burgos, B.L. Hsi, Human amnion as an adjunct in wound healing, Lancet 1 (1980) 1156–1158.
[50] C.E. Schmidt, J.M. Baier, Acellular vascular tissues: Natural biomaterials for tissue repair and tissue engineering, Biomaterials 21 (2000) 2215–2231.
[51] F. Sun, S. Pan, H.C. Shi, F.B. Zhang, W.D. Zhang, G. Ye, et al., Structural integrity, immunogenicity and biomechanical evaluation of rabbit decellularized tracheal matrix, J. Biomed. Mater. Res. A (2014) 1–11.
[52] L. Flynn, J.L. Semple, K.a. Woodhouse, Decellularized placental matrices for adipose tissue engineering, J. Biomed. Mater. Res. A 79 (2006) 359–369.
[53] R. Fu, Y. Wang, S. Liu, T. Shih, H. Lin, Y. Chen, et al., Review decellularization and recellularization technologies, Tissue Eng. 23 (2014) 621–630.
[54] J. Bao, Y. Shi, H. Sun, X. Yin, R. Yang, L. Li, et al., Construction of a portal implantable functional tissue-engineered liver using perfusion-decellularized matrix and hepatocytes in rats, Cell Transplant. 20 (2011) 753–766.
[55] F. Bolland, S. Korossis, S.P. Wilshaw, E. Ingham, J. Fisher, J.N. Kearney, et al., Development and characterisation of a full-thickness acellular porcine bladder matrix for tissue engineering, Biomaterials 28 (2007) 1061–1070.
[56] H.C. Ott, T.S. Matthiesen, S.-K. Goh, L.D. Black, S.M. Kren, T.I. Netoff, et al., Perfusion-decellularized matrix: using nature's platform to engineer a bioartificial heart, Nat. Med. 14 (2008) 213–221.
[57] H. Mertsching, J. Schanz, V. Steger, M. Schandar, M. Schenk, J. Hansmann, et al., Generation and transplantation of an autologous vascularized bioartificial human tissue, Transplantation 88 (2009) 203–210.